STUDIES OF THE ENERGETICS AND MECHANISMS OF ORGANOMETALLIC REACTIONS IN THE GAS PHASE

Thesis by

Linda F. Halle

In Partial Fulfillment of the Requirements

for the Degree of

Doctor of Philosophy

California Institute of Technology

Pasadena, California

1983

(Submitted April 1, 1983)

To my parents, Esther, and Oma

Acknowledgment

Many thanks go to Jack Beauchamp for his encouragement and guidance over the past four years. His confidence in me was invaluable.

It has been my particular good fortune to have started my graduate studies with Peter Armentrout, and a very special pleasure to have spent the last year working with Mary Mandich. My other friends and family, both in the Land of Sunshine and the Windy City, have provided support, good times, and good food, which will always be appreciated.

Acknowledgments are also due to the members of the various organic and organometallic chemistry groups at Caltech who were always obliging when asked if I could "borrow" compounds; to the Goddard group members, especially Art Voter, for their helpful discussions and computer programs and advice; to the staff of the Caltech shops, who were always ready with expert assistance; and to Sharon ViGario, who deserves special mention for the excellent and speedy typing of this thesis.

Financial support from Bell Laboratories, SOHIO, the Shell Companies Foundation, and Caltech is gratefully acknowledged.

Above all, thanks go to my husband Brian for making the years I spent at Caltech very happy ones.

Abstract

An ion beam apparatus is used to study reactions of the three first row group 8 atomic metal ions, Fe^+, Co^+, and Ni^+, as well as the diatomic FeH^+ species, with small organic molecules. The kinetic energy dependence of these processes is examined. Analysis of the thresholds for endothermic reactions yields bond strengths of the metal ion to various substituent groups. The thermochemical information derived in this manner and from more qualitative observations is used to assess the mechanisms by which these ions react with small organic molecules.

Chapter I provides a brief summary of some of the organometallic systems previously studied using the ion beam apparatus. Chapter II presents the culmination of our studies of reactions of the first row group 8 metal ions with alkanes in which the extensive use of deuterium- and ^{13}C-labeled compounds provides further elaboration of the mechanisms by which these ions activate carbon-carbon and carbon-hydrogen bonds.

Chapter III examines the consequences of incorporating a carbonyl group into the hydrocarbon from investigations of the reactions of Co^+ with aldehydes and ketones. Analysis of products formed at high relative kinetic energies are used in conjunction with thermochemical estimates to infer mechanistic details and construct qualitative reaction coordinate diagrams for the interactions of Co^+ with carbonyl compounds.

Chapter IV represents an extension of our determinations of metal-carbon bond strengths to include fluorinated substituents. In particular, measurements of the Ni^+-CH_2 and Ni^+-CF_2 bond energies are reported. The implication of these carbene bond strengths for the metathesis of fluorinated olefins is discussed.

Chapter V reports the first ion beam experiment of an organometallic fragment, the FeH^+ species. Thermochemical information is obtained from reactions involving proton transfer from, and hydride transfer to, FeH^+. We find that oxidative addition of FeH^+ to D_2 or hydrocarbons via Fe(IV) or four-centered intermediates is not a facile process, while reversible insertion of olefins into Fe^+-H occurs with moderate cross section at low energies. Preliminary results for the reactions of FeH^+ with alcohols, aldehydes, and ethers are also discussed.

TABLE OF CONTENTS

CHAPTER I

INTRODUCTION

Over the past several years, studies of organometallic reactions have been extended from condensed phases into the gas phase. In particular, the ion-molecule reactions of transition metal complexes have gained a considerable amount of attention since the initial mass spectrometric studies by Muller[1]. The scope of these investigations grew to include the application of the technique of ion cyclotron resonance spectrometry (ICR), which has been used extensively by several research groups to study reactions of ions generated by electron impact from metal carbonyl and cyclopentadienyl compounds[2-4]. Laser volatilization sources have also been developed for ICR spectrometers which allow the reactions of atomic metal ions to be examined[5,6].

Only thermoneutral reactions can be probed using straightforward ICR techniques. Much additional mechanistic and structural information can be acquired from the characterization of high energy products[7]. To this end, we have used an ion beam apparatus, described more completely in Chapter V, which permits the kinetic energy dependence of these reactions to be explored. Analysis of thresholds for endothermic processes using theoretical technique developed earlier[8,9] yields quantitative thermochemical information, including bond strengths of the ionic metal species to various substituent groups.

Initial ion beam studies from this laboratory reported reactions of atomic cobalt ions with alkanes in which formation of products due to carbon-carbon and carbon-hydrogen bond cleavage processes were observed[10]. Further experiments performed using alkenes as the neutral reactant yielded information on the intermediates involved in these reactions[11]. These studies were extended to involve investigations of reactions of the

other two first row group 8 metal ions, Fe^+ and Ni^+.[12]. Experiments using labeled alkanes provide greater detail of the pathways by which these reactions proceed. For example, it was discovered that Ni^+ effects a highly specific 1,4 dehydrogenation of hydrocarbons, instead of the more typical 1,2 process[13]. Further mechanistic information accrued from reactions with labeled alkanes for the three group 8 metal ions is presented in Chapter II of this thesis.

The introduction of a functional group, such as a carbonyl moiety, into the organic substrate guides the systematic disruption of the molecule by group 8 metal ions[14]. The interactions of Co^+ with aldehydes and ketones are presented in Chapter III. Reaction of Co^+ with formaldehyde, acetaldehyde, and acetone yields $CoCO^+$ as the major product at low energies. As the alkyl chains of the dialkyl ketones are extended, loss of alkenes and aldehydes predominate. However, if the alkyl chain is highly branched, the major product is loss of methane. This behavior is reminiscent of the reactions of Co^+ with alkanes[10].

In addition to the mechanistic studies described above, a fundamental contribution of the ion beam work has been the measurement of metal-hydrogen[15], metal-carbon[9,10,12], and metal-oxygen[16] bond dissociation energies[17]. This work has assisted in understanding the differences in reactivity of the metal ions with alkanes, as well as providing information on the electronic character of the metal ion-substituent bond. For example, the metal hydrogen and methyl bond dissociation energies correlate with the energy required to promote the metal ion from its ground state to the lowest state derived from the $3d^{n-1}4s^1$ configuration. This result implies that σ-bonding to the first row transition metals

involves substantial participation of the metal 4s orbital. No such correlation is found for $D^0(M^+\text{-}CH_2)$ or $D^0(M^+\text{-}O)$, presumably the result of variable amounts of π-bonding in these systems[17].

Because metal ligand bond strengths are sensitive to the electronic configuration of the metal ion, it is not surprising that enhanced reactivity might be seen for electronically excited metal species. This was, in fact, observed by comparing the reactions of electronically excited Cr^+ formed by electron impact from $Cr(CO)_6$ with those of Cr^+ formed in the ground state by surface ionization[18]. For example, reactions of ground state chromium ions (^6S derived from the configuration $3d^5$) with methane yields only CrH^+ in an endothermic process, while excited state Cr^+ (probably ^4D, derived from the configuration $3d^4 4s^1$) forms $CrCH_2^+$, $CrCH_3^+$, and CrH^+, all detected as exothermic products.

Chapter IV offers another variation of the thermochemical studies. In this chapter the determinations of the bond energies of two nickel carbenes, $Ni^+\text{-}CH_2$ and $Ni^+\text{-}CF_2$, are presented. The implication of these carbene bond strengths for the metathesis of various fluorinated olefins is discussed.

Future studies planned for the ion beam apparatus will involve the examination of reactions and thermochemistry of organometallic fragments. Chapter V reports the first of these efforts on the simplest type of fragment, a metal hydride ion. Thermochemical information is obtained from reactions involving proton transfer from, and hydride transfer to, FeH^+. We find that oxidative addition of FeH^+ to D_2 or hydrocarbons to give Fe(IV) intermediates (or reaction via four-center intermediates) is not a favorable process, while reversible insertion of olefins into the $Fe^+\text{-}H$ bond is a facile process. These results suggest that further

ion beam studies of organometallic fragments, such as metal hydrides and alkyls, will reveal a rich and interesting chemistry.

Selected References

1. Muller, J.; Fenderl, K. Chem. Ber. 1971, 104, 2199; Muller, J.; Fenderl, K., ibid. 1971, 104, 2207.
2. a) Weddle, G. H.; Allison, J.; Ridge, D. P. J. Am. Chem. Soc. 1977, 99, 105.
   b) Allison, J; Ridge, D. P. J. Am. Chem. Soc. 1979, 101, 4998.
3. a) Foster, M. S.; Beauchamp, J. L. J. Am. Chem. Soc. 1975, 97, 4808.
   b) Corderman, R. R.; Beauchamp, J. L. J. Am. Chem. Soc. 1976, 98, 5700.
   c) Stevens, A. E.; Beauchamp, J. L. J. Am. Chem. Soc. 1978, 100, 2584.
4. Jones, R. W.; Staley, R. H. Int. J. Mass Spec. Ion Phys. 1981, 39, 35.
5. Cody, R. B.; Burnier, R. C.; Reents, W. D., Jr.; Carlin, T. J.; McCrery, D. A.; Lengel, R. K.; Freiser, B. S. Int. J. Mass Spec. Ion Phys. 1980, 33, 37.
6. Jones, R. W.; Staley, R. H. J. Am. Chem. Soc. 1980, 102, 3794.
7. Armentrout, P. B.; Beauchamp, J. L. J. Am. Chem. Soc. 1980, 102, 1736.
8. Armentrout, P. B.; Beauchamp, J. L. Chem. Phys. 1980, 48, 315.
9. Armentrout, P. B.; Beauchamp, J. L. J. Chem. Phys. 1981, 74, 2819.
10. Armentrout, P. B.; Beauchamp, J. L. J. Am. Chem. Soc. 1981, 103, 784.
11. Armentrout, P. B.; Halle, L. F.; Beauchamp, J. L. J. Am. Chem. Soc. 1981, 103,6624.
12. Halle, L. F.; Armentrout, P. B.; Beauchamp, J. L. Organomet. 1982, 1, 963.
13. Halle, L. F.; Houriet, R.; Kappes, M.M.; Staley, R. H.; Beauchamp, J. L. J. Am. Chem. Soc. 1982, 104, 6293.
14. Burnier, R. C.; Byrd, G. D.; Freiser, B. S. J. Am. Chem. Soc. 1981, 103, 4360.

15. Armentrout, P. B., Beauchamp, J. L. Chem. Phys. 1980, 50, 37.

16. Armentrout, P. B.; Halle, L. F.; Beauchamp, J. L. J. Chem. Phys. 1982, 76, 2449.

17. Armentrout, P. B.; Halle, L. F.; Beauchamp, J. L. J. Am. Chem. Soc. 1981, 103, 6501.

18. Halle, L. F.; Armentrout, P. B.; Beauchamp, J. L. J. Am. Chem. Soc. 1981, 103, 962.

CHAPTER II

ACTIVATION OF C-H AND C-C BONDS IN ALKANES BY FIRST ROW GROUP 8 ATOMIC TRANSITION METAL IONS IN THE GAS PHASE. MECHANISTIC DETAILS FROM A STUDY OF DEUTERIUM AND ^{13}C-LABELED HYDROCARBONS.

ACTIVATION OF C-H AND C-C BONDS IN ALKANES BY FIRST ROW GROUP 8 ATOMIC TRANSITION METAL IONS IN THE GAS PHASE. MECHANISTIC DETAILS FROM A STUDY OF DEUTERIUM AND ^{13}C-LABELED HYDROCARBONS

L. F. Halle, Raymond Houriet,[1] and J. L. Beauchamp

Contribution No. 6782 from the Arthur Amos Noyes Laboratory of Chemical Physics, California Institute of Technology, Pasadena, California 91125.

Abstract: The first step in the interaction of saturated hydrocarbons with atomic Group 8 metal ions involves oxidative addition of either a C-H or a C-C bond to the metal. At low energies this is followed by unimolecular rearrangement and elimination of smaller alkanes or molecular hydrogen. The present report is a continuation of our ion beam studies of these processes, in which we make extensive use of deuterium and ^{13}C-labeled normal, branched, and cyclic alkanes to elucidate mechanistic details. While overall patterns of reactivity are similar, the labeling results reveal subtle differences in comparing the behavior of Fe^+, Co^+, and Ni^+. For example, dehydrogenation of linear alkanes by Ni^+ proceeds exclusively via a 1,4 elimination process, while dehydrogenation by Fe^+ and Co^+ occurs via a mixture of 1,4 and 1,2 eliminations and seems to be accompanied by some scrambling. In several cases involving the reactions of Fe^+, product distributions are best explained by assuming that β-alkyl transfers occur as one step in the decomposition of reaction intermediates.

The fragmentation of a hydrocarbon molecule by reaction with a Group 8 metal ion is highly specific and occurs without the extensive rearrangements which often accompany electron impact ionization. This suggests the use of gas-phase metal ion reactions as a novel chemical ionization technique to determine not only the structure but the original label distribution in a molecule.

Introduction

Considerable interest in the subject of C-H bond activation at transition metal centers has developed in the past several years, stimulated by the observation that even saturated hydrocarbons can react with little or no activation energy under appropriate conditions[2]. Interestingly, gas phase studies of the reactions of saturated hydrocarbons at transition metal centers were reported as early as 1973[3]. More recently, ion cyclotron resonance [4-7] and ion beam experiments[8-10] have provided many examples of activation of both C-H and C-C bonds of alkanes by transition metal ions. Facile addition of C-H or C-C bonds

Scheme I

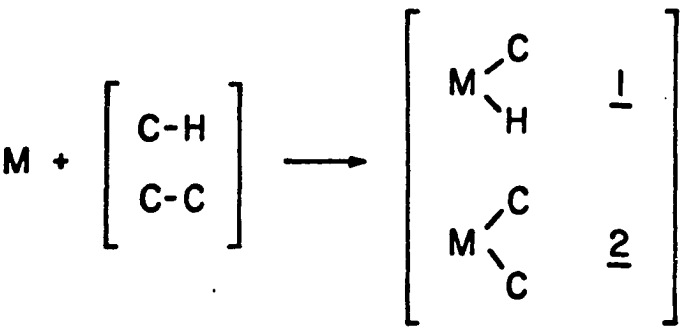

to metal centers requires first that the process be energetically feasible, preferably exothermic. Metal-hydrogen bonds in the range of 60 kcal/mole would require metal-carbon bond energies greater than 35 kcal/mole for 1 to be more stable than the reactants[11,12]. While this is not an unreasonable value, the requirement that metal-carbon bond energies exceed 40-45 kcal/mole to render 2 energetically accessible might at first appear restrictive. However, there are several estimates of metal-carbon bond energies in this range[15].

Recent studies in our lab have shown that metal-carbon bond energies in organometallic "fragment" ions can exceed the analogous metal hydrogen bond strengths (Table I)[8,9,16]. In part this result must be regarded as unique, and parallels involving coordinatively saturated complexes are not likely to be found. The polarizable methyl group stabilizes the charge more favorably than hydrogen, resulting in stronger metal-carbon bonds. This effect is diluted by additional polarizable ligands as well as by a dielectric medium in condensed phases.

Along with a detailed examination of their electronic structure[16], the above considerations argue against simple bond addivity in organometallic fragment ions. Hence, the metal-hydrogen and metal-carbon bond energies measured in our laboratory must be used cautiously in estimating the thermochemical changes attending formation of intermediates such as 1 or 2. An important additional observation is the formation of $M(CH_3)_2^+$ as an exothermic reaction of Fe^+, Co^+, and Ni^+ with acetone[17,18]. This requires that the sum of the first and second metal-carbon bond dissociation energies exceeds 96 kcal/mole[19]. Hence, we remain firmly convinced that insertion of these metal ions into C-C bonds is an exothermic process. Consistent with these observations are products derived from reactions in which the metal ion cleaves the carbon chain of the alkane at low relative kinetic energies[4-10]. These products, as well as those which occur via dehydrogenation processes, are listed in Table II for selected alkanes. The details of the product distributions have been discussed previously[8,9].

A general mechanism which has been proposed for the reaction of metal ions with hydrocarbons is shown in Scheme II for butane. Oxidative

Table I. Thermochemical Data[a,b]

Bond Energies	Fe^+	Co^+	Ni^+
$D^o(M^+ - H)$	58 ± 5	52 ± 4	43 ± 2
$D^o(M^+ - CH_3)$	69 ± 5	61 ± 4	48 ± 5
$D^o(M^+ - CH_2)$	96 ± 5	85 ± 7	86 ± 6

[a] All values in kcal/mol.

[b] See references 8,9,16.

Table II: Product Distributions for Reactions of Fe^+, Co^+, and Ni^+ with Alkanes Measured at ~0.5 eV Relative Kinetic Energy

		Neutral Products (irrespective of label)[a]									
M^+	Alkane	H_2	CH_4	C_2H_6	C_3H_8	C_4H_{10}	C_5H_{12}	C_6H_{14}	$2H_2$	$H_2 + CH_4$	$H_2 + C_2H_6$, $2CH_4$
Fe^+	propane	.18	.82								
	2-methylpropane[b]	.48	.52								
	butane	.20	.41	.39							
	-1,1,1,4,4,4-d_6	.16	.42	.42							
	pentane	.18	.27	.25	.24				.02	.04	
	-2,2,3,3,4,4-d_6	c	.44	.16	.41						
	hexane	.31	.12	.25	.12	.17					.03
	-1,1,1,6,6,6-d_6	.47	.16	.13	.07	.17					
	-2,2,5,5-d_4	.35	.16	.19	.09	.20					
	-3,3,4,4-d_4	.39	.21	.12	.09	.19					
	2,2-dimethylpentane[d]	.10	.31		.36	.03	.04				.03
	-5,5,5-d_3[d]	.10	.16		.50	.06	.07				.06
Co^+	propane	.75	.25								
	2-methylpropane	.27	.73								
	butane	.29	.12	.59							
	-1,1,1,4,4,4-d_6	.41	.10	.49							
	pentane	.30	.02	.59	.08					tr[e]	
	-2,2,3,3,4,4-d_6	.29	.06	.52	.14						
	hexane	.39		.35	.16	.04					
	-1,1,1,6,6,6-d_6	.37		.41	.18	.03					
	-2,2,5,5-d_4	.33		.45	.18	.04					
	-3,3,4,4-d_4	.43	.03	.29	.21	.04					

Table II - continued

M^+	Alkane	Neutral Products (irrespective of label)[a] H_2	CH_4	C_2H_6	C_3H_8	C_4H_{10}	C_5H_{12}	C_6H_{14}	$2H_2$	$H_2 + CH_4$	$H_2 + C_2H_6$, $2CH_4$
Ni^+	propane	.33	.67								
	propane[f]	.20	.80								
	-2-d_1[f]	.19	.81								
	2-methylbutane	.06	.94								
	-2-d_1	.07	.93								
	butane	.48	.06	.45							
	-1,1,1,4,4,4-d_6	.34	.09	.58							
	pentane[g]	.64	.01	.22	.13						
	-1,1,1,5,5,5-d_6	.52	.02	.34	.13						
	-2,2,3,3,4,4-d_6	.68		.19	.14						
	hexane[g]	.66	tr	.17	.11	.05					.02
	-1,1,1,6,6,6-d_6	.83		.09	.07	.02					
	-2,2,5,5-d_4	.81		.11	.06	.03					
	-3,3,4,4-d_4	.84		.06	.07	.03					
		.73		.12	.06	.03			.05		
		.81		.09	.07	.03					
	heptane	.63	.07	.12	.13	.05					
	2-methyl hexane										
		.66	.03	.01	.14	.13	.03				
		.67	.02	.01	.19	.10	.01				
		.68	.03	.01	.10	.17	tr				
		.76	.02		.12	.10					
		.77	.03		.10	.10					

Table II - continued

M^+	Alkane	Neutral Products (irrespective of label)[a] H_2	CH_4	C_2H_6	C_3H_8	C_4H_{10}	C_5H_{12}	C_6H_{14}	$2H_2$	$H_2 + CH_4$	$H_2 + C_2H_6$, $2CH_4$
	2,2-dimethylpentane										
		.64	.09	.03	.18	.06					
		.59	.06	.06	.19	.10					
		.49	.09	.05	.29	.09					
		.59	.09	.02	.21	.08	.01				
		.58	.07	.02	.23	.10	tr				
		.46	.07	.07	.27	.12	tr				
	octane										
	-1,1,1,8,8,8-d_6	.69		.03	.10	.11	.06	.01			

[a]For example, the "CH_4" column accounts for all methane losses, including ^{13}C and deuterium-labeled molecules.

[b]See footnote 37.

[c]The available amount of this compound was exhausted during the experiment. Consequently, the proportional loss of hydrogen could not be measured.

[d]Loss of C_2H_4 is also observed, see text.

[e]Trace amount observed.

[f]Measured at 0.9 eV relative kinetic energy.

[g]Product distributions listed are averages of two widely different data sets. Data taken at about the same time as labeled studies were performed show 73% dehydrogenation of pentane and 78% dehydrogenation of hexane.

Scheme II

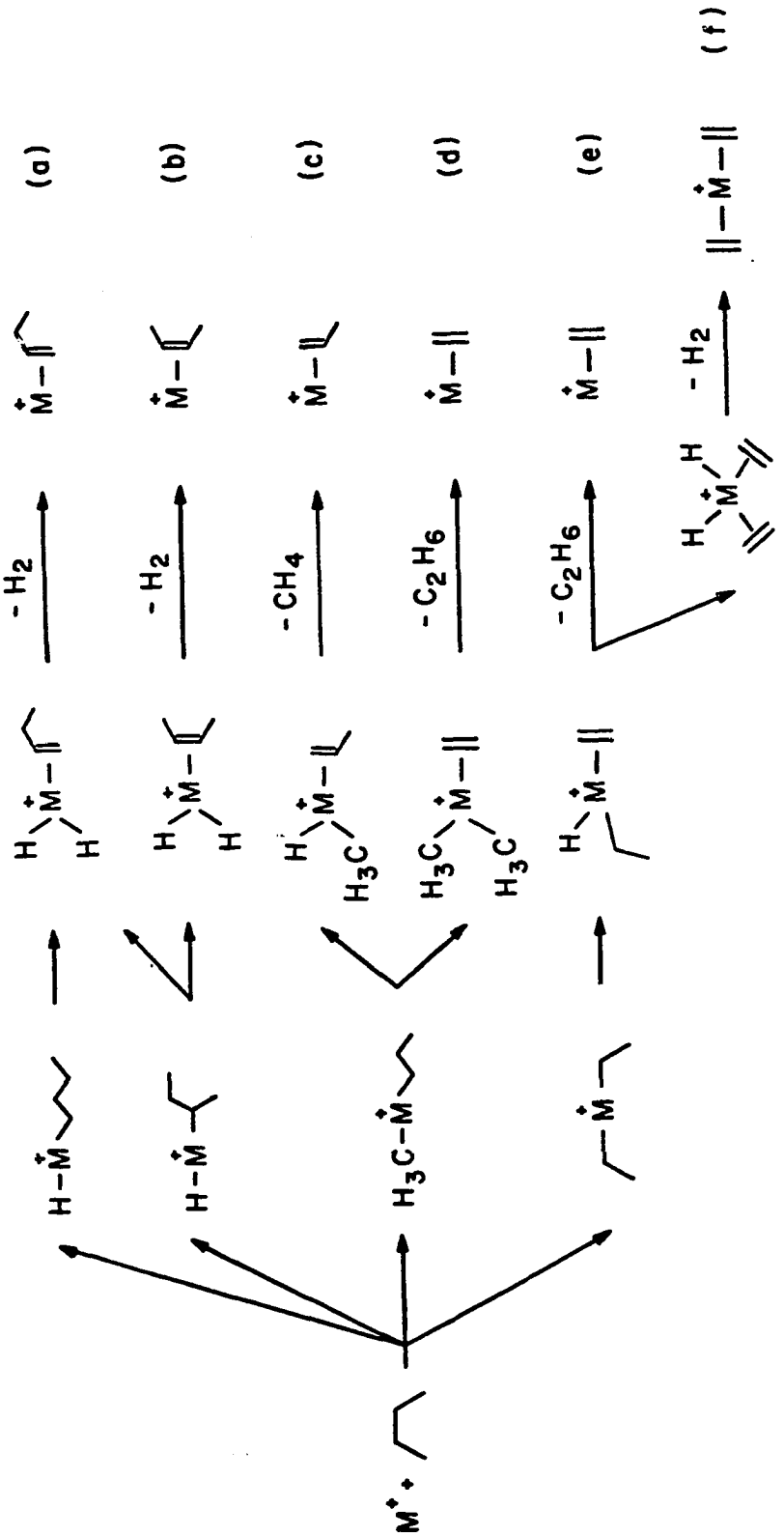

addition of C-H and C-C bonds to the metal yields reaction intermediates which further rearrange by β-H and β-alkyl shifts. The final step involves reductive elimination of hydrogen or an alkane from the metal center to yield observed products.

Several aspects of the proposed reaction mechanism shown in Scheme II deserve comment. The products are alkenes bound to the metal ion. Binding energies of group 8 metal ions to ethylene are in the range 40-70 kcal/mole[10,20]. Hence, it is the stability of the products which render the overall process substantially exothermic when effected by a transition metal ion.

Scheme II depicts a number of initial steps which arise from insertion of the metal ion into one of the two types of C-H bonds in butane (leading to structures 3 and 4) or one of the two types of C-C bonds (structures 5 and 6). A myriad of possible rearrangements can follow. Scheme II indicates what we believe to be the important subsequent rearrangement processes. To sort out which pathways occur for the different metal ions one needs information relating to the structure of the products. This can in part by obtained by varying the hydrocarbon structure. More sophisticated approaches include labeling the reactants[4a], ligand exchange reactions, and collision-induced dissociation studies of the product ions[4b,7,21].

Studies utilizing labeled hydrocarbons are few. Ridge and coworkers have reported that reaction of Fe^+ with $(CH_3)_3CD$ results in loss of CH_4 and HD, exclusively[4a]. In particular, dehydrogenation occurs via a 1,2 elimination process analogous to Scheme IIa or IIb[22]. There is no evidence in this case that β-H transfer processes are

reversible. In our laboratory the reaction of Co^+ with $CD_3CH_2CH_2CD_3$ has been studied[8]. Insertion of Co^+ into the central C-C bond leads mainly to formation of $Co(C_2H_2D_2)^+$ although a minor amount of $Co(C_2HD_3)^+$ was noted and attributed to reversible β-hydrogen transfer processes (see also Table IV). At higher kinetic energies the amount of hydrogen scrambling was reduced, consistent with a shorter lifetime of the reaction intermediate expected with higher internal energies. Dehydrogenation to form the cobalt-butene ion indicates loss of H_2, HD, and D_2; product yields were not reported but did not vary significantly with reactant ion kinetic energy.

Details of dehydrogenation reactions of nickel ions with a number of deuterated alkanes have also been reported[10]. The product distributions for these reactions are listed in Table III and indicate that at low energies, the dehydrogenation by Ni^+ of linear alkanes with alkyl chains of four or more carbons occurs exclusively by a 1,4 elimination process leading to structure 8, Scheme IIf. Metallacycle intermediates are not involved in these reactions. Instead, as shown for butane, the metal ion inserts into the internal carbon-carbon bond, followed by two β-hydrogen transfers onto the metal, resulting in loss of hydrogen atoms from the two end carbons. Reversible β-H transfers do not occur in these reactions. These results are supported by structural information obtained by Jacobson and Freiser using the technique of collision-induced dissociation (CID) of the product ions formed in a Fourier-transform mass spectrometer (FT-MS)[7,21]. The CID technique involves acceleration of a particular ion to a high kinetic energy. Subsequent collisions with neutral molecules convert translational energy to

Table III. Isotopic Product Distribution for Dehydrogenation of Deuterated Alkanes by Fe^+, Co^+, and Ni^+.

M^+	Alkane	Loss of H_2	Loss of HD	Loss of D_2
Fe^+	2-methylpropane-2-d_1 [b]		1.0	
	butane-1,1,1,4,4,4-d_6	0.59	0.18	0.23
	pentane-2,2,3,3,4,4-d_6	0.04	0.79	0.17
	hexane-1,1,1,6,6,6-d_6	0.58	0.42	
	hexane-2,2,5,5-d_4	0.47	0.43	0.10
	hexane-3,3,4,4-d_4	0.67	0.33	
Co^+	butane-1,1,1,4,4,4-d_6	0.18	0.31	0.51
	pentane-2,2,3,3,4,4-d_6	0.08	0.80	0.12
	hexane-1,1,1,6,6,6-d_6	0.65	0.35	
	hexane-2,2,5,5-d_4	0.46	0.21	0.33
	hexane-3,3,4,4-d_4	0.61	0.39	
Ni^+	propane-2-d_1	0.56	0.44	
	2-methylpropane-2-d_1		1.0	
	butane-1,1,1,4,4,4-d_6			1.0
	pentane-1,1,1,5,5,5-d_6		1.0	
	pentane-2,2,3,3,4,4-d_6		1.0	
	hexane-1,1,1,6,6,6-d_6	0.48	0.52	
	hexane-2,2,5,5-d_4	0.55		0.45
	hexane-3,3,4,4-d_4	0.47	0.53	
	hexane-1,1,6,6-d_4	0.71	0.29	
	hexane-3,3-d_2	0.80	0.20	

[a] Measured at ~0.5 eV relative kinetic energy unless otherwise noted.

[b] Reference 4a.

internal energy which can lead to fragmentation. The fragmentation pattern, or CID spectrum, is often characteristic of a particular structure. In the FT-MS experiments, $M(C_4H_8)^+$ ions, M = Fe, Co, Ni, were generated by reaction of M^+ with several different reactants, such as butane and larger n-alkanes, 2,2-dimethylpropane, and cyclopentanone. By comparing the CID spectra of the various $M(C_4H_8)^+$ ions, the authors concurred that Ni^+ dehydrogenates linear alkanes exclusively via a 1,4 elimination process (Scheme IIf). Their results indicate Co^+ dehydrogenates butane 90 ± 5% via Scheme IIf and 10 ± 5% by Scheme IIa-b, while Fe^+ dehydrogenates butane 30 ± 10% by Scheme IIf and 70 ± 10% by Scheme IIa-b[7,21].

In the present work we report reactions of first row group 8 metal ions with a variety of deuterium and ^{13}C-labeled hydrocarbons. Because there is little precedence for oxidative addition of unstrained C-C bonds to metal centers[23], our specific interests in carrying out these studies included not only comparing in greater detail the reactivity of the different group 8 metal ions, but also substantiating arguments in favor of Scheme II along with investigating the occurrence and mechanism of distal group eliminations (e.g., 1,4 dehydrogenation).

Experimental

The tandem ion beam mass spectrometer and experimental techniques have been described elsewhere[8]. Briefly, singly charged transition metal cations are formed by surface ionization using their respective metal chloride salts, $FeCl_3$, $CoCl_2 \cdot 6H_2O$, and $NiCl_2 \cdot 6H_2O$. The metal

ions are mass and energy selected before entering a collision chamber containing the reactant gas. Product ions scattered in the forward direction are detected using a quadrupole mass spectrometer coupled to a signal averager.

Labeled butane (1,1,1,4,4,4-d_6, 98% D) was obtained from Merck, Sharp, and Dohme. Other isotopically labeled compounds were synthesized by standard methods[24] and contained at least 99% D or 90% ^{13}C. The pressure of the alkane was kept constant at ~0.5 to 1.0 x 10^{-3} torr as measured by use of a capacitance manometer.

Because only limited amounts of most of the labeled compounds were available, the reactions were examined chiefly at one low energy, ~0.4 to 0.7 eV relative kinetic energy. Errors in product abundance are higher for minor products (±20% of reported value) than for major products (±10% of reported value). In some systems, product distributions are a very sensitive function of the relative kinetic energy[8,9]. Again, because of the limited availability of samples, this effect could not be explained in great detail. As a result, comparisons of product distributions even for substrates differing in their isotopic composition may have only semi-quantitative significance.

It is to be noted that neutral products are not detected in these experiments. However, the identity of these products can usually be inferred without ambiguity. Structures of the ionic products are inferred from results with the labeled compounds as well as thermochemical arguments.

Results and Discussion

Tables II - V list the product distribution for the three metal ions, Fe^+, Co^+, and Ni^+, reacting with labeled linear alkanes. In no case is ^{13}C scrambling evident, and deuterium scrambling in the inter-

Table IV. Distribution of Labeled Products in the Reactions of Fe^+, Co^+, and Ni^+ with Deuterated Alkanes[a]

M^+	Alkane	Neutral Products Corresponding to M(alkene)$^+$ Products																
		CH_4	CH_3D	CHD_3	C_2H_5D	$C_2H_4D_2$	$C_2H_3D_3$	$C_2H_2D_4$	C_2D_6	C_3H_8	$C_3H_6D_2$	$C_3H_5D_3$	$C_3H_4D_4$	$C_3H_3D_5$	$C_4H_8D_2$	$C_4H_7D_3$	$C_4H_6D_4$	$C_4H_4D_6$
Fe^+	2-methylpropane-2-d_1[b]	>0.90																
	butane-1,1,1,4,4,4-d_6			1.0				0.90	0.10									
	pentane-2,2,3,3,4,4-d_6	0.80	0.20				1.0				0.67		0.33					
	hexane-1,1,1,6,6,6-d_6			1.0			1.0					1.0					0.70	0.30
	hexane-2,2,5,5-d_4		1.0			1.0						1.0			1.0			
	hexane-3,3,4,4-d_4	1.0			1.0						1.0				0.33		0.67	
Co^+	butane-1,1,1,4,4,4-d_6			1.0			0.15	0.85	tr[c]									
	pentane-2,2,3,3,4,4-d_6	0.60	0.40			0.22	0.78				0.06		0.84	0.10				
	hexane-1,1,1,6,6,6-d_6[d]						1.0					1.0					1.0	
	hexane-2,2,5,5-d_4[d]		tr			1.0						1.0			1.0			
	hexane-3,3,4,4-d_4[d]	tr			1.0						1.0						1.0	
Ni^+	propane-2-d_1	1.0																
	2-methylpropane-2-d_1	1.0																
	butane-1,1,1,4,4,4-d_6			1.0				1.0										
	pentane-1,1,1,5,5,5-d_6						1.0						1.0					
	pentane-2,2,3,3,4,4-d_6						1.0						1.0					
	hexane-1,1,1,6,6,6-d_6						1.0					1.0					1.0	
	hexane-2,2,5,5-d_4					1.0						1.0			1.0			
	hexane-3,3,4,4-d_4				1.0						1.0						1.0	
	hexane-3,3-d_2									0.40	0.60				1.0			
	octane-1,1,1,8,8,8-d_6											1.0				1.0		

[a]Measured at ~0.5 eV relative kinetic energy unless otherwise noted. [b]Ref. 4a. [c]Trace amount [d]Resolution not good enough to detect products due to scrambling.

Table V. Distribution of Labeled Products in the Reactions of Ni^+ with ^{13}C-Labeled Alkanes[a]

Alkane	Neutral Products Corresponding to M(alkene)$^+$ Products						
	C_2H_6	$^{13}CCH_6$	C_3H_6	$^{13}CC_2H_8$	C_4H_{10}	$^{13}CC_3H_{10}$	$^{13}C_2C_2H_{10}$
hexane-1,6-$^{13}C_2$		1.0		1.0		1.0	
hexane-3,4-$^{13}C_2$[b]	1.0			1.0			1.0
hexane-2-$^{13}C_1$	0.50	0.50	0.50	0.50	0.50	0.50	

[a]Measured at ~0.5 eV relative kinetic energy.

[b]These spectra showed products due most likely to hexane-3-$^{13}C_1$ (~15-25% impurity), not included in table.

mediates appear to be a significant process only in the case of Co^+. A typical product, such as loss of a smaller alkane, can most often be explained by processes analogous to Schemes IIc and IIe. As an example, consider the reaction of Ni^+ with hexane-1,1,1,6,6,6-d_6. Little loss of methane is seen in the reactions of Ni^+ with the linear alkanes, most likely because of the high terminal C-C bond energy. In analogy with Schemes IIc and IIe, loss of ethane would proceed via insertion of the metal ion into the C2-C3 bond of hexane followed by transfer of the β-hydrogen on C4. Consistent with this expectation, only $C_2H_3D_3$ is lost from the 1,6-labeled hexane. Similarly, propane is lost only as $C_3H_5D_3$ and butane is eliminated as $C_4H_4D_4$, incorporating a terminal methyl and one deuterium atom from the opposite end of the molecule.

Table V lists the losses of alkane from reaction of Ni^+ with three ^{13}C-labeled hexanes. The products observed in these cases also are those expected via Schemes IIc and IIe. For example, loss of ethane involves a terminal carbon atom along with its nearest neighbor. Thus, $^{13}CCH_6$ is lost from hexane-1,6-$^{13}C_2$ and unlabeled ethane is lost from hexane-3,4-$^{13}C_2$.

Dehydrogenation

Table III lists the products due to dehydrogenation of alkanes by Fe^+, Co^+, and Ni^+. As mentioned above, nickel ions dehydrogenate linear alkanes larger than butane exclusively via a 1,4 elimination process at low energies[10,21]. Iron and cobalt ions dehydrogenate alkanes by both this 1,4 pathway and the 1,2 elimination process depicted in Schemes IIa and IIb. The bond strengths of Ni^+ to H and CH_3 (Table I) suggest that the overall energetics of insertion into a C-H bond may be

unfavorable. Insertion into C-C bonds appears more reasonable on energetic grounds, which can explain the preference of Ni^+ to react via the 1,4 elimination pathway[25]. Iron and cobalt ions have higher first bond energies to a hydrogen atom, and undergo the "easier" 1,4 elimination process only part of the time. Jacobson and Freiser estimate from CID spectra that Co^+ and Fe^+ dehydrogenate butane 90 $\pm$ 5% and 30 $\pm$ 10% by Scheme IIf, respectively[7]. It is more difficult to determine these proportions from our data because a small amount of scrambling (see below) complicates the analysis. However, our results for loss of D_2 from butane-1,1,1,4,4,4-d_6, Table III (see also Table VI), with Fe^+ and especially Co^+ is less than what the CID results would predict.

Data in Table VI indicate that as the relative kinetic energy is increased, the proportion of 1,4 loss (loss of D_2) decreases in the reaction of the three metal ions with butane-1,1,1,4,4,4-d_6. For Ni^+, loss of H_2 becomes competitive with loss of D_2 above 1 eV, with equal amounts at 2eV.

The small amount of H_2 loss from pentane-2,2,3,3,4,4-d_6 in the reactions of Co^+ and Fe^+ cannot be explained by either a strict 1,2 or 1,4 process. Either α-hydrogen elimination occurs or some scrambling takes place. The former is considered unlikely since no loss of H_2 is seen in reactions with 2,2-dimethylpentane[8,9]. A plausible scrambling mechanism is shown in Scheme III. While scrambling processes seem to be negligible for both Fe^+ and Ni^+, they also account for some ionic products due to loss of alkanes in Co^+ reactions[8] as discussed below.

Loss of Alkane

Tables IV and V list the label distribution in alkane loss products from the interaction of the three group 8 metal ions with the n-alkanes.

Table VI. Percentage of Loss of X_2(X = H,D) in the Reactions of Fe^+, Co^+, and Ni^+ with Butane-1,1,1,4,4,4-d_6 at Several Energies

	Loss of H_2:HD:D_2			
	Relative Kinetic Energy (eV)			
M^+	0.26	0.52	1.0	2.0
Fe^+	71:5:25	46:30:24	60:26:14	
Co^+	15:28:57	16:28:56	36:18:45	
Ni^+	0:0:100	0:0:100	14:0:86	50:?:50

Scheme III

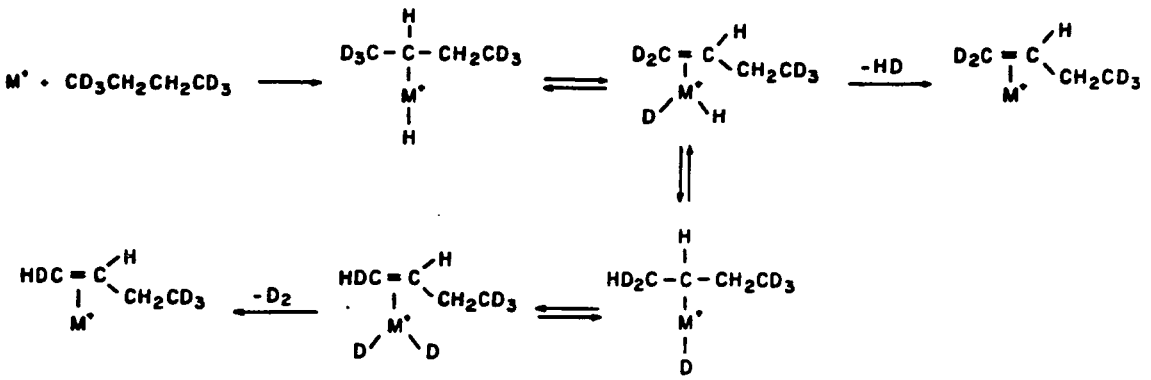

For each metal ion, slightly different sets of products are observed. The products of Ni^+ reactions are strictly consistent with Scheme IIc and IIe, where the metal cation inserts into a C-C bond followed by a β-H transfer and elimination of an alkane. However, somewhat unexpected products arise in both the Fe^+ and Co^+ reactions. For example, focusing on the Fe^+ reactions, 10% of the loss of ethane from butane-1,1,1,4,4,4-d_6 is C_2D_6, and 30% of the loss of butane from n-hexane involves the carbon atoms in the 1,2,3 and 6 positions[26]. These products can be explained by a mechanism in which Fe^+ inserts into the C1-C2 bond of butane or the C3-C4 bond of hexane, after which the terminal β-methyl group migrates onto the metal. This leads to elimination of ethane from butane, and butane from hexane, as shown in Scheme IV (which is analogous to Scheme IId).

Scheme IV

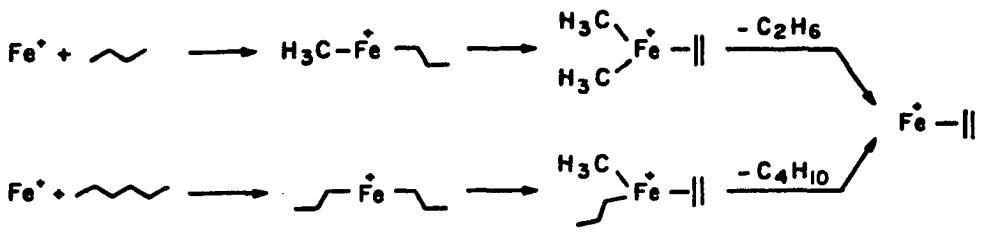

This also accounts for the loss of $C_3H_6D_2$ from pentane-2,2,3,3,4,4-d_6 and $C_5H_9D_3$ from 2,2 dimethylpentane-5,5,5-d_3 (Table IX). Though rarely observed, β-alkyl transfers have been noted in solution studies as well[27].

Loss of C_2D_6 from reaction of butane-1,1,1,4,4,4-d_6 with Fe^+ increases in proportion to loss of $C_2H_2D_4$ (Scheme IIe) with increasing energy. Loss of C_2D_6 is also seen at higher energies in the reactions of Co^+ and Ni^+ with butane-1,1,1,4,4,4-d_6. The occurrence of β-methyl transfers at very low energies in the Fe^+ reactions, and to a lesser extent in the Co^+ reactions (see Table IV), may be due to a higher methyl bond energy of the intermediates (5 or 7) involved in these reactions. However, thermochemical data for these more complex species are not known.

Table VII lists the methane losses expected via Scheme IIc as well as those experimentally observed. There are several mechanisms that can explain these products. For example, Fe^+ may insert into a terminal C-C bond followed by either an α- or δ-hydrogen transfer, processes (1) and (2). As discussed above, α-hydrogen transfers are

Table VII. Loss of Methane in the Reaction of Fe^+ with Deuterated Hexanes at ~0.5 eV Relative Kinetic Energy.

	Hexane		
	1,1,1,6,6,6-d_6	2,2,5,5-d_4	3,3,4,4-d_4
Experimentally observed	CHD_3	CH_3D	CH_4
Expected by analogy with Scheme IIc	CHD_3	CH_4	CH_3D
Expected from Scheme V	CHD_3	CH_3D	CH_4

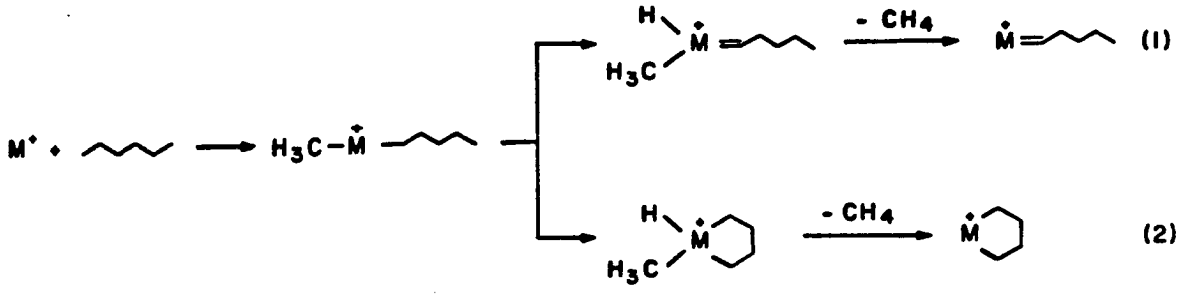

not considered likely[8]. Metallacycle intermediates[28] have been proposed in studies of the interactions of cobalt ions with cycloalkanes[29] and the dehydrogenation of 2,2,3,3-tetramethylbutane[8,9]. We are not aware of any precedent which provides support for the possible existence of the high oxidation states required by the intermediates in processes 1 and 2. Scheme V also yields the observed methane

Scheme V

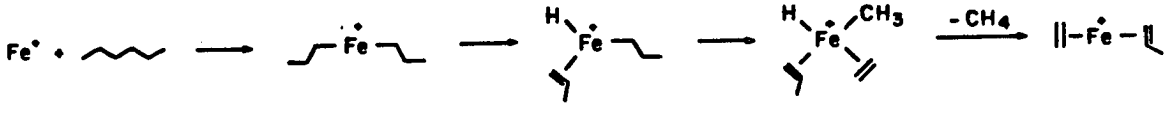

losses, and remains consistent with Schemes IId and IV. Here Fe^+ inserts into the central bond of hexane, followed by β-hydrogen and β-methyl transfers onto the metal center and reductive elimination of methane. This also accounts for the loss of CH_4 from pentane-2,2,3,3,4,4-d_6 (insertion into the C2-C3 bond followed

by methyl [C1] and β-hydrogen [from C5] transfers) and CH_3D (and perhaps some CD_3H) from 2,2-dimethylpentane-5,5,5-d_3, Table IX. It is surprising that an iron ion, which makes a bond of 68 kcal/mol to one methyl radical (Table I), preferentially inserts into an internal rather than a terminal C-C bond which is only ~4 kcal/mol stronger[11,31]. It is possible that the second metal carbon bond is substantially weaker and accounts for this selectivity, or that the metal ion alkyl bond strength is larger for the larger alkyls. However, this does not account for the relatively large amount of methane lost in the reaction of Fe^+ with butane.

As noted above, smaller amounts of products which may occur through Schemes IV and V appear in the reactions of Co^+ ions as well, as exemplified by the loss of CH_4 and $C_3H_6D_2$ in the reaction with pentane-2,2,3,3,4,4-d_6. There are yet other products observed only in the Co^+ reactions, such as loss of $C_2H_3D_3$ from butane-1,1,1,4,4,4-d_6 and loss of $C_2H_4D_2$ and $C_3H_3D_5$ from pentane-2,2,3,3,4,4-d_6 which occur via other pathways. These products <u>decrease</u> in proportion to the Scheme IIc- and IIe-type products with increasing energy (also noted in Ref. 8). Their occurrence can be explained either by allowing for α-hydrogen transfers as in reaction 1, again considered unlikely for reasons discussed above, or as already mentioned, via a scrambling mechanism similar to Scheme III[8]. Studies of the hexane reactions were not done in such detail due to limited amounts of the compounds, so that scrambling products could not be examined with certainty.

Reactions of Metal Ions with Branched Alkanes

The product distributions for the reactions of the metal ions with the heptane isomers (Tables VIII and IX) display the expected influence of branching in the alkane, namely an increase in the loss of CH_4 from the intermediate complex[8,9]. This is due in part to the increased number of sites for methane loss, as well as the decrease in the terminal carbon-carbon bond energy.

The loss of alkane from the Ni^+-isoheptane complex consists essentially of propane and butane in comparable amounts (Table II). The results obtained with labeled samples, Table VIII, indicate that these two products are both formed from the same intermediate, 9, Scheme VI.

Scheme VI

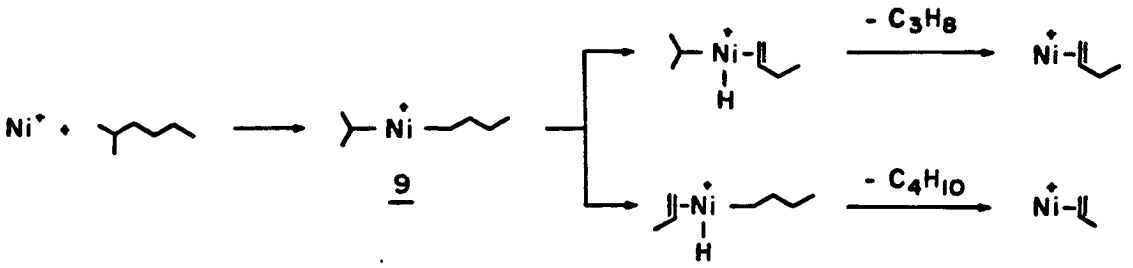

It thus appears that Scheme VII involving insertion into the C3-C4 bond is not contributing to the formation of these products. This suggests that

Scheme VII

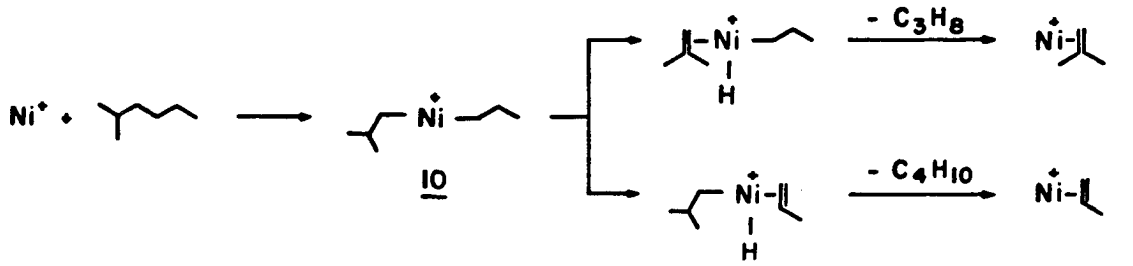

Table VIII. Distribution of Labeled Products in the Reactions of Ni^+ with ^{13}C-Labeled 2-Methylhexane and 2,2-Dimethylpentane[a]

	Neutral Products												
Alkane	CH_4	$^{13}CH_4$	C_2H_6	$^{13}CCH_6$	C_3H_8	$^{13}CC_2H_8$	$^{13}C_2CH_8$	C_4H_{10}	$^{13}CC_3H_{10}$	C_5H_{12}	$^{13}CC_4H_{12}$	$2CH_4$	$CH_4 + {}^{13}CH_4$
	1.0			1.0	1.0				1.0	1.0			
	1.0			1.0	1.0				1.0	1.0			
	1.0		1.0		1.0				1.0		1.0		
	b		b		1.0				1.0	b			
	1.0		b			1.0		1.0		b			
		1.0	1.0				1.0	1.0		b			
	1.0					1.0		1.0				.70	.30
	1.0					1.0		1.0				1.0	
	1.0					1.0		1.0				1.0	
	1.0				1.0				1.0			b	
	~.60	~.40			1.0				1.0			~.50	~.50

[a]Measured at ~0.6 eV relative kinetic energy.

[b]Distributions not measured (product peaks very small).

Table IX. Distribution of Labeled Products in the Reactions of Fe^+ and Ni^+ with 2,2-Dimethylpentane-5,5,5-d_3 [a]

	Neutral Products										
M^+	H_2	HD	CH_4	CH_3D	CD_3H	$C_3H_5D_3$	C_4H_{10}	$C_5H_{11}D$	$C_5H_9D_3$	$2CH_4$	$CH_4 + CHD_3$
Fe^+	.76	.24	.09	.27	.64	1.0	1.0	.44	.56	.43	.57
Ni^+	1.0		b			1.0	1.0			.64	.36

[a]Measured at ~0.6 eV relative kinetic energy.

[b]Distributions not measured (product peaks very small).

Ni^+ selectively inserts into the weakest carbon-carbon bond, resulting in the formation of intermediate 9 rather than 10[32]. The small amount of ethane loss (~1%), however, must occur from insertion into the internal C4-C5 bond.

The reaction of Ni^+ with the tertiary heptane isomer, 2,2-dimethylpentane, displays product distribution and label retention compatible with the formation of intermediate 11 which subsequently loses either

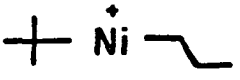

11

C_3H_8 or C_4H_{10} in accordance with Schemes IIc and IIe. In this case, no ethane is lost since there is no hydrogen in a β position to the metal following insertion into the C_3-C_4 bond.

The loss of methane from both heptane isomers reacting with Ni^+ occurs exclusively with a methyl group originating in the branched part of the alkane. This is in contrast to the behavior of Fe^+ (Scheme V), since no CH_3D is lost from the tertiary isomer. Instead, insertion into the branched methyl-carbon bond is favored, followed by a β-hydrogen transfer.

The loss of two molecules of methane occurs in the reactions of both Fe^+ and Ni^+ with 2,2-dimethylpentane. The second step of this process may be related to the mechanism by which loss of methane is thought to occur in the reaction of Co^+ with 2-methyl-2-butene[33]. This is illustrated in Scheme VIII for 2,2-dimethylpentane-5,5,5-d_3. The initial methane loss leads to formation of the internal olefin, 2-methyl-2-pentene. It can rearrange to give either the 2-methyl-3-pentene or 2,2-dimethyl-1-pentene isomer bound to the metal. The metal ion can then insert into the allylic

Scheme VIII

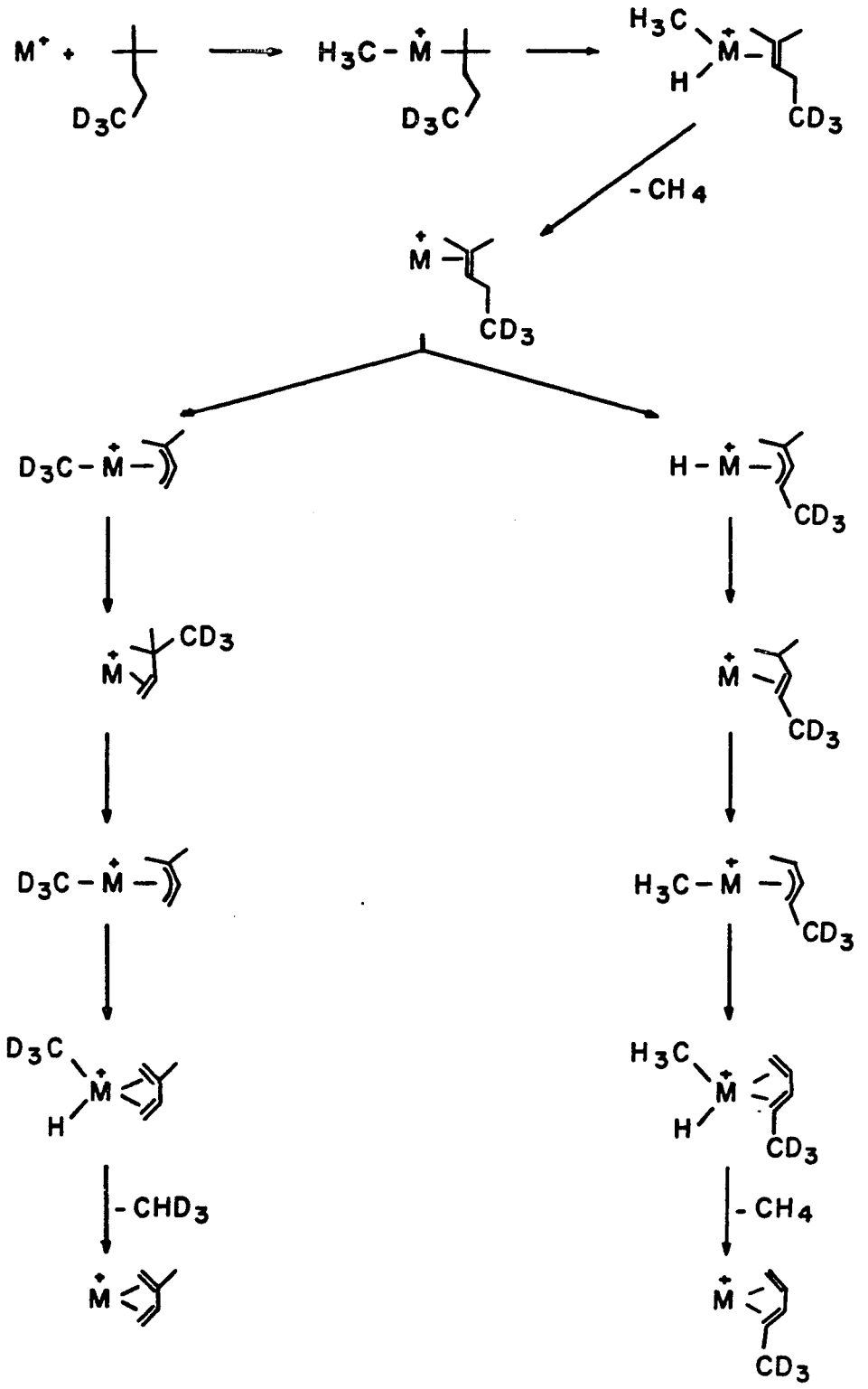
M+ +
D3C
H3C - M
D3C
H3C
H
M
CD3
- CH4
M
CD3
D3C - M
H - M
CD3
M
CD3
M
CD3
D3C - M
H3C - M
CD3
D3C
H
M
H3C
H
M
CD3
- CHD3
- CH4
M
M
CD3

C-C bond, abstract a β-hydrogen, and eliminate methane. This has been proposed to be the general mode of reaction in the interactions of Co^+ with alkenes[33].

One type of product not previously observed is the exothermic loss of ethylene, C_2H_4, in the reaction of Fe^+ with 2,2-dimethylpentane-5,5,5-d_3. This product is probably formed via insertion into the C2-C3 bond followed by β-methyl transfer to give structure 12. Loss of ethylene (~18% of the

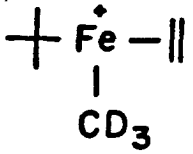

12

product distribution at 0.3 eV relative kinetic energy) is preferred over loss of $C_5H_9D_3$ (5% at 0.3 eV). This suggests that the activation energy for reductive elimination of the alkane is fairly high.

Reactions of Ni^+ with Cycloalkanes

Table X lists the product distributions for reactions of Ni^+ with several cycloalkanes. The reactions with cyclobutane, cyclopentane, and cyclohexane, both at low and high energies (high energy data are not presented[34]) are virtually identical[35] to the analogous reactions of Co^+ which were discussed in detail in a previous paper[29]. These data are presented here to compare to the reactions of Ni^+ with methylcyclopentane and methylcyclohexane which were studied using labeled compounds as well (Tables XI and XII). Table X indicates that dehydrogenation is a major process in reactions of Ni^+ with simple cycloalkanes, accounting for 40% to over 70% of the reaction. The major product in reactions

Table X. Product Distributions for Reactions of Ni^+ with Cyclic Alkanes Measured at 0.5 eV Relative Kinetic Energy

Alkane	Neutral Products (irrespective of label)						
	H_2	CH_4	C_2H_4	C_3H_6	C_4H_8	$2H_2$	CH_4+H_2
 [a]	.41		.48				
	.61		.30	.03		.05	
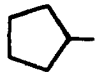	.20	.46	.01	.05		.03	.24
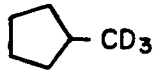	.33	.45		.04			.19
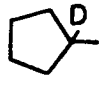	.18	.58		.04			.20
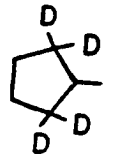	.22	.57	.01	.10			.11
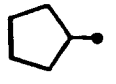	.24	.46	.01	.08			.21
	.76			.21		.03	
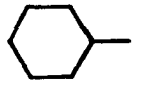	.18	.39		.10	.01	.01	.29
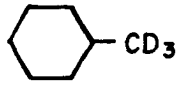	.26	.47		.06	.02		.19

[a] Also observed at this energy is an 11% loss of CH_3, see ref. 35.

Table XI. Product Distributions for Reactions of Ni^+ with Labeled Methylcyclopentanes and Cyclohexane (measured at ~0.6 eV relative kinetic energy)[a]

Alkane	Neutral Products													
	H_2	HD	CH_4	CH_3D	CHD_3	C_3H_6	C_3H_5D	$C_3H_4D_2$	$C_3H_3D_3$	$C_4H_5D_3$	CH_4 + H_2	CH_4+HD, CH_3D+H_2	CH_3D_3 +HD	CHD_3 +H_2
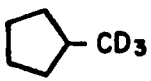	.70	.30			1.0	.30	?		.70					1.0
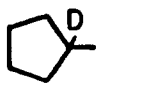		1.0	1.0			.50	.50				1.0			
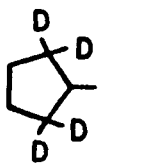	.60	.40		1.0				1.0				X	X	
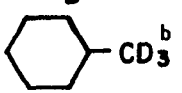 [b]	mostly				1.0	mostly	X	X	X	mostly				1.0

[a] X's are entered when it is difficult to separate mass peaks to determine product ratios.

[b] Spectrum seemed to show lingering amounts of previous sample.

Table XII. Product Distribution for the Reaction of Ni^+ with ^{13}C Labeled Cyclopentanone (measured at 0.55 eV relative kinetic energy)

	Neutral Products				
Alkane	H_2	$^{13}CH_4$	C_3H_6	$^{13}CC_2H_6$	$^{13}CH_4 + H_2$
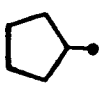	1.0	1.0	.50	.50	1.0

with the methylcycloalkanes is loss of methane, and methane in combination with hydrogen. This pattern of reactivity suggests that methane is eliminated as a first step in the reactions of the methylcycloalkanes, followed by dehydrogentation.

Some mechanistic details can be elucidated with the aid of data given in Tables XI and XII for reaction of Ni^+ with labeled methylcyclopentane and methylcyclohexane. Dehydrogenation appears to always involve the tertiary hydrogen as indicated by the methylcyclopentane-1-d_1 results in which only HD loss is observed. This process probably proceeds via insertion into the weak tertiary C-H (or C-D)bond, followed by a β-hydrogen transfer to the metal, most often the secondary β-hydrogen, Scheme IX. Loss of methane always involves the exocyclic carbon.

Scheme IX

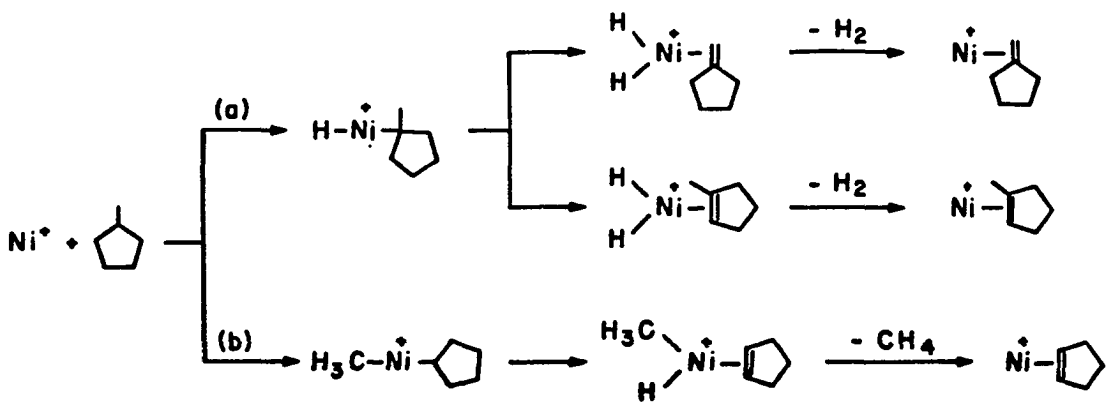

The small amounts of cleavage products make verification of the pathways leading to these products (including the possibility of scrambling) difficult.

Nickel ions dehydrogenate 2-methylpropane-2d_1, presumably in a process analogous to Scheme IX, producing only loss of HD by a

1,2 elimination process. It was argued above that dehydrogenation by Ni^+ of linear alkanes larger than propane occurs via a 1,4 elimination in which the first step is insertion into a C-C rather than C-H bond. Insertion into a C-H bond in the case of 2-methylpropane and methylcyclopentane may be favored due to a low tertiary C-H bond strength. Unfortunately, these results yield no information on the mechanism of dehydrogenation of simple cycloalkanes, which may proceed in a similar pathway as depicted in Scheme IX, or occur via a 1,4 process such as in Scheme X.

Scheme X

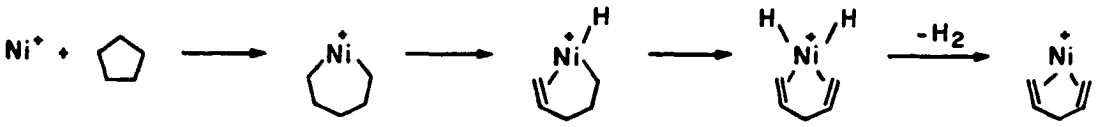

In contrast to the reactions of Co^+ and Ni^+ with cycloalkanes, loss of alkenes is not a prominent pathway in the reactions of Fe^+ with cyclopentane and cyclohexane[6,36]. Single and multiple dehydrogenation account for greater than 95% of product distribution at low energies in these reactions[6,34]. This may be due to a greater facility of Fe^+ to insert into C-H bonds resulting from a greater bond strength to hydrogen atoms (see Table I).

Isotope Effects

Deuterium or ^{13}C labeling of the alkanes does not appear to greatly

alter the distribution of products, as shown in Tables II and X[37]. Because of the small fractional mass difference between a ^{13}C and ^{12}C nucleus, any isotope effect caused by this labeling is expected to be small. None can be inferred from the present data. Deuterium substitution might lead to observable isotope effects in at least three different processes. These include (1) insertion of the metal into C-H bonds, (2) transfer of β-hydrogen to the metal center, and (3) the rate of reductive elimination of alkanes from metal hydrido-alkyl intermediates. Since the observed reaction processes are formulated as multistep sequences, it is difficult to establish isotope effects for individual steps, especially when different reaction pathways operate competitively. In the first instance the data for dehydrogenation of propane-2-d_1 by Ni^+ suggest no isotope effect on the relative probabilities of insertion into otherwise equivalent C-H and C-D bonds[37,38]. This assumes, however, that insertion into the secondary C-H bond initiates the dehydrogenation process. In the reaction of Ni^+ with butane-1,1,1,4,4,4-d_6, the decomposition of 13 involves reductive

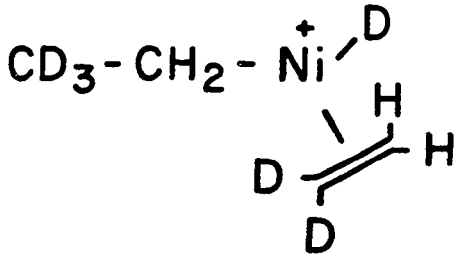

13

elimination of CD_3CH_2D occurring in competition with a β-D transfer. In 4-center rearrangements of chemically activated species, transfer of a β-H can be favored over a β-D transfer by a factor ranging from 2 (at high levels of excitation) to 6 or more (near threshold), depending on the excess internal energy[39]. The loss of ethane from $CD_3CH_2CH_3CD_3$ in the reaction with Ni^+ is somewhat more prominent than from unlabeled butane (Table II). In light of the previous discussion this appears reasonable, provided that the isotope effect associated with reductive elimination of CH_3CH_2D vs. CH_3CH_3 (in the case of unlabeled butane) from intermediate 13 is smaller than that for β-D vs. β-H transfer. Halpern and coworkers have reported a comparison of the rates of reductive elimination of methane from $[PtH(CH_3)(PPh_3)_2]$ and $[PtD(CH_3)(PPh_3)_2]$ which reveals a primary isotope effect of k^H/k^D = 3.3 ± 0.3[40]. This suggests that a marked isotope effect should be apparent in the loss of CH_3CH_2D vs. CH_3CD_3 in the reaction of Ni^+ with butane-1,1,1-d_3 since the former involves both a β-D transfer and rupture of the Ni^+-D bond of $[(CH_2CD_2)NiD(C_2H_5)]^+$. Unfortunately, the labeled precursor which would confirm this conjecture was not readily available to us. This discussion makes it clear, however, that it is difficult to assign isotope effects on product distributions (Tables II and X) to isotope effects in individual reaction steps.

Conclusion

The specific goal of the present study was to understand the mechanistic details by which hydrocarbons are cleaved to first row group 8 metal ions. Despite the apparent similarity of the reactions

with alkanes, somewhat different pathways are significant for the three ions. This can in part be attributed to differences in reaction thermochemistry. For example, nickel ions dehydrogenate linear alkanes with a chain of four or more carbons via a 1,4 elimination process which has as its first step insertion into a C-C rather than C-H bond, Scheme IIf[7,10]. This pathway is apparently favored due to the low nickel ion-hydrogen bond strength as discussed above (Table I). Iron and cobalt ions make stronger first bonds to hydrogen, and undergo a mixture of both 1,2 and 1,4 dehydrogenation processes. In the alkane elimination reactions, β-methyl transfers seem to play an important role in the reactions of Fe^+ with alkanes, and to a lesser extent in Co^+ reactions. This may be due to a higher Fe^+-methyl bond energy of the intermediates (such as 5 or 7). The appearance of β-methyl transfer products at higher energies in the reactions of Co^+ and Ni^+ lends support to this assumption. It is not clear why all of the loss of methane in the reaction of Fe^+ with hexane appears to occur via combined β-methyl and β-hydrogen transfer processes (Scheme V), while ~20% of the loss of methane in reaction with pentane is via a pathway analogous to Scheme IIc. Scrambling of the intermediates in the reactions of deuterated alkanes with Co^+ (and to a lesser extent with Fe^+) is a significant process at low energies[8]. No scrambling is observed in reactions of Ni^+ with these alkanes.

Differences in reactivity among the three metal ions are also noted with the cycloalkanes. While a substantial amount of ring cleavage products (loss of alkene) occurs in the interaction of Co^+[29] and Ni^+ with cyclopentane and cyclohexane, multiple dehydrogenation accounts for almost all of the products seen in the analogous reactions of Fe^+[6,34,36].

Marked bond insertion selectivity is also noted in these reactions[32]. For example, little insertion into terminal C-C bonds is observed even in the reactions of Fe^+, which has a high first bond energy to a methyl radical. This suggests that perhaps the second metal-ion ligand bond is weak enough to account for this selectivity, or that bonds to larger alkyl fragments are much greater than to methyl groups, or a combination of both effects.

The present studies reveal that group 8 metal ions react with ^{13}C and deuterium-substituted alkanes to give highly specific label retention in the products. This is in contrast to ion-molecule reactions of organic species, which can lead to totally scrambled products[41]. This suggests the use of these gas-phase metal ion reactions as a tool to determine the original label distribution in a molecule. For example, by looking at the product ratio for loss of methane to loss of ethane from butane in the reaction with nickel ions, the amount of ^{13}C at interior versus exterior positions can be determined. Because mass spectrometry is used to detect the products, this technique could be quite useful for identifying isotopically labeled reactants when only small amounts of the compound are available.

Acknowledgment

We wish to thank Dr. Peter Armentrout for helpful discussions about this paper. This research was supported in part by the U.S. Department of Energy. Graduate fellowship support from Bell Laboratories and SOHIO (L.F.H.) is gratefully acknowledged.

References

1. On leave from École Polytechnique Fédérale, CH 1007 Lausanne, Switzerland.
2. (a) Parshall, G. W. Catalysis 1977, 1, 335.
   (b) Crabtree, R. H.; Mellea, M. F.; Mihelcic, J. M.; Quirk, J. M. J. Am. Chem. Soc. 1982, 104, 107.
   (c) Janowicz, A. H.; Bergman, R. G. Ibid. 1982, 104, 352.
3. Müller, J.; Goll, W. Chem. Ber. 1973, 106, 1129.
4. (a) Allison, J.; Freas, R. B.; Ridge, D. P. J. Am. Chem. Soc. 1979, 101, 1332.
   (b) Freas, R. B.; Ridge, D. P. Ibid. 1980, 102, 7129.
5. (a) Uppal, J. S.; Johnson, D. E.; Staley, R. H. J. Am. Chem. Soc. 1981, 103, 508.
   (b) Jones, R. W.; Staley, R. H. J. Phys. Chem. 1982, 86, 1387.
   (c) Kappes, M. M.; Staley, R. H. J. Am. Chem. Soc., submitted.
6. Byrd, G. D.; Burnier, R. C.; Freiser, B. S. J. Am. Chem. Soc. 1982, 104, 3565.
7. Jacobson, D. B.; Freiser, B. S. J. Am. Chem. Soc., submitted for publication.
8. Armentrout, P. B.; Beauchamp, J. L. J. Am. Chem. Soc. 1981, 103, 784.
9. Halle, L. F.; Armentrout, P. B.; Beauchamp, J. L. Organomet. 1982, 1, 963.
10. Halle, L. F.; Houriet, R.; Kappes, M. M.; Staley, R. H.; Beauchamp, J. L. J. Am. Chem. Soc. 1982, 104, 6293.

11. Supplementary heats of formation of hydrocarbons are taken from: Cox, J. D.; Pilcher, G. "Thermochemistry of Organic and Organometallic Compounds"; Academic Press: New York, 1970.

12. It has been estimated that the activation energy for reductive elimination of cyclohexane from $(C_5Me_5)(Me_3P)Ir(H)(C_6H_{11})$ is approximately 30 kcal/mol, and that the activation barrier for the reverse process is small in comparison (Bergman, R. G., private communication). This implies that the sum of the iridium carbon and hydrogen bonds is ~125 kcal/mole (using $D(c\text{-}C_6H_{11}\text{-}H) = 95.5 \pm 1$ kcal/mol from McMillen, D. F.; Golden, D. M.: Ann. Rev. Phys. Chem. 1982, 33, 493). This value is not inconsistent with known thermochemical data. A bond energy of 49 ± 11 kcal/mol has been measured for $D(Ir\text{-}C(O)CH_3)$[13], and bond strengths of 65-70 kcal/mol for metal hydrogen bonds are not unreasonable[14].

13. Yoneda, G.; Lin, S.-M.; Wang, L.-P.; Blake, D. M. J. Am. Chem. Soc. 1981, 103, 5768.

14. See Stevens, A. E.; Beauchamp, J. L. J. Am. Chem. Soc. 1982, 103, 190, for estimates of metal-hydrogen bond energies in protonated transition metal complexes.

15. (a) Dias, A. R.; Salema, M. S.; Martinho Simões, J. A. J. Organomet. Chem. 1981, 222, 69.

    (b) Tel'noi, V. I.; Rabinovich, I. B. Russian Chem. Rev. 1977, 46, 689.

16. Armentrout, P. B.; Halle, L. F.; Beauchamp, J. L. J. Am. Chem. Soc. 1981, 103, 6501.

17. Burnier, R. C.; Byrd, G. D.; Freiser, B. S. J. Am. Chem. Soc. 1981 103, 4360.

18. Halle, L. F.; Crowe, W.; Armentrout, P. B.; Beauchamp, J. L., to be submitted for publication.

19. McMillen, D. F.; Golden, D. M.; Ann. Rev. Phys. Chem. 1982, 33, 493. $\Delta H_f(CH_3)$ = 35.1 ± 0.15 kcal/mol.

20. Armentrout, P. B.; Halle, L. F.; Beauchamp, J. L. J. Am. Chem. Soc. 1981, 103, 6624.

21. Jacobson, D. B.; Freiser, B. S.; J. Am. Chem. Soc., in press.

22. Note that this is also true for the reaction of Ni^+ with 2-methylpropane-2-d_1, see Table III.

23. Shilov, A. E.; Shteinman, A. A. Coord. Chem. Rev. 1977, 24, 97.

24. We are very grateful to Professor Tino Gaumann for providing us with samples of labeled alkanes.

25. Dehydrogenation of an alkane resulting in formation of two olefins requires ~20-30 kcal/mol more energy than dehydrogenation forming one olefin, for example, $C_4H_{10} \rightarrow 2C_2H_4 + H_2$ (ΔH = 55 kcal/mol) vs. $C_4H_{10} \rightarrow C_4H_8 + H_2$ (ΔH = 27 kcal/mol)[11]. The extra metal-olefin bond more than compensates for the extra energy required.

26. Loss of butane from hexane involving carbon atoms in the 1,2,3, and 6 positions versus the 1,2,4, and 6 positions could not be distinguished with the labeled compounds we had, but the latter case seems unlikely.

27. See, for example, Watson, P. L.; Roe, D. C. J. Am. Chem. Soc. 1982, 104, 6471.

28. For examples of metallacycles in solution phase studies see: Grubbs, R. H. Prog. Inorg. Chem. 1978, 24, 1 or Stone, F. G. A. Pure Appl. Chem. 1972, 30, 551.

29. Armentrout, P. B.; Beauchamp, J. L. J. Am. Chem. Soc. 1981, 103, 6628.

30. The dehydrogenation of 2,2,4,4-tetramethylbutane can also be explained by a 1,4 elimination mechanism similar to Scheme IIf. Namely, the metal ion inserts into the central C-C bond followed by a β-H tranfer from both ends and loss of H_2 off the metal center.

31. $\Delta H_f(n\text{-}C_5H_9\cdot)$ was calculated by assuming $D(n\text{-}C_5H_9\text{-}H) = D(n\text{-}C_3H_7\text{-}H)$. $D(n\text{-}C_3H_7\text{-}H) = 97.9 \pm 1$ kcal/mol, and $\Delta H_f(CH_3)$ from ref. 19.

32. The selectivity of Fe^+, Co^+ and Ni^+ in inserting into C-C bonds has been discussed previously in the literature[7-9]. Note that in determining the proportion of insertion of Fe^+ into terminal C-C bonds, these references do not account for β-methyl transfers (Schemes IId, IV and V).

33. Armentrout, P. B.; Halle, L. F.; Beauchamp, J. L. J. Am. Chem. Soc. 1981, 103, 6624.

34. Halle, L. F.; Beauchamp, J. L., unpublished results.

35. In the reaction of Ni^+ with cyclobutane, loss of CH_3 to yield a $Ni(C_3H_5)^+$ ion accounts for 11% of the product distribution with a cross section of 4Å^2 at ~0.5 eV relative kinetic energy. As an exothermic process, the formation of this product implies that $D(Ni^+\text{-}C_3H_5) > 67$ kcal/mol ($\Delta H_f(C_3H_5\cdot) = 39.1$ kcal/mol from Rossi, M.; King, K. D.; Golden, D. M. J. Am. Chem. Soc. 1980, 101, 1223)[11,19]. $Co(C_3H_5)^+$ accounts for less than 1% in the analogous reaction of Co^+ at the same energy and appears as an endothermic product. $Fe(C_3H_5)^+$ is not observed in the reaction of Fe^+ with cyclobutane[34].

36. In the reaction of Fe^+ with cyclobutane, $Fe(C_2H_4)^+$ accounts for ~85% of the product distributions at energies from 0.5 eV to 1.0 eV relative kinetic energy[34].

37. A similar branching ratio was observed for products of the reaction of Fe^+ with 2-methylpropane and 2-methylpropane-d_{10} studies using an ion cyclotron resonance spectrometer[4a].

38. It is strange that no loss of D_2 is observed in the reaction of Fe^+ or Co^+ with hexane-3,3,4,4-d_4, a product expected via a 1,2 dehydrogenation process. (Less than 5% would go undetected.)

39. Bomse, D. S.; Woodin, R. L.; Beauchamp, J. L. J. Am. Chem. Soc. 1979, 101, 5503.

40. Abis, L.; Sen, A.; Halpern, J. J. Am. Chem. Soc. 1978, 100, 2915.

41. Franklin, J. L., "Ion Molecule Reactions," Vol. 1; Franklin, J. L., ed., Plenum Press: New York, 1972.

CHAPTER III

REACTIONS OF ATOMIC COBALT IONS WITH ALDEHYDES AND KETONES. OBSERVATION OF DECARBONYLATION PROCESSES LEADING TO FORMATION OF METAL ALKYLS AND METALLACYCLES IN THE GAS PHASE.

REACTIONS OF ATOMIC COBALT IONS WITH ALDEHYDES AND KETONES. OBSERVATION OF DECARBONYLATION PROCESSES LEADING TO FORMATION OF METAL ALKYLS AND METALLACYCLES IN THE GAS PHASE

L. F. Halle, W. E. Crowe[1a], P. B. Armentrout[1b], and J. L. Beauchamp

Contribution No. 6812 from the Arthur Amos Noyes Laboratory of Chemical Physics, California Institute of Technology, Pasadena, California 91125.

Abstract

An ion beam apparatus is used to study the reactions of singly charged cobalt positive ions with several aldehydes and ketones as a function of relative kinetic energy. Deuterium labeling is used to provide mechanistic information. Decarbonylation yielding $CoCO^+$ is the dominant process in the reactions of Co^+ with formaldehyde, acetaldehyde, and acetone at low energies. At ~0.5 eV relative kinetic energy cross sections for formation of $CoCO^+$ from these neutrals are 0.25, 29, and 80 $Å^2$, respectively, indicating that formaldehyde is much less reactive than the alkyl-substituted species. An ion corresponding to $Co(CH_3)_2^+$ is formed as an exothermic product in the reaction of Co^+ with acetone. The analogous product is also observed in the reactions of Fe^+ and Ni^+ with acetone. This indicates that the sum of the first two methyl bond energies to first row group 8 metal ions is greater than 96 kcal/mol, which supports the conclusion of earlier studies that metal ion insertion into unactivated carbon-carbon bonds of saturated hydrocarbons is an exothermic process.

As the alkyl chains of the dialkyl ketones are extended, loss of alkene and aldehyde dominate the product distributions at low energies. If one of the alkyl groups is highly branched, the major product is due to loss of methane. Decarbonylation of cyclopentanone yields $Co(C_4H_8)^+$, suggested to be a metallacycle, and its subsequent dehydrogenation product $Co(C_4H_6)^+$ as the major species formed in exothermic processes at low relative kinetic energies.

Analysis of products formed at high relative kinetic energies are used in conjunction with thermochemical estimates to infer mechanistic

details and construct qualitative reaction coordinate diagrams for the interaction of metal ions with carbonyl compounds. Some interesting conclusions can be reached from an inspection of these diagrams. For example, reaction of coordinatively unsaturated metal dialkyls and hydrido alkyls with carbon monoxide will lead to the reductive elimination of alkanes rather than formation of ketones and aldehydes. The results of this work are compared to earlier ion cyclotron resonance studies of related reactions at thermal energies.

Introduction

Studies in our laboratory have provided detailed insights into the mechanism and energetics of reactions of atomic transition metal ions with hydrocarbons[2-6]. These studies have utilized a specially designed ion beam apparatus which permits the relative kinetic energy to be varied over a wide range, making it possible to characterize not only exothermic reactions but endothermic and "high energy" processes as well. Ancillary information is provided by ion cyclotron resonance (ICR) studies[6]. In the present work we employ these experimental methods to examine the reactions of first row group 8 atomic transition metal ions, mainly Co^+, with organic molecules containing the carbonyl group as a structural moiety.

There have been several recent studies of the gas phase reactions of metal ions with aldehydes and ketones[7-12]. Corderman and Beauchamp[7] first reported ICR studies of the decarbonylation (e.g., reaction 1)

$$CpNi^+ + CH_3CHO \rightarrow CpNi(CO)^+ + CH_4 \qquad (1)$$

by $CpNi^+$ ($Cp \equiv \eta^5\text{-}C_5H_5$). Interestingly, this species was unreactive with acetone and formaldehyde. Using ICR techniques, Freiser and coworkers have examined the reactions of Cu^+ and Fe^+ with ketones[8,9]. While copper ions either dehydrate ketones or cleave them into an enol (or ketone) and alkene, Fe^+ exhibits a richer variety of reactions[9]. These include dehydrogenation and decarbonylation processes, along with generation of alkenes, alkanes, and smaller ketones. Kappes and Staley[11], as well as Ridge[12] and coworkers have also examined reactions of atomic transition ions with a range of cyclic and acyclic ketones.

In the present paper we report detailed studies of the reactions of Co^+ with acetone, acetaldehyde and formaldehyde, using the variable kinetic energy in the ion beam experiment as an important parameter to probe the mechanism and energetics of processes analogous to reaction 1. Less extensive results are presented for more complex cyclic and acyclic ketones. Deuterium labeling is employed to provide additional mechanistic information.

Experimental

The ion beam apparatus and experimental techniques have been described in detail[2]. Briefly, singly charged cobalt ions are formed by thermal dissociation and surface ionization of $CoCl_2 \cdot 6H_2O$ on a heated rhenium ribbon. The metal ions are mass selected and decelerated to the desired energy before entering a collision chamber containing the reactant gas. Product ions scattered in the forward direction are focused into a quadrupole mass filter and detected by using a channeltron electron multiplier operated in a pulse-counting mode.

All unlabeled samples were commerically available. Deuterated acetone was obtained from Stohler Isotope Chemicals (99.5 atom % D). Labeled 2-butanone and 3-pentanone were obtained by repetitive exchange with D_2O (99.8 atom % D) in the presence of small amounts of NaOD[13]. The ketones were separated from the aqueous phase by ether extractions which were dried with anhydrous $MgSO_4$. The ether was distilled off, with a final separation made by gas chromotography. Mass spectrometric analysis indicated preparation of 2-butanone-α,α'-d_5 with 98.0 atom % D and 3-pentanone-α,α'-d_4 with 97.5 atom % D. NMR analysis performed for

the 3-pentanone confirmed selective deuteration at the α-position. Cyclopentanone-α,α'-d_4 was prepared by adding 25 ml of D_2O and 2 drops of NaOD to 1 ml of cyclopentanone. The mixture was stirred under reflux at 70^0 C for 24 hours. As with the ketones described above, cyclopentanone was extracted with ether and dried over $MgSO_4$. The ether was distilled off with a final separation by GC. Mass spectrometric analysis indicated labeling to an extent of 96 atom % D.

Reaction cross sections for specific products, σ_i, are obtained by using equations 2 and 3, which relate the total cross-section, σ, the

$$\sigma = \frac{1}{n_o l} \ln [(I_o + \sum I_i)/I_o)] \quad (2)$$

$$\sigma_i = \sigma I_i / \sum I_i \quad (3)$$

number density of the target gas, n_o, and the length of the collision chamber, l (5 mm), to the transmitted reactant ion beam intensity, I_o, and the sum of the product ion intensities, $\sum I_i$. Except as noted, the pressure of the target gas, measured by using an MKS Baratron Model 90H1 capacitance manometer, is kept low, usually $<1 \times 10^{-3}$ torr. It has been previously noted that cross sections for reactions with heavier hydrocarbons were not accurately reproducible[2], presumably due to substantial loss of elastically scattered Co^+ from the reactant beam. Branching ratios were found to be reproducible, and the results for the larger ketones are reported in this manner.

Results and Discussion

The product distributions for the reactions of cobalt ions with several aldehydes and ketones are listed in Tables I through IV. We consider first the series $(CH_3)_2CO$, CH_3CHO, and H_2CO, where methyl groups are sequentially replaced with hydrogen atoms.

Acetone. Data for the reaction of Co^+ with acetone are shown in Figure 1. Cross sections for processes 4 and 5 are large at low energies

$$Co^+ + CH_3COCH_3 \xrightarrow{90\%} Co(CO)^+ + C_3H_6 \quad (4)$$

$$Co^+ + CH_3COCH_3 \xrightarrow{10\%} Co(CH_3)_2^+ + CO \quad (5)$$

and decrease with increasing energy, indicating that both reactions are exothermic. The identities of these products were checked using CD_3COCD_3.

Also seen at low energies is the Co^+—acetone adduct, with the diadduct appearing at higher pressures. A log-log plot of $\sigma_i p$ (equation 2) versus p, where p is the pressure of the target gas, is shown in Figure 2 for the major products at a relative kinetic energy of 1 eV. The slopes of the lines for $Co(CO)^+$ and $Co(CH_3)_2^+$ are 0.99 and 1.18, respectively, which are close to the value expected for a purely bimolecular process (i.e., the cross sections for production of these species are independent of pressure). The slope for the cobalt ion acetone adduct in Figure 2 is 1.86, indicating a termolecular process. This product may result either from collisional stabilization of the reaction intermediate in processes 4 and 5 or by further reaction of the products of these reactions with acetone (ligand displacement processes). Although the data are limited, the slope for the diadduct

Table I. Product Distributions for Reactions of M^+ with Aldehydes and Ketones

Neutral Reactant	M^+	Neutral Products (irrespective of label)[a,b]													
		CO	H_2	CH_4	C_2H_6	C_3H_8	C_4H_{10}	C_2H_4	C_4H_8	C_2H_4O	$H_2+C_2H_4O$	C_3H_6O	$H_2+C_3H_6O$		MH
H_2CO	Co^+		1.0												
CH_3CHO	Co^+			1.0											
	Fe^+			1.0											
$(CH_3)_2CO$	Co^+	.10			.90										
	Ni^+	.12			.88										
$-\alpha,\alpha'-d_6$	Co^+	.10			.90										
	Fe^+	.07			.93										
	Ni^+	.06			.94										
$C_2H_5\overset{O}{\overset{\|}{C}}CH_3$	Co^+		.07	.18		.10		.49		.15					
$-\alpha,\alpha'-d_5$	Co^{+c}		tr	.19		.08		.61		.12					
	Fe^+		.30	.15		.10		.38		.07					
$(C_2H_5)_2CO$	Co^+		.05		.08		.04	.70				.12			
	Fe^{+d}		.29		.15[d]			.26[d]				.15[d]			
$-\alpha,\alpha'-d_4$	Co^+		.04		.04		.03	.74				.10			
$(CH_3)_3C-\overset{O}{\overset{\|}{C}}CH_3$	Co^+			.88					.01	.07	.01				.04
	Fe^+			1.0											
$(CH_3)_3C-CH_2\overset{O}{\overset{\|}{C}}CH_3$	Co^+			.76					.06	.13		.03	.02[e]		.02[e]

a) The data from the reactions of labeled compounds were used to determine product ratios for the unlabeled reactants when two products coincided at the same mass. See text for discussion of structure of the neutral products.

Table I. Continued

b) The data for Fe^+ are taken from ICR studies of Reference 9. All other product distributions listed are from ion beam reactions measured at ~0.5 eV relative kinetic energy.

c) The d) Because the reaction of Fe^+ with 3-pentanone-α,α'-d_4 was not performed, one cannot distinguish between loss of acc(C_2H_6 and H_2CO, C_2H_4 and CO, and between loss of C_3H_6O and C_4H_{10}. The sum of this product distribution from Reference 2 adds up to ~85% of the total reaction.

d) Because the reaction of Fe^+ with 3-pentanone-α,α'-d_4 was not performed, one cannot distinguish between loss of C_2H_6 and H_2CO, C_2H_4 and CO, and between loss of C_3H_6O and C_4H_{10}. The sum of this product distribution from Reference 2 adds up to ~85% of the total reaction.

e) These products have the same mass and cannot be distinguished from each other in this reaction.

Table II. Product Distributions for the Reactions of M^+ with Cyclopentanone

Neutral Reactant	M^+	Neutral Products (irrespective of label) CO[a]	H_2	C_4H_8[b]	H_2+CO[c]	CO+C_2H_4
Cyclopentanone	Co^{+}[d,e]	.44		.02	.52	.02
	Fe^{+}[f]	.30	.11	.10	.49	
	Co^{+}[f,g]	.08	.05	.05	.82	
	Ni^{+}[f]	.39		.13	.48	
	Ni^{+}[h]	.50		.17	.33	
-α,α'-d_4	Co^{+}[d]	.50		.02	.46	.02

a) See Reference 39.

b) This product cannot be distinguished from loss of CO + C_2H_4. (With the labeled compound, a peak at 87 amu appeared, attributed to loss of $C_4H_4D_4$ in this table, but it could be due to loss of CO + C_2D_4.)

c) The neutral product may be H_2CO.

d) Product distributions measured at 0.6 eV relative kinetic energy using the ion beam apparatus.

e) Data from reactions of the labeled compound were used to determine branching ratios in the reactions with the unlabeled reactants when two products coincided at the same mass. See footnote b of this table.

f) Data taken from ICR studies of Reference 10.

g) See Reference 40.

h) Data taken from ICR studies of Reference 6.

Table III. Distribution of Labeled Products in the Reactions of M^+ with Labeled Ketones[a,b]

		HD	CH_3D	CHD_3	$C_2H_4D_2$	C_3HD_5	$C_4H_6D_4$	C_2H_3D	$C_2H_2D_2$	C_2HD_3O	C_2D_4O	$C_3H_4D_2O$	$C_3H_3D_3O$
2-butanone-α,α'-d_5	Co^+	1.0	?	1.0		1.0		.19	.81	.79	.21		
	Fe^+	1.0		1.0		1.0			1.0	1.0			
3-pentanone-α,α'-d_4	Co^+	1.0			1.0		1.0	.12	.88			.86	.14

a) Distributions for Co^+ reactions measured in ion beam at ~0.5 eV relative kinetic energy. Data for Fe^+ taken from ICR studies of Reference 9.

b) See text for discussion of structure of the neutral products.

Table IV. Distribution of Label for Reaction of Co^+ with Cyclopentanone-α,α'-d_4 to Yield $Co[C_4(H,D)_6]^+ + (H,D)_2 + CO$ [a]

Isotopic Hydrogen Product	Fractional Distribution
H_2	.48
HD	.35
D_2	.17

a) Measured at 0.6 eV relative kinetic energy.

Figure 1. Variation in reaction cross section for the interaction of Co^+ with acetone as a function of kinetic energy in the center of mass frame (lower scale) and laboratory frame (upper scale).

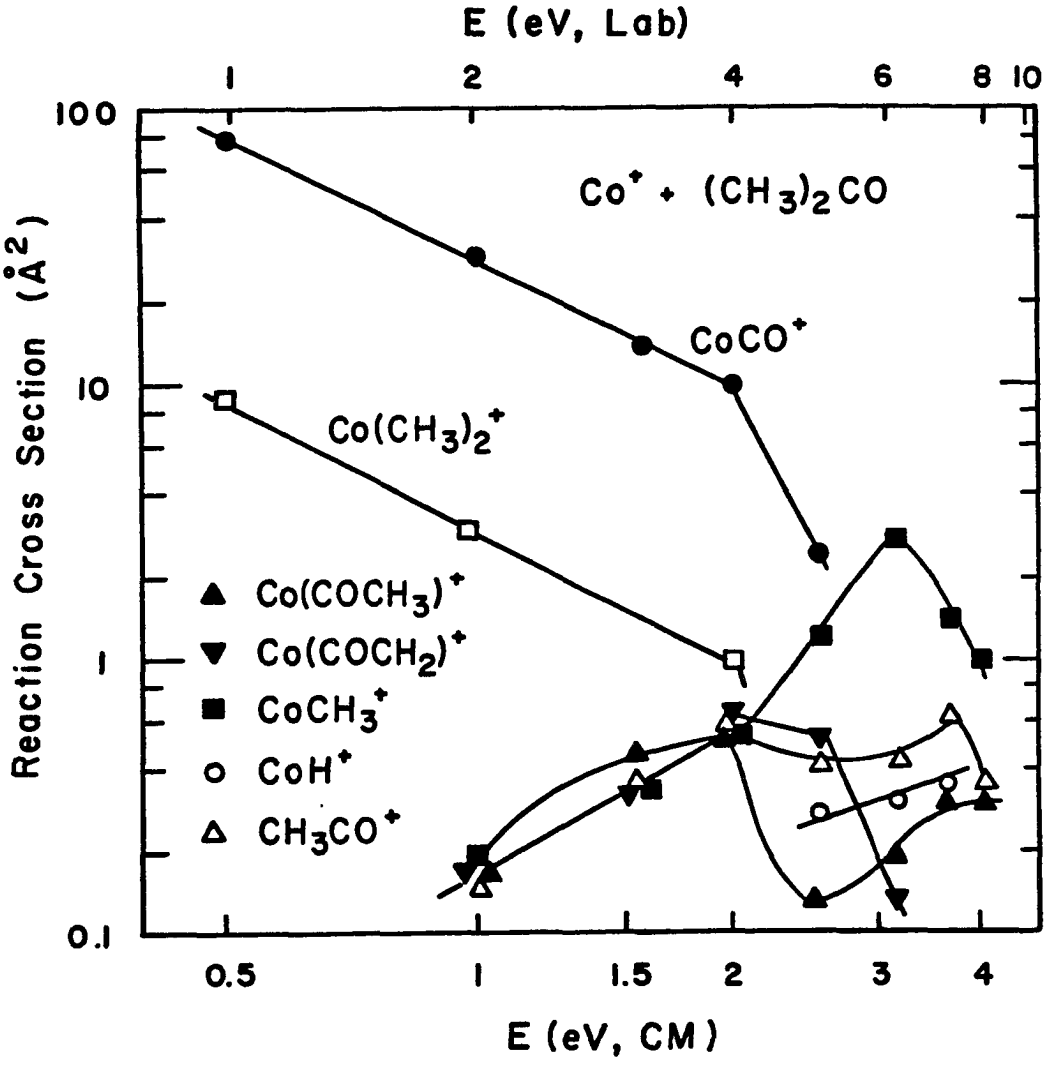
E (eV, Lab)
1
2
4
6
8
10
100
10
1
0.1
Reaction Cross Section (Å²)
Co⁺ + (CH₃)₂CO
CoCO⁺
Co(CH₃)₂⁺
Co(COCH₃)⁺
Co(COCH₂)⁺
CoCH₃⁺
CoH⁺
CH₃CO⁺
0.5
1
1.5
2
3
4
E (eV, CM)

Figure 2. Plot of the product of the reaction cross section and pressure, $\sigma_i p$, vs. pressure for the major products of the reaction of Co^+ with acetone at 1 eV relative kinetic energy. The slopes of the lines drawn are 0.99 [$CoCO^+$], 1.18 [$Co(CH_3)_2^+$], 1.86 [$Co(C_3H_6O^+$], and 6.73 [$Co(C_3H_6O)_2^+$].

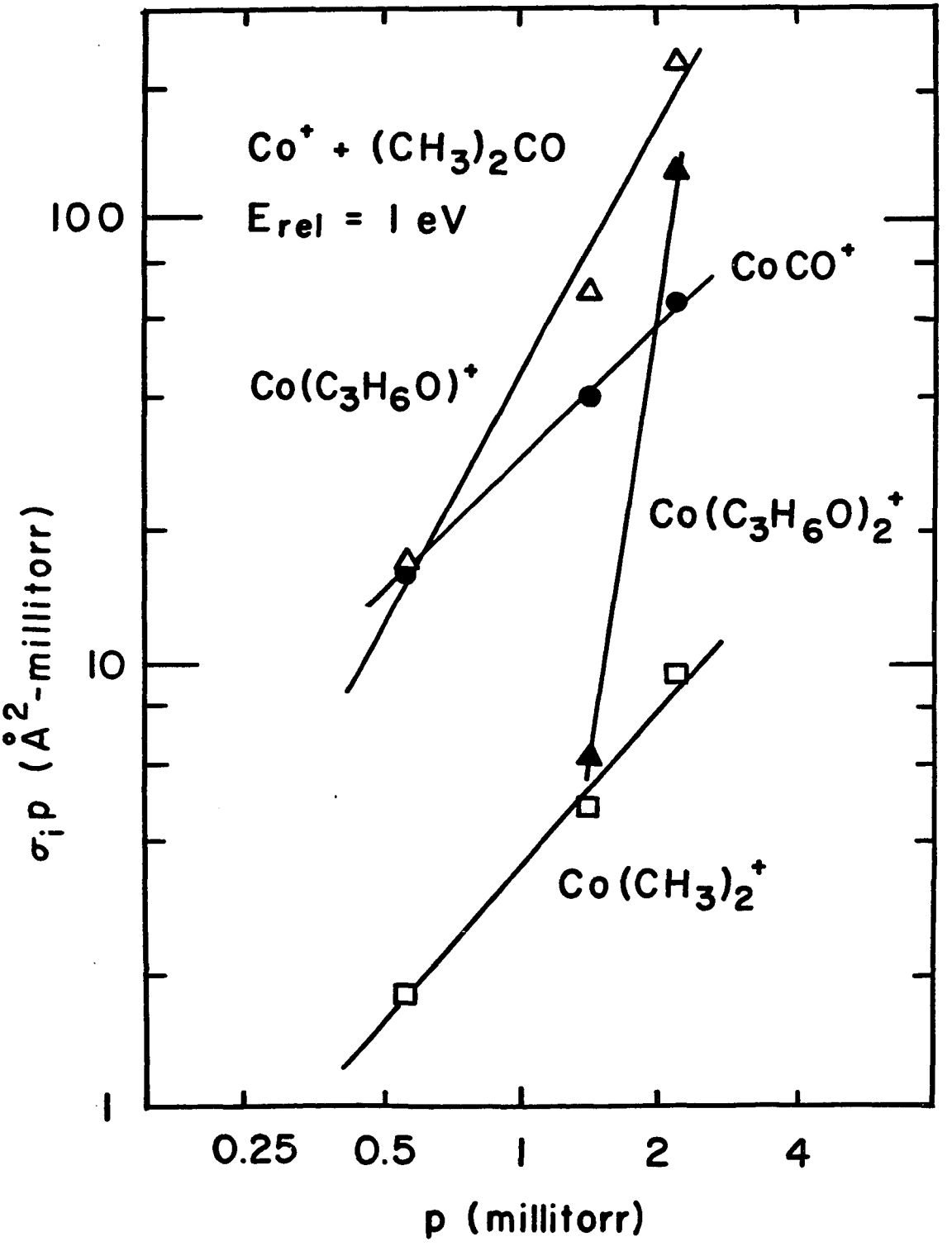
Co+ + (CH3)2CO
Erel = 1 eV
CoCO+
Co(C3H6O)+
Co(C3H6O)2+
Co(CH3)2+
100
10
1
0.25
0.5
1
2
4
σi p (Å2-millitorr)
p (millitorr)

in Figure 2 suggests an even higher order process.

The low energy products can be accounted for by the steps depicted in Scheme I. The general reaction coordinate diagram is shown in

Scheme I

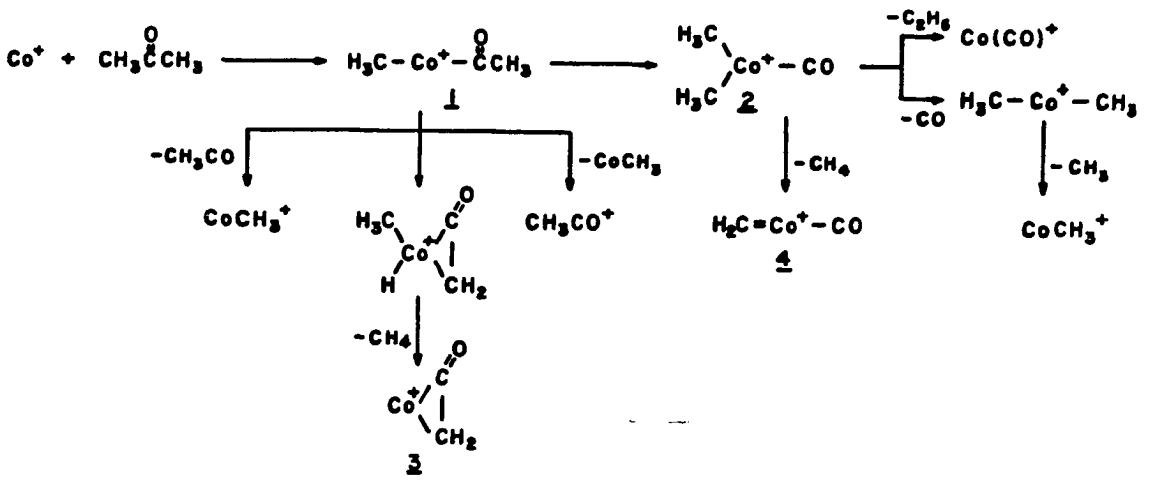

Figure 3. Cobalt ions insert into the C-CO bond of acetone, followed by a methyl migration onto the metal center to form 2. This type of methyl shift has many precedents in the literature[14]. Intermediate 2 can either reductively eliminate ethane, resulting in formation of the major product, $Co(CO)^+$, or lose CO to give the dimethyl species, $(CH_3)_2Co^+$. The decomposition of acetone into CO and two methyl radicals requires 96 kcal/mol[15,16](Table V). Thus, the exothermic production of $(CH_3)_2Co^+$ indicates that the sum of the two methyl bond dissociation energies to Co^+ exceeds this amount. This same limit applies to the ions $(CH_3)_2Fe^+$ [9] and $(CH_3)_2Ni^+$ [17], formed in the analogous exothermic

Table V. Reaction Enthalpies Used in Text

	ΔH (kcal/mol)[a]
$H_2CO \rightarrow HCO + H$	87
$\rightarrow CO + 2H$	103.7
$\rightarrow CO + H_2$	-0.3
$CH_3CHO \rightarrow CH_3CO + H$	86.0
$\rightarrow HCO + CH_3$	82.5
$\rightarrow CO + H + CH_3$	100.5
$\rightarrow CO + CH_4$	-4.6
$(CH_3)_2CO \rightarrow CH_3CO + CH_3$	81.2
$\rightarrow CO + 2CH_3$	95.7
$\rightarrow CO + C_2H_6$	5.3
$\rightarrow CO + H_2 + C_2H_4$	38.0
$\rightarrow CH_3COCH_2 + H$	98.3
$CH_3COC_2H_5 \rightarrow CH_3CO + C_2H_5$	77.1
$\rightarrow C_2H_5CO + CH_3$	80.6
$\rightarrow CO + CH_3 + C_2H_5$	91.6
$\rightarrow CO + C_3H_8$	5.8
$\rightarrow CO + CH_4 + C_2H_4$	25.2
$\rightarrow COCH_3 + C_2H_4 + H$	115.8
$\rightarrow HCOCH_3 + C_2H_4$	29.8
$\rightarrow CH_3COCH_2 + CH_3$	75.4

Table V. Continued

	ΔH (kcal/mol)[a]
$(C_2H_5)_2CO \rightarrow COC_2H_5 + C_2H_5$	77.4
$\rightarrow CO + 2C_2H_5$	87.0
$\rightarrow CO + C_4H_{10}$	4.9
$\rightarrow CO + C_2H_4 + C_2H_6$	27.4
$\rightarrow COC_2H_5 + C_2H_4 + H$	116.0
$\rightarrow HCOC_2H_5 + C_2H_4$	28.6
$\rightarrow CH_2COC_2H_5 + CH_3$	86.4

a) From references 15 and 16

reactions of Fe^+ and Ni^+ with acetone (Table I). These results confirm an earlier contention that processes involving insertion of first row group and metal ions into C-C bonds of alkanes are exothermic[2,3,18].

At higher energies reactions 6-9 are observed. Observation of energy thresholds for these processes indicates that they are endothermic reactions or have fairly high activation energies.

$$Co^+ + (CH_3)_2CO \longrightarrow \begin{cases} CH_3CO^+ + CoCH_3 & (6) \\ CoCH_3^+ + CH_3CO & (7) \\ Co(CH_2CO)^+ + CH_4 & (8) \\ Co(COCH_3)^+ + CH_3 & (9) \end{cases}$$

The second of these has a maximum cross section of 3 $\mathring{A}^2$ at 3.1 eV. The remainder are minor products, with maximum cross sections less than 1 $\mathring{A}^2$. All four have thresholds between 0.5 and 1.0 eV. It is difficult to say which process has the lowest threshold. The endothermic reactions 6-9 of Co^+ with acetone provide additional clues as to the nature of reaction intermediates involved in the formation of $CoCO^+$ and $Co(CH_3)_2^+$ at low energy. For example, simple cleavage of the metal-acyl bond in 1 would yield the products of reactions 6 and 7. These reactions dominate at higher energies due to their favorable frequency factors[19]. Thresholds and product ion abundances for both processes are comparable, indicating that the ionization energies of CH_3Co and CH_3CO are similar. Earlier estimates give the ionization potential of $CoCH_3$, IP[$CoCH_3$], in the range of 6.70 eV to 7.36 eV[2], to be compared with IP[CH_3CO] = 7.04 eV[16,20]. Pyrolysis of acetone yields ketene and methane (reaction 10)[21], a process which is endothermic by

$$(CH_3)_2CO \rightarrow CH_2CO + CH_4 \qquad (10)$$

20 kcal/mol[15]. The binding energy of ketene to Co^+ is very likely in excess of this amount (see Appendix), rendering the overall process exothermic. The data in Figure 1 indicate that reaction 8 requires ~15 kcal/mol excess energy to be observed, suggesting that the process has a moderate activation energy. Possible structures for the product are indicated by 3 and 4. Our estimates (see Appendix) suggest that 3 and 4 have comparable stabilities[22]. Plausible mechanisms leading to 3 and 4 involve β-hydrogen transfer starting from 1, and elimination of CH_4 from 2, respectively. Apparently, these processes have frequency factors or activation energies which do not allow them to compete with the major pathways except at high internal energies.

Reaction 9 is interesting since this product might result from cleavage of the metal-methyl bond in either 1 or 2. Thermochemical estimates (see Appendix) indicate that $(CH_3)CoCO^+$ is more stable than $Co(COCH_3)^+$ by ~20 kcal/mol (i.e., methyl migration from the carbonyl to the metal is exothermic). Hence, the metal-methyl bond in 2 can be cleaved at a lower energy than in 1. It is possible that both processes are occurring, giving rise to the unusual structure in the cross section shown for this process in Figure 1.

The semi-quantitative potential energy diagram shown in Figure 3 is useful for further discussing the reactions of Co^+ with acetone. Thermochemical data used to construct this diagram are discussed in detail in the appendix. The initial interaction generates a chemically activated species, 5, with an internal energy approximately equal to

Figure 3. Simplified reaction coordinate diagram for the interaction of Co^+ with acetone (●), acetaldehyde (■), and formaldehyde (▲). The curve is drawn through the points calculated for the acetone reaction.

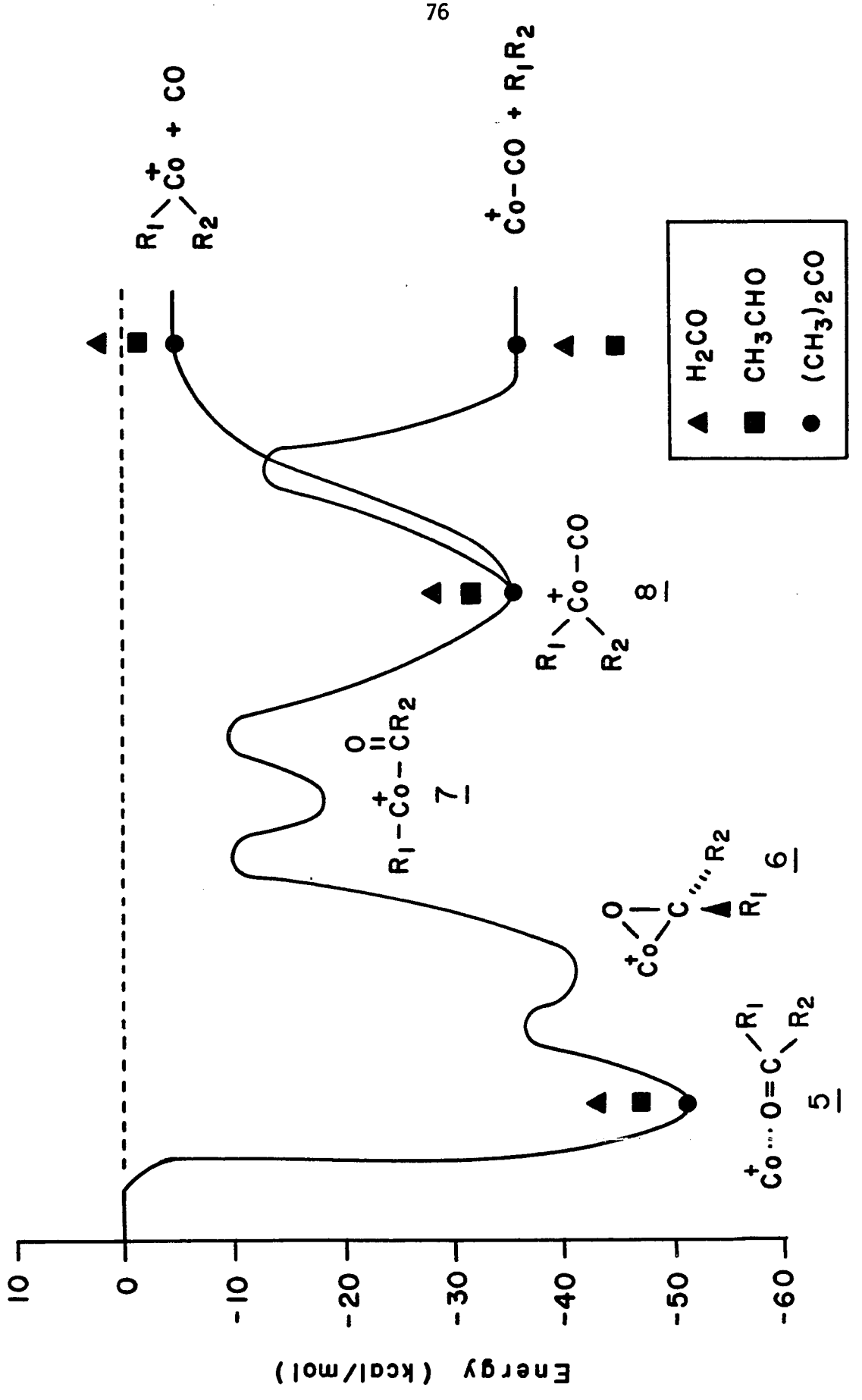
Energy (kcal/mol)
10
0
-10
-20
-30
-40
-50
-60
$R_1-\overset{+}{C}o + CO$
R_2
$\overset{+}{C}o-CO + R_1R_2$
H_2CO
CH_3CHO
$(CH_3)_2CO$
$\overset{+}{C}o\cdots O=C(R_1)(R_2)$ 5
$\overset{O}{\underset{\overset{+}{C}o}{|}}-C(R_1)(R_2)$ 6
$R_1-\overset{+}{C}o-\overset{O}{\overset{\|}{C}}R_2$ 7
$R_1-\overset{+}{C}o-CO$ R_2 8

the binding energy of acetone to Co^+ (51 kcal/mol). This species may have either a linear geometry with respect to the carbonyl group, which is characteristic of an electrostatic interaction (e.g., with Li^+[23]), or a bent structure, such as 9, depending on the degree of covalent

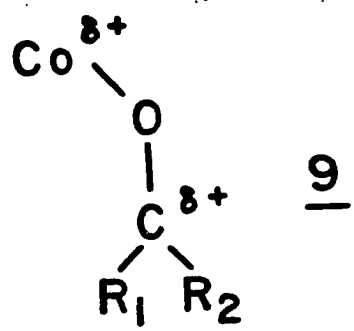

9

bonding. The precursor to the methyl shift onto the metal is probably 7, with η^2-bound acetone. Although we think the linear structure is more stable (see Appendix), the mode of bonding shown for acetone in 7 is characteristic of the binding of aldehydes and ketones to metals in coordinatively saturated complexes[24].

Rearrangement of 5 to allow interaction of Co^+ with the π system of the carbonyl group is followed by addition of the metal ion to one of the two C-C bonds of acetone, yielding 7. A methyl migration from CO to the metal forms 8, which can reductively eliminate ethane or lose CO. The minor product, $Co(CH_3)_2^+$ is only slightly exothermic, while $Co(CO)^+$ is 35 kcal/mol exothermic. The activation energy for reductive elimination of ethane from 8 is expected to be high[25]. If this were not the case, $Co(CH_3)_2^+$ would not be formed competitively in the reaction of Co^+ with acetone. This barrier is also consistent with the observation that the reverse process, insertion of $Co(CO)^+$ into the carbon-carbon bond of an alkane[26], is not observed. In contrast, bare cobalt ions readily add

to carbon-carbon bonds of alkanes[2]. Loss of CO from 8, a simple bond cleavage process, is not expected to have an activation energy much in excess of the endothermicity. The fact that the ratio of $Co(CH_3)_2^+$ to $CoCO^+$ remains relatively constant as a function of translational energy indicates that activation energies for processes 4 and 5 are comparable.

Acetaldehyde. The only product formed at low energies in the reaction of cobalt ions with acetaldehyde is $Co(CO)^+$, process 11.

$$Co^+ + CH_3CHO \rightarrow Co(CO)^+ + CH_4 \qquad (11)$$

The data for this reaction are shown in Figure 4, and indicate that reaction 11 is an exothermic process. Adduct formation at the lowest energies is also prominent. At higher energies, endothermic formation of CH_3CO^+, CoH^+, and $CoCH_3^+$ occurs. A species corresponding to $Co(H)(CH_3)^+$ is not observed at any energy.

Scheme II shows a mechanism by which reaction 11 can occur. After

Scheme II

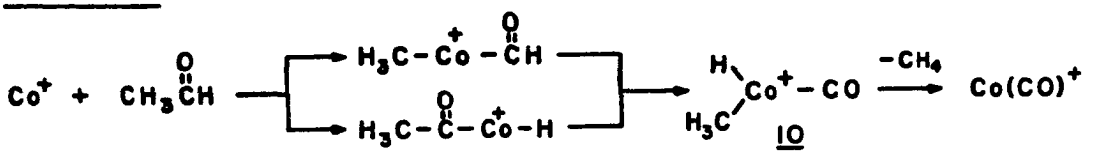

Figure 4. Variation in reaction cross section for the interaction of Co^+ with acetaldehyde as a function of kinetic energy in the center of mass frame (lower scale) and laboratory frame (upper scale).

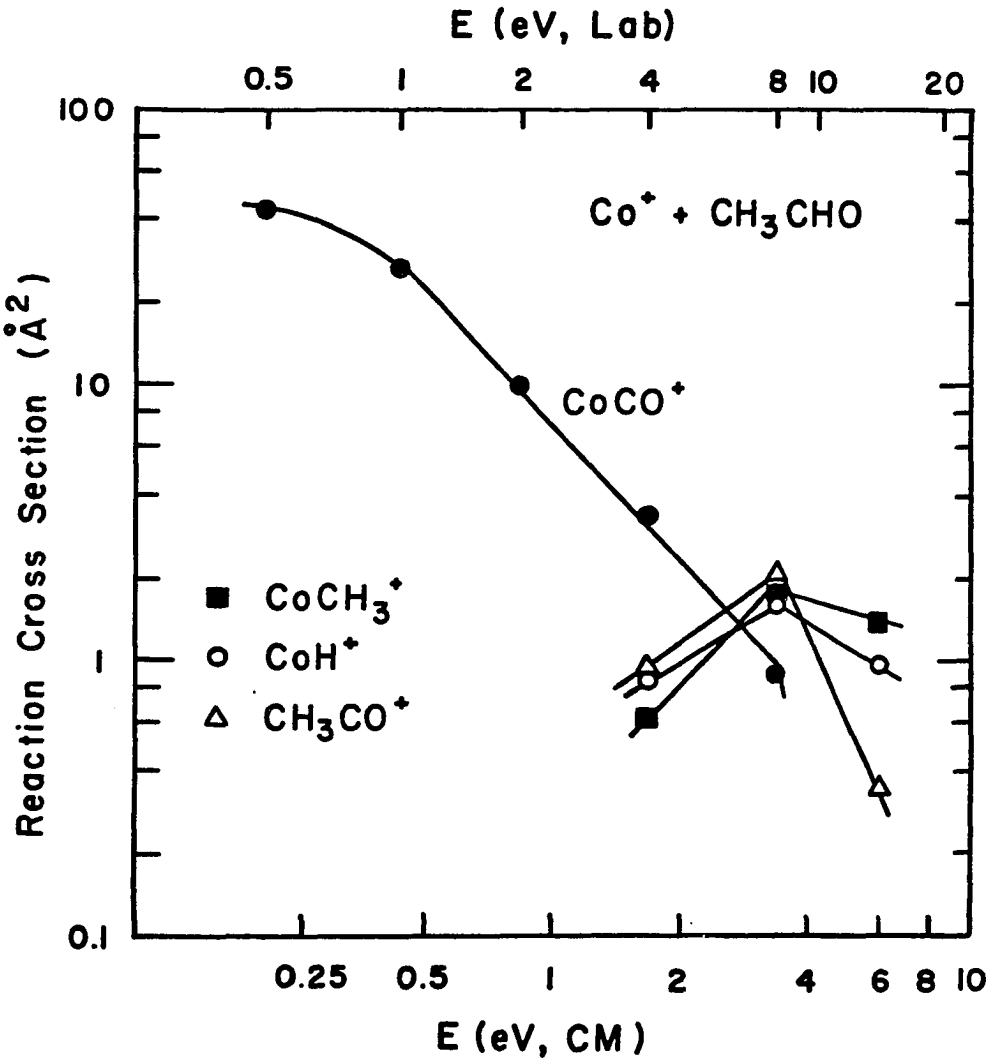
E (eV, Lab)
0.5
1
2
4
8
10
20
100
10
1
0.1
Reaction Cross Section (Å²)
Co⁺ + CH₃CHO
CoCO⁺
CoCH₃⁺
CoH⁺
CH₃CO⁺
0.25
0.5
1
2
4
6
8
10
E (eV, CM)

an initial interaction with the carbonyl moiety, Co^+ inserts into the H-CO or C-CO bond of acetaldehyde. Methyl or hydrogen migration from CO onto the metal then precedes reductive elimination of CH_4. The absence of the $Co(H)(CH_3)^+$ species may indicate that the process is endothermic (this would be the case if $D[HCo^+-CH_3]$ were less than 49 kcal/mol), or that the activation energy for the reductive elimination of methane from 10 is very low[25]. Thermochemical data in Table A1 are chosen such that formation of $Co(H)(CH_3)^+$ is 2 kcal/mol endothermic, as shown in Figure 3.

We would like to be able to say whether Co^+ adds first to the C-CO or H-CO bond of acetaldehyde. Using the thermochemical estimates given in the appendix, there is little difference in the energy of 7 for $R_1 = H$, $R_2 = CH_3$ and $R_1 = CH_3$, $R_2 = H$. The above results for acetone indicate that cobalt ions do insert into the C-CO bond and that methyl migration from CO to the metal center can occur. Results discussed below for formaldehyde suggest that either addition of Co^+ to the H-CO bond or the subsequent hydrogen transfer is a difficult process. At higher energies, insertion of Co^+ into both the C-CO and H-CO bond is suggested by observation of the endothermic products $CoCH_3^+$ and CoH^+. Based on the value IP(CoH) = 7.3 ± 0.1 eV[2], formation of CoH^+ should require only ~5 kcal/mol more energy than $COCH_3^+$[16,20]. At 1.7 eV relative kinetic energy, slightly above threshold, comparable amounts of these two products are observed. The appearance of HCO^+ was not examined.

Formaldehyde. Cobalt ions react with formaldehyde to form $Co(CO)^+$, equation 12. Data for this reaction are shown in Figure 5. Surprisingly,

Figure 5. Variation in reaction cross section for the interaction of Co^+ with formaldehyde as a function of kinetic energy in the center of mass frame (lower scale) and laboratory frame (upper scale).

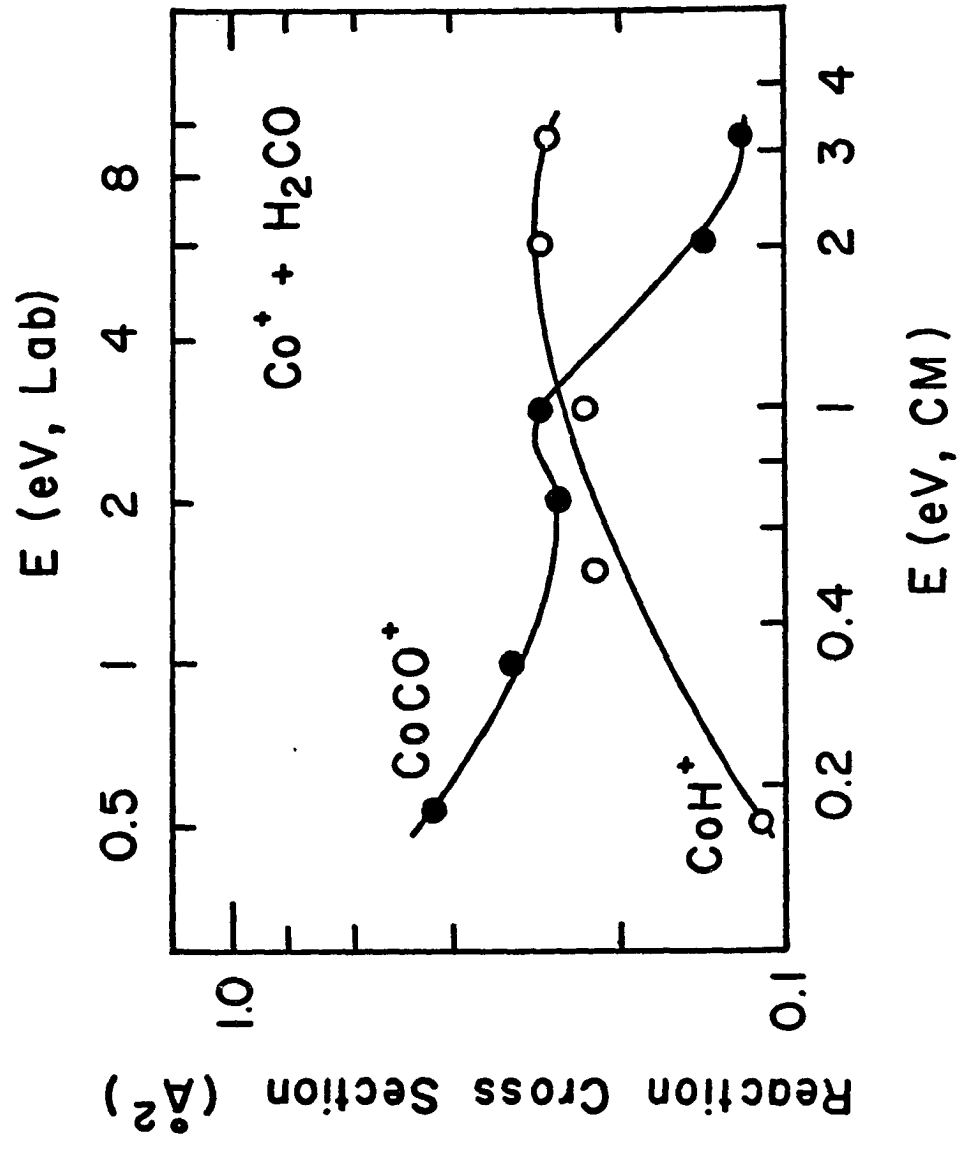
Reaction Cross Section (Å²)
10
0.1
E (eV, Lab)
0.5
1
2
4
8
E (eV, CM)
0.2
0.4
1
2
3
4
Co⁺ + H₂CO
CoCO⁺
CoH⁺

unlike the results for the $Co(CO)^+$ ion formed in reactions 4 and 11, the cross-section for reaction 12 is very small at low energies (<1 $Å^2$) and decreases slowly with energy. A small amount of CoH^+ is seen at low energies, but the cross section for this product increases with increasing energy, suggesting an endothermic process. The dihydrido species $Co(H)_2^+$ is not observed at any energy examined.

The decarbonylation processes seen in these gas phase reactions have their parallels in condensed phase studies. For example, certain rhodium[27] and osmium[28] complexes are known to react with acetaldehyde to form the metal hydridoacyl compound. Upon heating, the hydridoacyl undergoes migratory deinsertion followed by reductive elimination to yield the metal carbonyl complex and an alkane. Similarly, hydrido formyl complexes of Ir(III)[29] and Os(0)[24a] have been prepared by the direct oxidative addition of the C-H bond of formaldehyde. Formation of the hydrido formyl is probably preceded by formation of a complex containing a π-bound H_2CO entity, analogous to the chemically activated species, 6[24a]. When heated, the hydrido formyl complexes decompose with one product of the decomposition being hydrogen gas[24a].

It is not clear why decarbonylation of formaldehyde by gas phase ions should be less facile than that of acetaldehyde or acetone. The energetics involved in the conversion of the organic substrates, R_1COR_2, where R_1,R_2 = H or CH_3, to $R_1CO + R_2$ are given in Table V. Cleavage of the H-CO bond requires only ~5 kcal/mol more energy than cleavage of the H_3C-CO bond. Using the thermochemical estimates from Table A1, Figure 3 places 7 at approximately the same energy relative to reactants for acetone, acetaldehyde and formaldehyde.

Some distinctions can be made in comparing the present results to condensed phase studies. The metal-carbon bond energies in organometallic fragment ions often exceed the analogous metal-hydrogen bond strengths because the polarizable methyl group stabilizes the charge more favorably than hydrogen[30]. This effect is diluted by additional polarizable ligands as well as by a dielectric medium. Thus metal-hydrogen bonds are expected to be stronger than metal-carbon bonds in solvated complexes or those with more ligands attached. Hence, unsolvated bare metal ions may be uniquely suited as reagents for decarbonylation of ketones.

Interestingly, reactions of Ni^+ and Rh^+ with formaldehyde yield $M(CO)^+$ as the only product ion at low energies, again with a very small cross section[17]. The reactions of Ni^+ might be expected to be similar to Co^+, given the similar types of products observed in the reactions of the three first row group 8 metal ions with alkanes[3]. However, at low energies Rh^+ exclusively dehydrogenates alkanes, including ethane[31]. Because of this selectivity toward C-H bond insertion in alkanes, one might expect a greater reactivity towards the C-H bonds of formaldehyde. This does not occur.

The small cross sections for reactions of metal ions with formaldehyde in the gas phase may have less to do with overall thermochemistry than with the relative magnitude of reaction and dissociation rates for the initially formed adduct, 5. Little of the adduct is seen in the formaldehyde reactions, while it is quite prominent at low energies in the acetone and acetaldehyde reactions.

The rate of dissociation of the chemically activated intermediate, 5, to regenerate the reactants varies considerably with the number of

vibrational degrees of freedom in the adduct. More importantly, an RRKM analysis indicates the ratio of unimolecular reaction to dissocation at a given level of internal energy increases with increasing substitution of CH_3 for H. With formaldehyde it is possible that dissociation is significantly faster than the initial rearrangement step leading to decarbonylation[32].

Larger Dialkyl Ketones. Once the ketone has a longer alkyl chain, a greater variety of products appears. For example, Figure 6 depicts the data for the reaction of Co^+ with 2-butanone. Butanone-α,α'-d_5 was used to identify the products listed in Table I. A number of pathways can lead to the same product as shown in Scheme III. The initial insertion product can be to either of the C-CO bonds of the ketone. If insertion occurs into the weaker OC-C_2H_5 bond, a β-hydrogen can be transferred to the metal to form 13. Structure 13 can lose ethene or rearrange further to 15. Here again, loss of ethene, or loss of acetaldehyde can take place. Alternatively, structure 16 may be generated if insertion into either C-CO bond is followed by an alkyl migration onto the metal center. This intermediate may be a common precursor to all product ions. Losses of methane, ethene, and carbon monoxide can follow. Because ethene is more strongly bound to metal cations than CO[33], structure 16 would be expected to lose more CO than ethene. However, no $Co(C_3H_3D_5)^+$ is observed. This suggests that loss of CHD_3 precedes loss of ethene and loss of CO from 16. Likewise, because the binding energy of acetaldehyde to Co^+ is expected to be much greater than that of ethene, intermediate 15 most likely loses only ethene[7]. This leaves 13 or 17 as the likely precursors to the Co(ethene)$^+$ product.

Figure 6. Variation in reaction cross section for the interaction of Co^+ with 2-butanone as a function of kinetic energy in the center of mass frame (lower scale) and laboratory frame (upper scale).

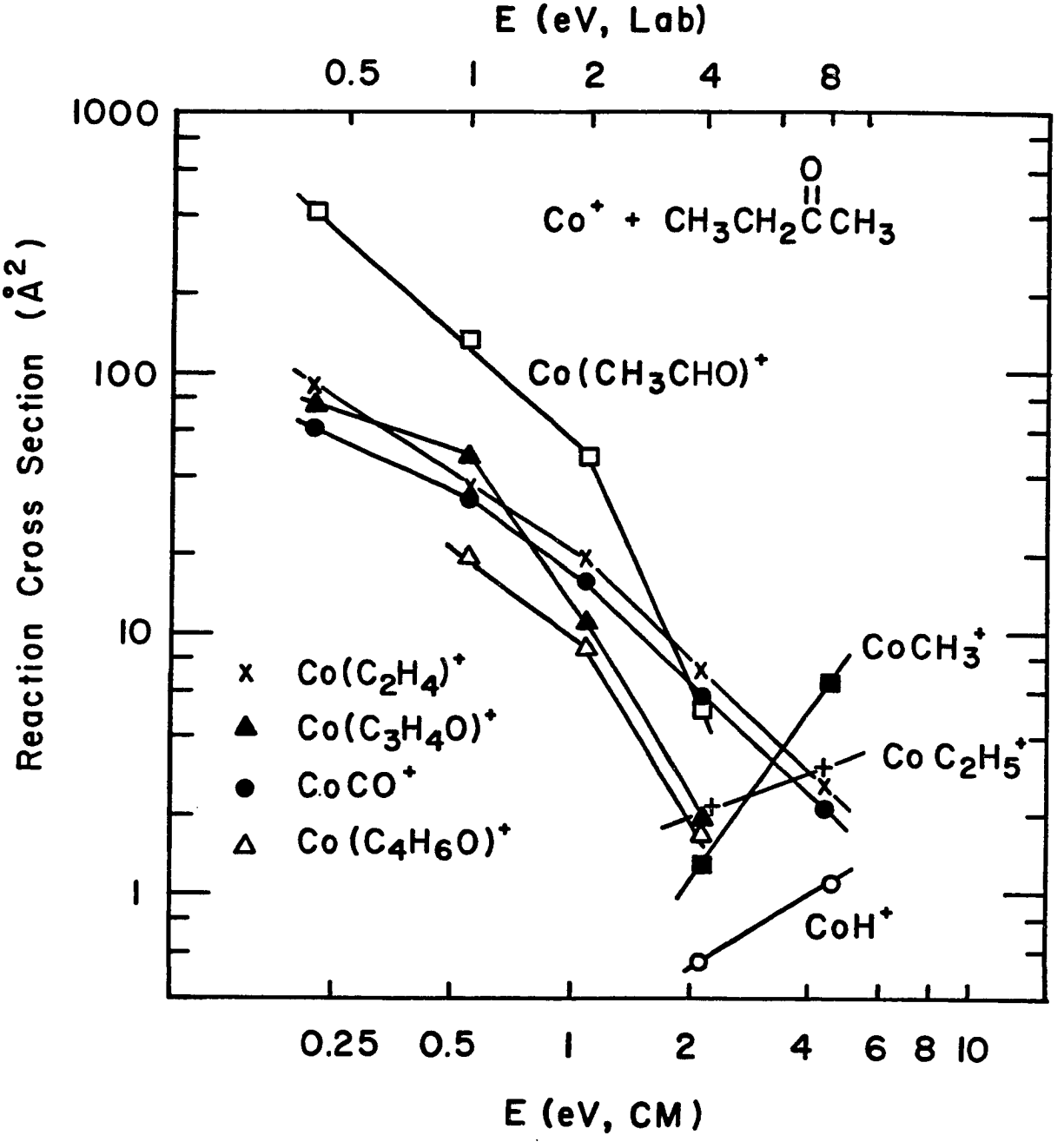
E (eV, Lab)
0.5
1
2
4
8
1000
100
10
1
Reaction Cross Section (Å²)
Co⁺ + CH₃CH₂C(=O)CH₃
Co(CH₃CHO)⁺
x Co(C₂H₄)⁺
▲ Co(C₃H₄O)⁺
● CoCO⁺
△ Co(C₄H₆O)⁺
CoCH₃⁺
Co C₂H₅⁺
CoH⁺
0.25
0.5
1
2
4
6
8
10
E (eV, CM)

Scheme III

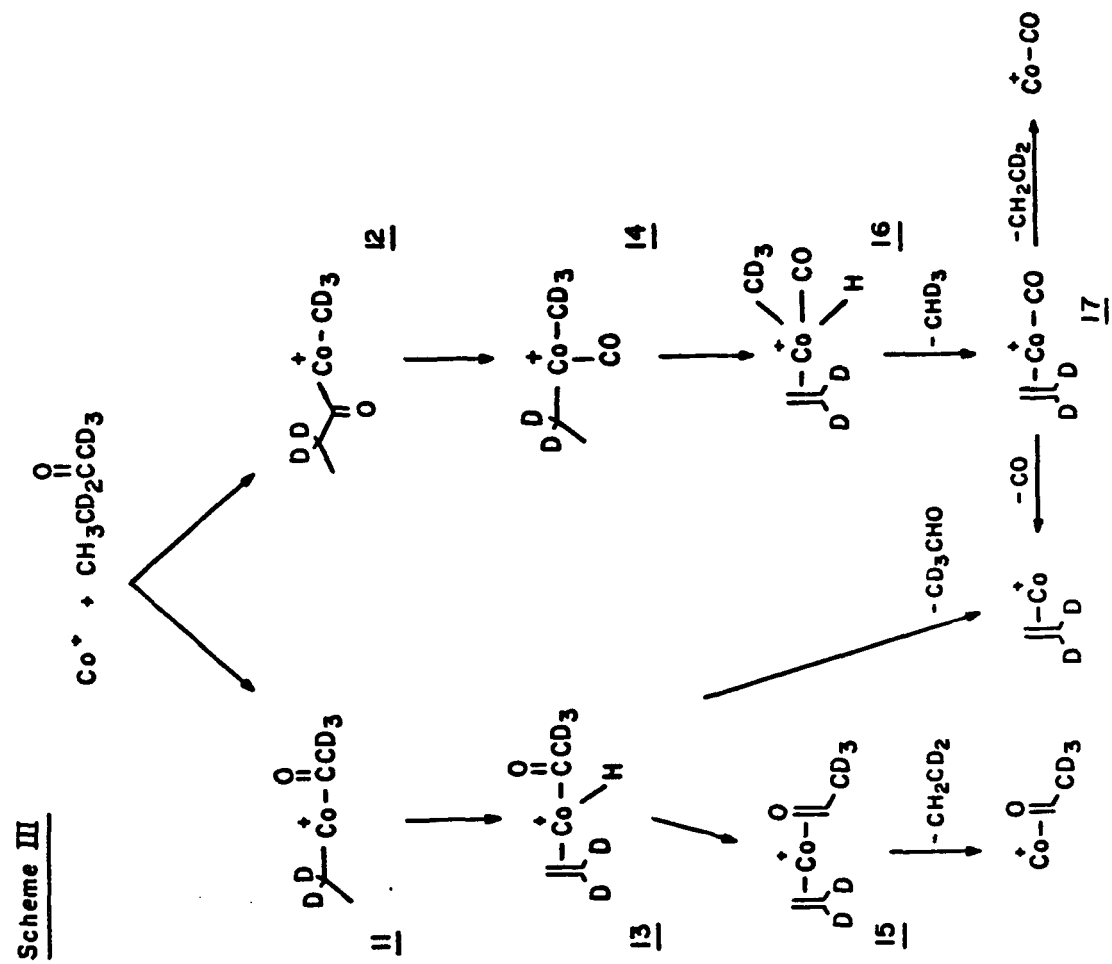
Co⁺ + CH3CD2CCD3
11
12
13
14
15
16
17
-CD3CHO
-CO
-CH2CD2
-CH2CD2
-CHD3

The species corresponding to $Co(C_2HD_3O)^+$ is expected to be a cobalt ion bound to acetaldehyde. Exothermic formation of $Co(H)(COCD_3)^+$ from butanone would imply that $D[HCo^+-COCD_3] > 63$ kcal/mol (Tables V and A1). If this were the case, the $Co(COCH_3)^+$ species should appear at much lower energies (~0.5 eV) than it does in the reaction of Co^+ with acetone.

In contrast to the reaction with acetone, simple loss of CO is not observed. This may suggest that alkyl migration from CO onto the metal ion is slow compared to β-hydrogen transfers, i.e., 13 is formed more rapidly than 14. Another possibility, although unlikely, is that formation of $Co(CH_3)(C_2H_5)^+$ from reaction with butanone is endothermic. This would result if the sum of the two metal-carbon energies were less than 92 kcal/mol[15,16].

Reaction of Co^+ with butanone may also proceed via initial insertion into other bonds of the ketone. A small amount of dehydrogenation which occurs exclusively via loss of HD from the butanone-α,α'-d_5 is observed. Dehydrogenation most likely proceeds via insertion of the metal into the C-H or C-D bond of the ethyl group followed by β-D(H) transfer and loss of HD. The resulting ionic product is stabilized by a conjugated π system to which the metal can bind, structure 18[34].

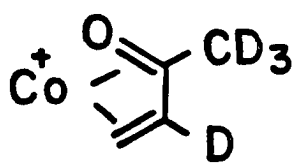

18

The major loss of CH_2CD_2 (81%) from the 2-butanone-α,α'-d_5 is rationalized as indicated in Scheme III. At the lowest energies, loss of

C_2H_3D appears as well. The proportion of the latter decreases with increasing energy. This product is probably formed via a scrambling process. Scheme IV shows how this scrambling can occur once intermediate

Scheme IV

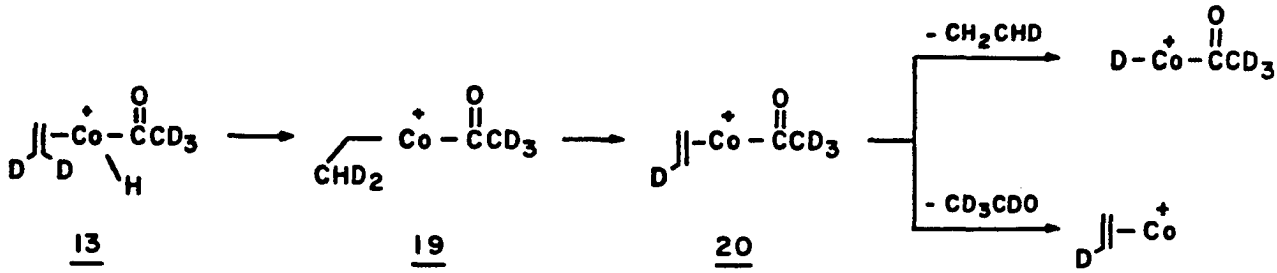

13 is formed (Scheme III). The hydrogen which has been transferred onto the metal may be reversibly transferred back onto either end of the alkene. If it returns to the deuterated carbon, intermediate 19 is formed. This ion can undergo a β-D transfer to form 20. Now either C_2H_3D or acetaldehyde-d_4 can be eliminated. Both of these products are observed. The analogous scrambling mechanism can in principle proceed via 16, leading to loss of CD_4 as well. This may occur, though it is difficult to ascertain from our data. It is of interest to note that pathways similar to those depicted in Scheme IV appear to play a significant role in the low energy reactions of Co^+ with alkanes[2,35].

Products appearing at higher energies include $CH_3CD_2^+$, CD_3CO^+

$COCD_2CH_3^+$, $CoCD_3^+$, $Co(CD_2CH_3)^+$, $Co(COCD_3)^+$, and $Co(COCD_2CH_3)^+$. These may be formed by dissociation of intermediates 11 and 12 by simple cleavage of the Co^+-carbon bonds. The $CoCH_3^+$ and $Co(CD_2COCD_3)^+$ ions are also observed at higher energies[36], and must be generated by insertion into the C3-C4 bond. The cross-section for the $CoCD_3^+$ ion is slightly greater than that for $CoCH_3^+$ at the energies where these products first appear. This is consistent with the slightly lower $OC-CD_3$ bond energy (Table V). These two cobalt-methyl ions account for > 50% of the product distribution at 8 eV, the highest relative kinetic energy examined.

Insertion into both C-H and C-D bonds takes place. The ratio of CoH^+ to CoD^+ is roughly 1:1 at relative kinetic energies from 1 eV ($\sigma_H \sim 0.3$ $\AA^2$) to 8 eV ($\sigma_H \sim 1.1$ $\AA^2$). Because the ratio of H:D in the labeled butanone is 3:5, the equivalent amounts of CoH^+:CoD^+ may indicate a favoring of C-H bond insertion over C-D bond insertion. However, this trend does not continue in the 3-pentanone-α,α'-d_4 discussed below.

Products observed in the reaction of Co^+ with 3-pentanone are listed in Table I. The products formed at low energies can be explained as indicated in Scheme V, which depicts processes similar to those in Scheme III. Cobalt ions add first to a C-CO bond of the ketone. Beta-hydrogen abstraction off the ethyl group leads to 22, or ethyl migration to the metal yields 24. Loss of propanal or ethene from 22, loss of butane from 24, and loss of ethane from 23 lead to most products observed at low energies. As is the case in the butanone reaction, the $Co(C_3H_3D_2O)^+$ ion is expected to be a cobalt ion bound to an aldehyde, in this case propanal, rather than a hydrido acyl. Exothermic production

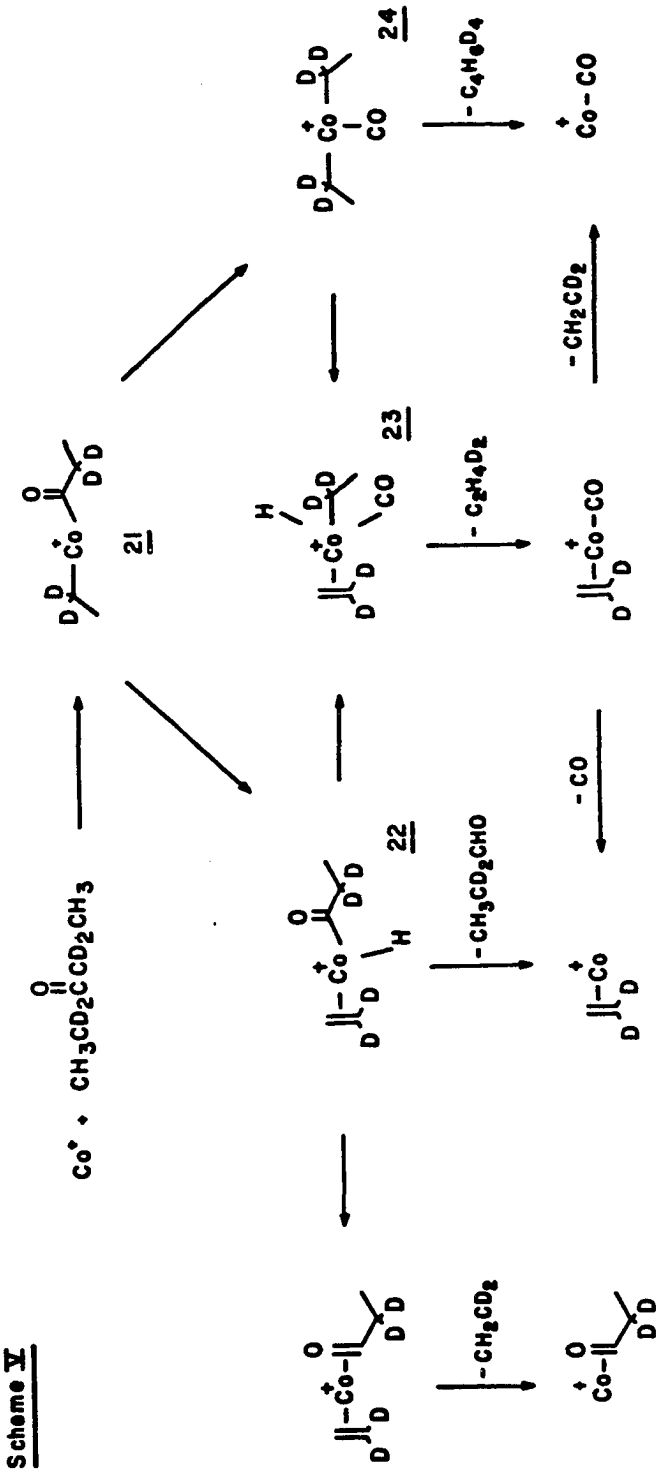
Scheme V
Co⁺ + CH3CD2CCD2CH3
21
22
23
24
-CH2CD2
-CH3CD2CHO
-C2H4D2
-CO
-C4H8D4

of the latter would imply $D[HCo^+-COC_2H_5] > 64$ kcal/mol (Tables V and A1). This is unlikely for reasons discussed above.

A small amount of dehydrogenation, lost exclusively as HD from the 3-pentanone-$\alpha,\alpha'-d_4$, is also observed at low energies. In analogy to structure 18, the dehydrogenation product is thought to be a cobalt ion bound to an α,β-unsaturated ketone, in this case, 1-pentene-3-one. As in the case of 2-butanone-$\alpha,\alpha'-d_5$, a small amount (~2%) of $Co(CH_2CO)^+$ also appears as an exothermic process in the reaction with 3-pentanone-$\alpha,\alpha'-d_4$ [34].

Scrambling processes similar to those depicted in Scheme IV for 2-butanone-$\alpha,\alpha'-d_5$ are also apparent in the reactions of Co^+ with 3-pentanone-$\alpha,\alpha'-d_4$, Table II. Analogous to Scheme IV, 22 can exchange the metal bound hydrogen atom for one of the vinyl deuteriums, leading to loss of propanal-$\alpha,\alpha'-d_3$ or C_2H_3D. Because of the small amount of product due to loss of ethane, it could not be determined if scrambling processes occur during its formation as well.

At higher energies, Co^+ is seen to insert into all C-C and C-H bonds of the molecule. Simple cleavage products of intermediate 21, $CD_2CH_3^+$ and $Co(CD_2CH_3)^+$, and of 25, $CoCH_3^+$ and $Co(CH_3CD_2COCD_2)^+$, are

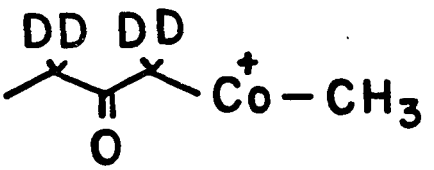

25

observed. Some $Co(CD_2CO)^+$ appears at these high energies as well, and is probably due to a complex rearrangement of 25. The ratio of $CoH^+:CoD^+$ is ~1.2 from 1.2 eV to 20 eV in the center of mass frame, with a maximum

cross section observed of ~1.7 $Å^2$. A statistical ratio accounting for the number of hydrogen to deuterium atoms would be 1,5.

As the alkyl chain on the ketone becomes more complex, more of the product distribution is due to loss of an alkane. For example, 88% of the observed products in the reaction of Co^+ with 3,3-dimethyl-2-butanone are accounted for by loss of methane, and 76% loss of methane is observed in the reaction with 4,4-dimethyl-pentanone. Scheme VI depicts two pathways, a and b, through which methane can be lost from the dimethylbutanone. Both of these pathways have precedence in other reactions of cobalt ions. Path a is analogous to the proposed mechanism for loss of methane with 2,2-dimethylpropane[2]. The metal ion inserts into the terminal C-C bond, a β-hydrogen is transferred to the metal, and reductive elimination of CH_4 occurs. This can result in a cobalt ion bound to an α,β-unsaturated ketone. Alternatively, and consistent with Schemes III and V, Co^+ can enter the OC-C3 bond, followed by a methyl migration off the CO and a β-hydrogen transfer to the metal center, path b. In addition, processes similar to those depicted earlier with 2-butanone and 3-pentanone occur, such as loss of acetaldehyde and alkene (butene in this case). The cobalt-butene ion can further dehydrogenate by allylic hydrogen abstractions to form $Co(C_4H_6)^+$[37]. This product was also observed in the reaction of Co^+ with 2-methylpropene[4]. The structure of the $Co(C_4H_6)^+$ ion is uncertain. It may be a cobalt ion trimethylene methane complex. Other possibilities would result if substantial rearrangment is required before dehydrogenation occurs. High energy products include cobalt-carbon cleavage products of 26, 27, and 28, namely CH_3CO^+, $C_4H_9^+$, $C_4H_9CO^+$, and $CoCH_3^+$. The CoH^+ ion is also observed.

Loss of methane from 4,4-dimethyl-2-pentanone can also be accounted for by two pathways. The first, shown in Scheme VII a, is directly

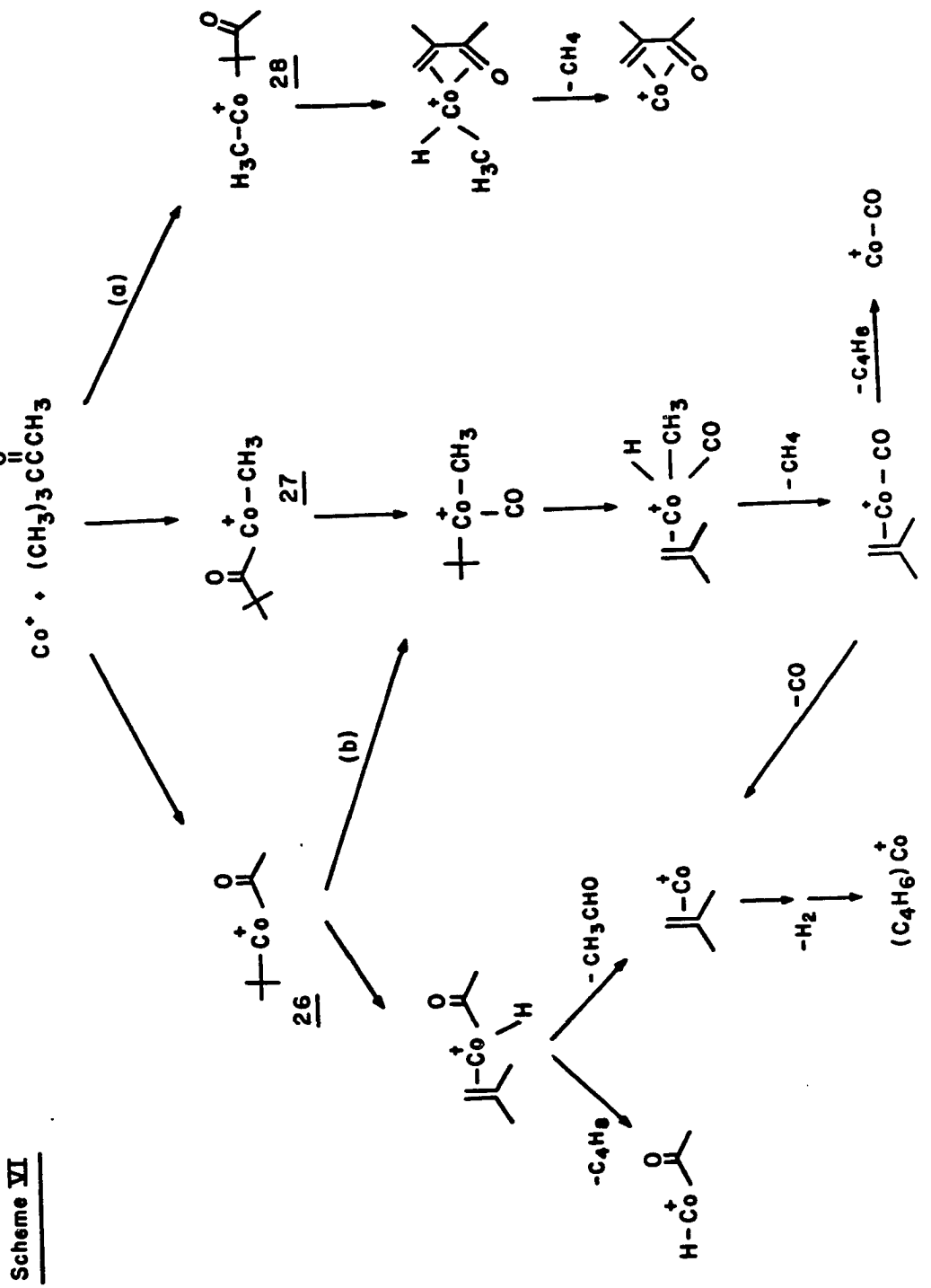

Scheme VI

Scheme VII (a)

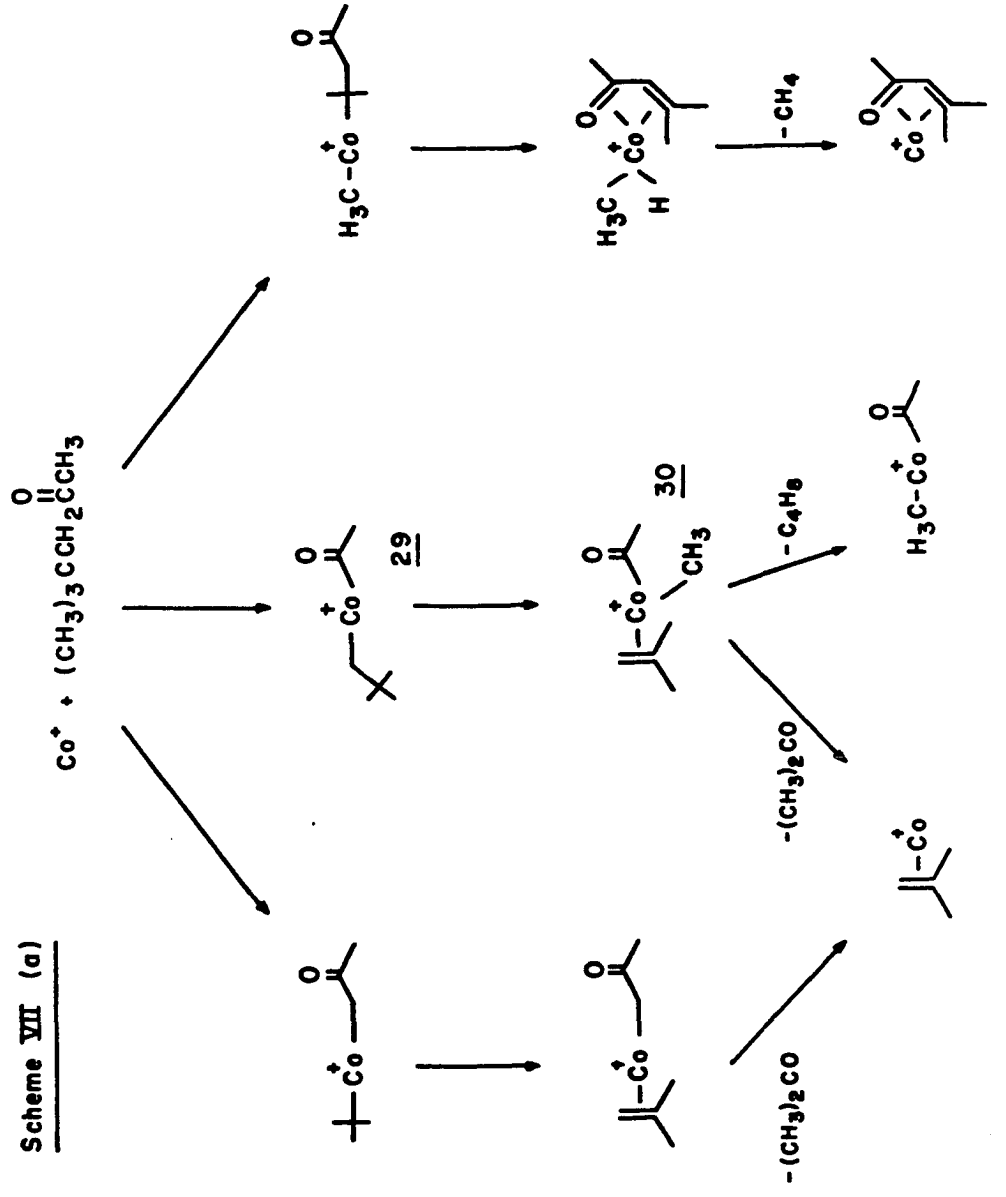

analogous to Scheme VIa. Here too, the product can be the metal ion bound to an α,β-unsaturated ketone. Another possible pathway is through Scheme VII b. Intermediate 30 is formed from 29 via a β-methyl transfer to the metal. Beta-methyl transfers have been noted in the reaction of Fe^+ with deuterated alkanes at low energies, and also with Co^+ at slightly higher energies[3,38]. Intermediate 30 can lose either acetone or butene, or abstract an allylic hydrogen from the 2-methylbutene to which it is bound[4]. Loss of methane, or loss of acetaldehyde leading to 31 can then occur. This ion may abstract an allylic hydrogen to form $Co(C_4H_6)^+$. The latter product may also be formed by dehydrogenation of the $Co(C_4H_8)^+$ ion (as in Scheme VI).

Cyclopentanone. The major products of the reaction of cobalt ions with cyclopentanone at low energies are loss of CO and loss of CO and H_2, equations 12 and 13[39]. These products are formed in approximately equal

$$Co^+ + \text{cyclopentanone} \begin{cases} \longrightarrow Co(C_4H_8)^+ + CO & (12) \\ \longrightarrow Co(C_4H_6)^+ + (CO + H_2) & (13) \end{cases}$$

amounts at very low relative kinetic energies, while the $Co(C_4H_6)^+$ ion accounts for over 80% of the product distribution at slightly higher energies[40] (~1 eV). A small amount (~2% each) of loss of butene and C_3H_4O (see Table II) is also observed at low energies, with slightly larger amounts (~4% each) at 1 eV. The low energy products were identified using cyclopentanone-α,α'-d_4[39]. At higher energies, a product with mass 101 appears, which corresponds to $Co(COCH_2)^+$ or $Co(C_3H_6)^+$.

The proposed pathway for loss of CO is similar to the previously described reactions with ketones. The metal ion inserts into the C-CO bond of cyclopentanone, followed by an alkyl shift onto the

Scheme VII (b)

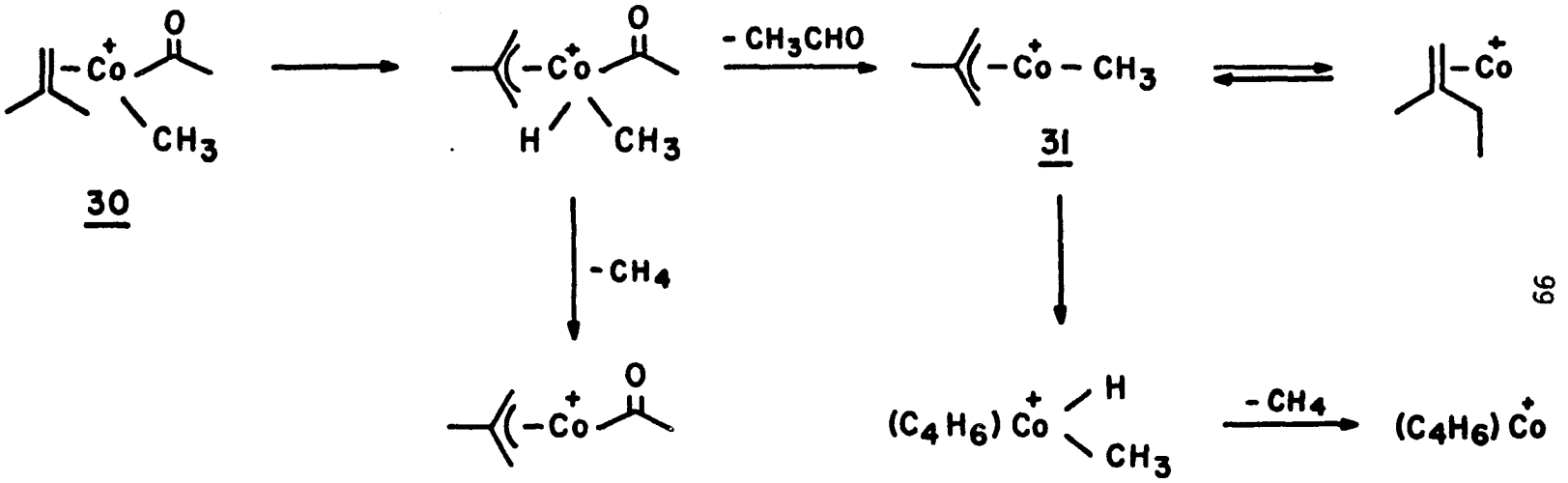

metal center. Ion cyclotron resonance spectroscopy experiments have shown that $M(C_4H_8)^+$ ions, M = Fe^+, Ni^+, formed from reaction of M^+ with cyclopentanone are unreactive with HCN. This suggests the C_4H_8 unit remains intact[6,10] for these two species. Similar studies were not done on the cobalt product. Reactions of Fe^+, Co^+, and Ni^+ with cyclobutanone are reported to form metallacyclobutanes[41]. In analogy to these systems, the decarbonylation process is expected to initially form the metallacyclopentane, 32. Subsequent dehydrogenation leads to the $Co(1,3\text{-butadiene})^+$ ion. Cleavage of the metallacycle leads to loss of ethene.

The metallacyclopentane, 32, has also been proposed as an intermediate in the reaction of Co^+ with cyclobutane[5]. The major products of this reaction at low energies are dehydrogenation and loss of ethene, equations 14 and 15. The ionic products of reactions 14 and 15 are

$$Co^+ + c\text{-}C_4H_8 \longrightarrow Co(C_4H_6)^+ + H_2 \qquad (14)$$

$$Co^+ + c\text{-}C_4H_8 \longrightarrow Co(C_2H_4)^+ + C_2H_4 \qquad (15)$$

the same as those observed in the reaction of Co^+ with cyclopentanone, which supports the supposition that 32 is a common intermediate in both reactions.

Studies using cyclopentanone-α,α'-d_4 indicate that some scrambling processes occur. For example, Scheme VIII predicts the $Co(ethene)^+$ ions from the labeled compound should be $Co(C_2H_2D_2)^+$. While this is the major $Co(ethene)^+$ product, the ions $Co(C_2H_3D)^+$,[42] $Co(C_2HD_3)^+$, and $Co(C_2D_4)^+$ are also observed with intensities ~14% that of the $Co(C_2H_2D_2)^+$ peak at 1.2 eV relative kinetic energy. A $Co(C_2H_4)^+$ product is also

Scheme VIII

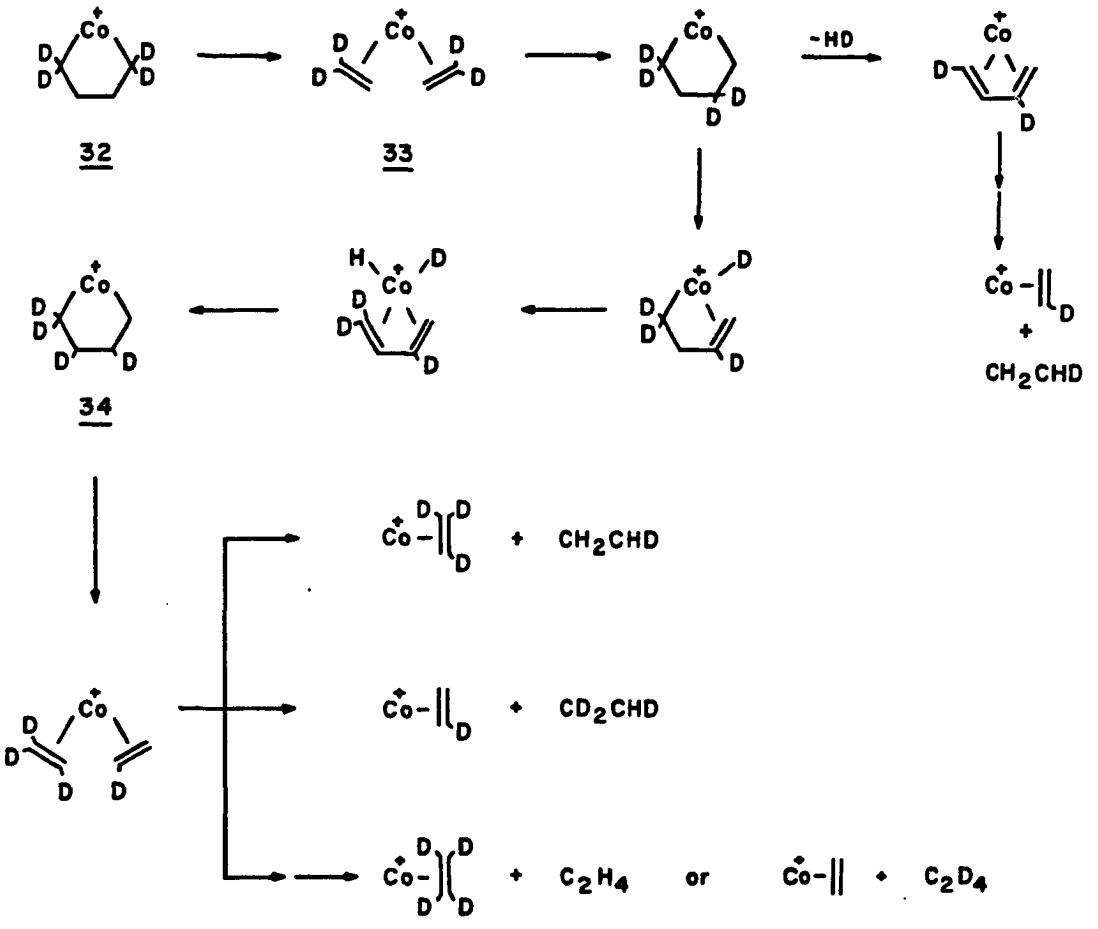

probably formed, but we cannot distinguish between this product and $Co(CO)^+$ which has the same mass. Scheme VIII proposes a possible mechanism to account for these products. The metallacycle 32, shown to cleave to form a bis-ethene complex 33 which may reform the metallacycle with one of the deuterated carbon atoms in the beta position. Beta-hydrogen and β-deuterium then switch back and forth from carbon to metal center. At some point, the dehydrogenation or cleavage of the metallacycle with loss of ethene occurs. Thus, 34 can lead to both $Co(C_2H_3D)^+$ and $Co(C_2HD_3)^+$. Dehydrogenation of 34 may involve loss of H_2, HD, or D_2. In viewing the complexity of Scheme VIII, it is important to bear in mind that the $Co(ethene)^+$ species is a very minor product[43].

The overall process for the reaction of Co^+ with cyclopentanone is analogous to that shown for acyclic ketones in Figure 3. Formation of the species corresponding to $R_1R_2Co^+$ is much more prominent in the cyclic ketone. This is presumably due to constraints imposed by the cyclic structure on the reductive elimination of R_1R_2 which, in this case, is the somewhat strained cyclobutane ring. Moreover, the formation of the $R_1R_2Co^+$ product from reaction with cyclopentanone should be a more exothermic process. A semi-quantitative potential energy diagram for the interaction of Co^+ with cyclopentanone is shown in Figures 7 and 8. Figure 7 is constructed using arguments analogous to those used to discuss Figure 3, with the thermochemical estimates listed in Table A1. The decomposition of 35 to the metallacycle involves simple bond cleavage and is not expected to have much of an activation barrier. On the other hand, the reductive elimination of R_1R_2 to form $CoCO^+$ is expected to exhibit an activation barrier since the reverse process is

Figure 7. Simplified reaction coordinate diagram for the interaction of Co^+ with cyclopentanone.

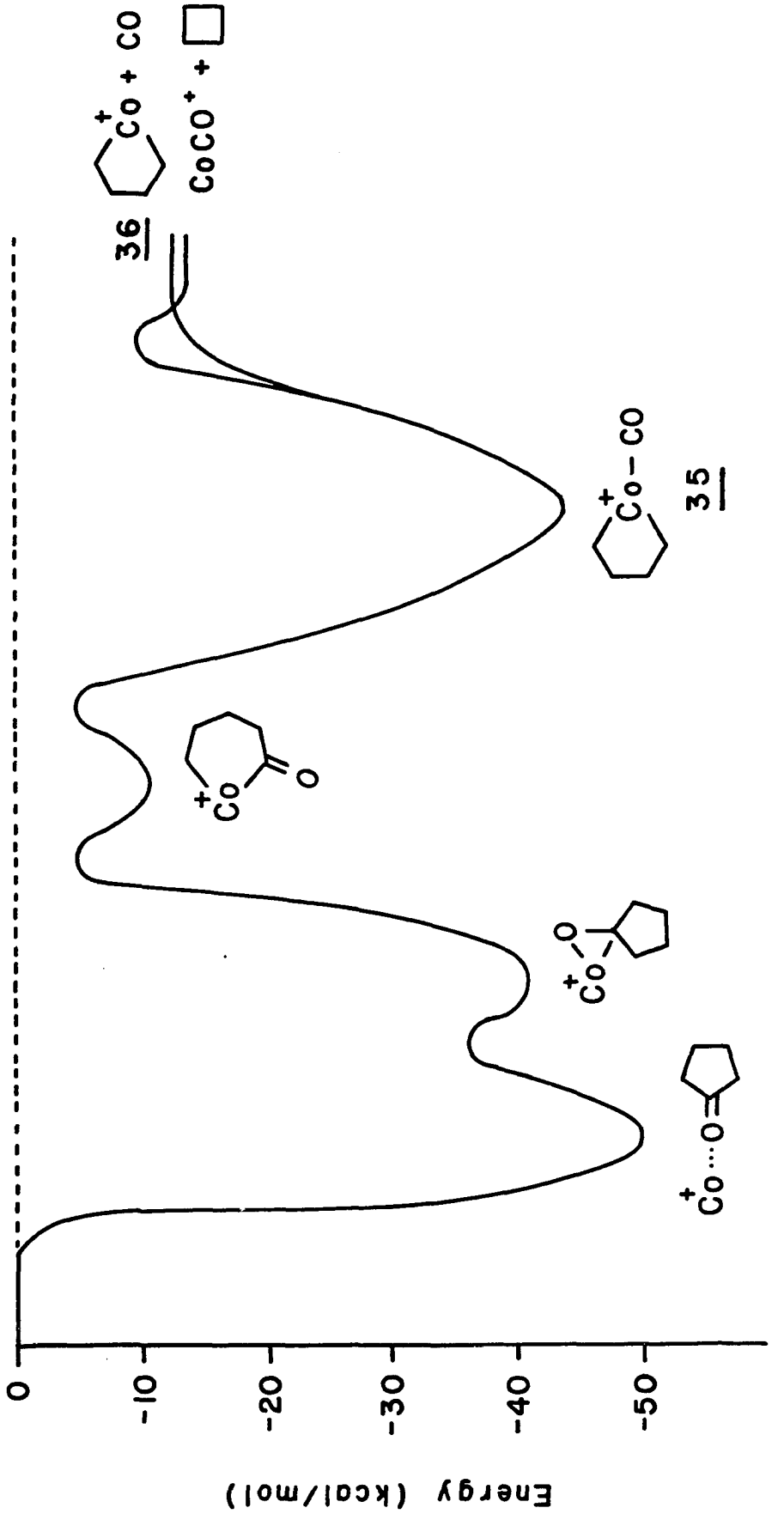
Energy (kcal/mol)
0
-10
-20
-30
-40
-50
36
35
Co + CO
CoCO+ +
Co-CO
Co...O

Figure 8. Simplified reaction coordinate diagram for decomposition of the metallacyclopentane formed in the interaction of Co^+ with cyclopentanone.

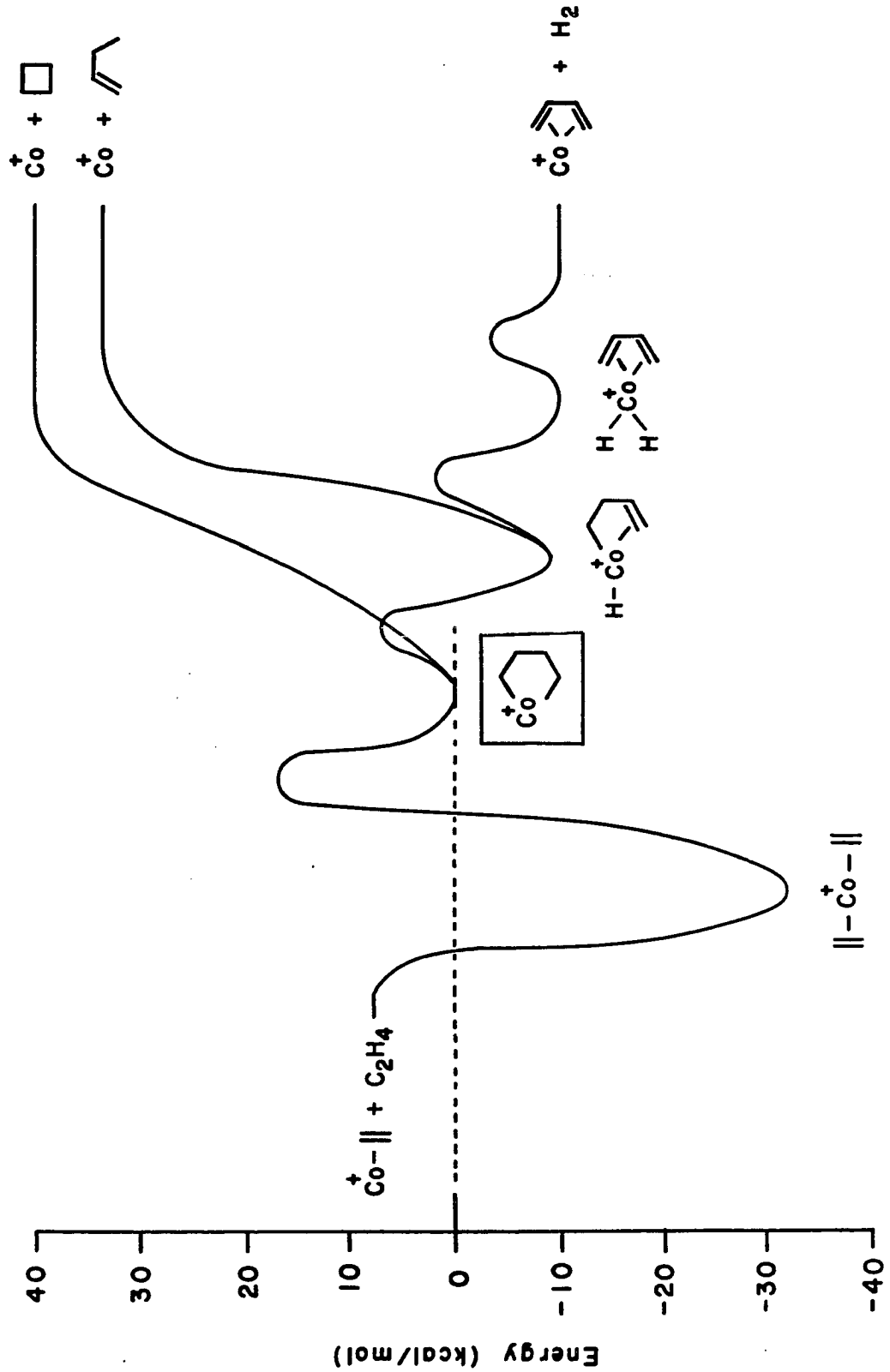
Energy (kcal/mol)
40
30
20
10
0
-10
-20
-30
-40
+ H2
+ C2H4

not seen in the gas phase[26].

A reaction coordinate diagram for the further decomposition of the metallacycle 36 is sketched in Figure 8. Dehydrogenation is the major product of this decomposition. Cleavage of the metallacycle to form $Co(C_2H_4)^+$ is shown as an endothermic process. The reverse reaction, addition of C_2H_4 to $M(C_2H_4)^+$ to form the metallacycle, would be detectable in gas phase studies by the subsequent dehydrogenation which leads to the formation of $Co(C_4H_6)^+$. Examples of these olefin-coupling processes in solution are numerous[44]. However, ICR experiments designed to discover systems for which this reaction occurs in the gas phase have not been successful[45,46]. This suggests an appreciable activation energy for metallacycle formation.

The diagram in Figure 8 predicts that reaction of Co^+ with cyclobutane and 1-butene will result in the formation of $Co(C_4H_6)^+$ and $Co(C_2H_4)^+$. This is consistent with previously reported studies of these reactions[4,5]. While the diagram in Figure 8 is quite complex, it is not constructed to show every intermediate which may be involved. For example, a π-allyl complex is probably formed in the interaction of Co^+ with 1-butene[4]. This species is not shown in Figure 8.

Conclusion

The present results for the reactions of Co^+ with ketones and aldehydes complement and are in general agreement with the previous studies of Fe^+ by Freiser and coworkers (Table I)[9]. The ability to vary kinetic energy in a quantitative fashion in the present study has provided additional insights into the mechanism and energetics of

observed reactions. Using thermochemical data which have recently become available, we have attempted to construct reaction coordinate diagrams such as shown in Figures 3, 7, and 8 which are at least semi-quantitative in describing reaction energetics.

Proposed reaction mechanisms for bare cobalt ions have close parallels in solution phase studies of cobalt and rhodium complexes[27,47-49]. The known chemistry of rhodium(I) complexes is of particular interest since species have been identified which decarbonylate aldehydes[27,47]. Compared to metal complexes in solution, however, bare metal ions in the gas phase are very reactive, capable of disrupting a complex structure in a single bimolecular encounter. This destructive behavior results from a desire on the part of the metal ions to become ligated, a process which is achieved by converting complex aldehydes and ketones into smaller molecular fragments, including alkanes, alkenes, carbon monoxide and hydrogen. It is clear, however, that insights into the synthesis of molecules can be gained by learning how they come apart and then considering what would be required to force the process in the reverse direction. For example, alkenes, hydrogen and carbon monoxide can be assembled to form aldehydes (hydroformylation process) using organometallic catalysts. Whereas group 8 metal ions oxidatively add to the C-CO bond of ketones (e.g., intermediates 1 or 8), reductive elimination via RH_2C-C(O)R bond coupling has been proposed to occur in the formation of ketones by reaction of acyl chlorides with alkyl cobalt and alkyl-rhodium complexes[48]. While Co^+ forms alkenes in the reactions with ketones described above, it has been suggested that ethene may insert into the Rh-H bond of $RC(O)-Rh(H)(PPh_3)_2Cl$ to generate $RC(O)C_2H_5$[50]. There are several salient

features of the proposed reaction coordinate diagrams that relate to the possible formation of molecular species. Reaction of $Co(CH_3)_2^+$ with CO may lead to formation of acetone by moving to the left along the potential energy diagram shown in Figure 3. The system does not have sufficient energy for acetone to be released, however, and the only reaction path available to the system will be to move back to the right and reductively eliminate ethane. In fact, any experiment which started with a stabilized Co^+-acetone complex and added increasing amounts of excitation would result in formation of the decarbonylation products. Removal of acetone could be achieved by a ligand displacement reaction, or by modifying the potential energy surface by attachment of spectator ligands which increase the activation energies for the initial step in the decarbonylation reaction.

Similar diagrams constructed for the reaction of Co^+ with cyclopentanone indicate that reaction of Co^+ with cyclobutane and 1-butene should yield $Co(C_2H_4)^+$ and $Co(C_4H_6)^+$. In fact, these processes are observed[4,5]. On the other hand, Figure 8 is constructed such that reaction of $Co(C_2H_4)^+$ with C_2H_4 will not yield the $Co(C_4H_6)^+$ ion. This conclusion is supported by unsuccessful searches for systems where this process occurs. For example, Ridge and coworkers have looked at the reactions of $Co(NO)(CO)_n^+$, n = 1-3, with C_2D_4[46]. Only ligand exchange reactions are observed. Similar results were reported by Jones and Staley for reactions of $CpCo^+$ with C_2D_4[51]. In analogy to the Co^+-acetone complex described above, at somewhat higher energies the Co^+-ethene adduct should be able to react with another molecule of ethene to form the metallacyclopentane. A high pressure ion source, now being constructed for the beam apparatus

will allow us to generate these sorts of adducts and monitor the kinetic energy dependence of their reactions.

Acknowledgment

This research was supported in part by the U.S. Department of Energy. Graduate fellowship support from Bell Laboratories and the Shell Companies Foundation (L.F.H.) is gratefully acknowledged.

Appendix

While there is a growing collection of thermochemical data for organometallic compounds[30, 52,53], there are few data from systematic examination of bond strengths of M-CO, M-R, M-COR, $(R)_nM$-CO, etc., in gas or condensed phase studies[54]. Transferring values known for one system to another can be used only as a first approximation. With this background in mind, the thermochemical estimates used in sketching the potential energy diagrams in Figures 3, 7 and 8 are listed in Table AI. Some of the considerations involved in assigning these values are discussed below.

The binding energies of aldehydes and ketones to Co^+ are not known. Jones and Staley have studied the relative bond dissociation energies for two ligand complexes of Co^+, $\delta D(Co^+-2L)$, with several organic molecules, including acetone and acetaldehyde[55]. Plotting $D(CpNi^+-L)$[56], where Cp = $\eta^5-C_2H_5$, versus $\delta D(Co^+-2L)$, one obtains a line of slope ~0.5, suggesting that the difference in binding energy of various ligands to Co^+ and $CpNi^+$ is similar. The absolute values of the binding energies of acetone and acetaldehyde to $CpNi^+$ are known[56], and the binding energies of formaldehyde and cyclopentanone to $CpNi^+$ can be predicted from their proton affinities[56,57]. These values are used as estimates for the binding energies of these compounds to Co^+, listed in Table AI. Because ketene is protonated on the methylene carbon rather than on oxygen[58], its proton affinity will not be related to its binding energy to $CpNi^+$ in a similar fashion. However, CO is not observed to displace ketene from $CpFe(CH_2CO)^+$[59]. Thus, we assume $D[Co^+-(CH_2CO)] > D[Co^+-CO]$.

The two ligand binding energies to Co^+ of the oxygen bases studied

Table AI. Thermochemical Estimates Used in Constructing Reaction Coordinate Diagrams

Bond	Binding Energy (kcal/mol)
$Co^+ \cdots O{=}CH_2$	43
$Co^+ \cdots O{=}CHCH_3$	47
$Co^+ \cdots O{=}C(CH_3)_2$	51
$Co^+ \cdots O{=}$ 	50
$Co^+ \ldots (CH_2CO)$	>40
Co^+-H	52 ± 4[a]
Co^+-CH_3	61 ± 4[a]
$Co^+{=}CH_2$	85 ± 7[a]
$(H)Co^+$-H	50
$(H_3C)Co^+$-H	41
$(H_3C)Co^+$-CH_3	40
Co^+-CO	40
RCo^+-CO	35
$(R_1)(R_2)Co^+$-CO	30
$H_2C{=}Co^+$-CO	30
Co^+-C(O)R	60
$(H_3C)Co^+$-C(O)R	40
HCo^+-C(O)R	50

Table AI. Continued.

Bond	Binding Energy (kcal/mol)
$Co^+-(C_2H_4)$	50
$(C_2H_4)Co^+-(C_2H_4)$	40
$Co^+-(C_4H_6)$	56

[a]Reference 30.

by Jones and Staley can also be correlated to binding energies to Li^+[55]. The slope of the line in the correlation plot of Li^+-L binding energies versus the relative dissociation enthalpy per ligand for Co^+ of the oxygen base ligands, ethers and alcohols, as well as ketones and aldehydes, is 1.10. This suggests that the mode of binding of the different ligands to Co^+ is similar in character to the binding of these ligands to Li^+. Calculations have shown that the Li^+-base bond is basically electrostatic[23]; thus, Li^+ binds to the lone pair on oxygen in these systems. Because of these considerations, the chemically activated species initially formed, structure 5 in Figure 3, is shown as binding end-on to the oxygen atom of the carbonyl group. Rearrangement can then lead to a π-bound complex.

The bond energies $D^o(Co^+\text{-}H)$ and $D^o(Co^+\text{-}CH_3)$ are known from previous ion beam studies[2]. Combining the methyl bond energy with the information that $D^o(Co^+\text{-}2CH_3) > 96$ kcal/mol (see above) gives a lower limit of $D^o[(H_3C)Co^+\text{-}CH_3] > 35$ kcal/mol. We have set $D^o[(H_3C)Co^+\text{-}CH_3]$ equal to 40 kcal/mol. Because the polarizable methyl group stabilizes the metal cation more than H, $D^o[(H_3C)Co^+\text{-}CH_3]$ will be smaller than $D^o[(H)Co^+\text{-}CH_3]$. The latter is chosen to be 50 kcal/mol. Thus, $D^o[(H_3C)Co^+\text{-}H] = 41$ kcal/mol, and likewise should be less than $D^o[HCo^+\text{-}H]$, to which a value of 50 kcal/mol is assigned.

Unfortunately, there are no estimates for binding energies of acyl and formyl groups to the gas phase ions. On the basis of some condensed phase studies, it has been suggested that metal alkyl and acyl bond energies are simliar[52,60-62]. The acyl and formyl binding energies listed in Table AI are equal to the methyl bond energy estimates.

The binding energy of CO to cobalt ions has also not been measured. The binding energy of CO to $CpNi^+$ is 40 kcal/mol[63]. Photoionization mass spectrometry studies have determined the appearance potentials for $Fe(CO)_n^+$, n = 1-5, and $Ni(CO)_n^+$, n = 1-4[64]. An average value for the binding energy of one CO to a metal ion from the above studies is ~40 kcal/mol. This value is listed in Table AI for $D[Co^+-CO]$. This binding energy should decrease as more polarizable ligands are added onto the metal.

Additional, and more speculative, estimates used in constructing the diagrams in Figure 7 and 8 are also listed in Table AI. Because the ring strain in 4- and 5-membered metallacylces is often found to be small[65], the binding energy for $(R_1R_2)-Co^+$, where R_1R_2 is $\cdot CH_2(CH_2)CH_2\cdot$, is estimated to be 5 kcal/mol less than $D[Co^+-2CH_3]$[66]. Previous studies have determined a lower bound for the binding energy of ethene to Co^+ of 36 kcal/mol[4]. The energies listed in Table AI reflect the fact that ethene is observed to displace CO in many gas phase organometallic systems[6,33,46,51]. Because $Co(C_4H_6)^+$ is not formed at low energies in the reaction of Co^+ with n-butane[2], the binding energy of Co^+ to butadiene is suggested to be less than ~56 kcal/mol[15].

References

1. Present address: a) Department of Chemistry, Yale University, New Haven, CT 06520, b) Department of Chemistry, University of California, Berkeley, CA 94720.
2. Armentrout, P. B.; Beauchamp, J. L. J. Am. Chem. Soc. 1981, 103, 784.
3. Halle, L. F.; Armentrout, P. B.; Beauchamp, J. L. Organomet. 1982, 1, 963.
4. Armentrout, P. B.; Halle, L. F.; Beauchamp, J. L. J. Am. Chem. Soc. 1981, 103, 6624.
5. Armentrout, P. B.; Beauchamp, J. L. J. Am. Chem. Soc., 1981, 103, 6628.
6. Halle, L. F.; Houriet, R.; Kappes, M. M.; Staley, R. H.; Beauchamp, J.L. J. Am. Chem. Soc., 1982, 104, 6293.
7. Corderman, R. R.; Beauchamp, J. L. J. Am. Chem. Soc. 1976, 98, 5700.
8. Burnier, R. C.; Byrd, G. D.; Freiser, B. S. Anal. Chem. 1980, 52, 1641.
9. Burnier, R. C.; Byrd, G. D.; Freiser, B. S. J. Am. Chem. Soc. 1981, 103, 4360.
10. a) Jacobson, D. B.; Freiser, B. S. J. Am. Chem. Soc. 1983, 105, 736. b) Jacobson, D. B.; Freiser, B. S. ibid., submitted for publication.
11. Kappes, M. M.; Ph. D. Thesis, Massachusetts Institute of Technology, 1981.
12. Ridge, D. P.; Allison, J. "Twenty Sixth Annual Conference on Mass Spectrometry and Allied Topics," 1978, p. 224.
13. Caserio, M. C.; Beauchamp, J. L. J. Am. Chem. Soc. 1972, 94, 2638.
14. Kuhlman, E. J.; Alexander, J. J. Coord. Chem. Rev. 1980, 33, 195. Flood, T. C.; Jenson, J. E.; Statler, J. A. J. Am. Chem. Soc. 1981, 103, 4410. Migratory insertion processes have also been noted in

cationic iron systems: Magnuson, R. H.; Zulu, S.; T'sai, W.-M.; Giering, W. P. J. Am. Chem. Soc. 1980, 102, 6888.

15. Supplementary heats of formation of organic molecules are taken from Cox, J. D.; Pilcher, G., "Thermochemistry of Organic and Organometallic Compounds," Academic Press: New York, 1970.

16. Heats of formation of organic radical species are taken from McMillen, D. F.; Golden, D. M., Ann. Rev. Phys. Chem. 1982, 33, 493.

17. Halle, L. F.; Beauchamp, J. L.,unpublished results.

18. Carbon-carbon bond dissociation energies of alkanes are typically in the range of 70 to 90 kcal/mol[16].

19. Robinson, P. J.; Holbrook, K. A. "Unimolecular Reactions," Wiley: London, 1972.

20. Traeger, J. C.; McLoughlin, R. G.; Nicholson, A. J. C. J. Am. Chem. Soc. 1982, 104, 5318.

21. Williams, J. W.; Hurd, C. D. J. Org. Chem. 1940, 5, 122.

22. The fact that $CoCH_2^+$ is not observed as a prominent reaction product at higher energies may suggest that 3 is somewhat more stable.

23. Woodin, R. L; Houle, F. A.; Goddard, W. A. III Chem. Phys. 1976, 14, 461.

24. a) Brown, K. L.: Clark, G. R.; Headford, C. E. L.; Marsden, K.; Roper, W. R. J. Am. Chem. Soc. 1979, 101, 503.

b) Walther, D. J. J. Organomet. 1980, 190, 393.

c) Driessen, W. L.; Groeneveld, W. L. Recl. Trav. Chem. 1969, 88, 1977.

25. Activation energies for reductive elimination of ethane and methane from platinum complexes are discussed in: Brown, M. P.; Puddephatt,

R. J.; Upton, C. E. E. J. Chem. Soc., Dalton Trans. 1974, 2457, and Abis, L; Sen, A.; Halpern, J. J. Am. Chem. Soc. 1978, 100, 2915.

26. Freas, R. B.; Ridge, D. P. J. Am. Chem. Soc. 1980, 102, 7129.

27. Milstein, D. Organomet. 1981, 1, 1549.

28. Headford, C. E. L.; Roper, W. R.; J. Organomet. Chem. 1980, 98, C7.

29. Thorn, D. L. Organomet. 1982, 1, 197; Thorn, D. L. J. Am. Chem. Soc. 1980, 102, 7109.

30. Armentrout, P. B.; Halle, L. F., Beauchamp, J. L. J. Am. Chem. Soc. 1981, 103, 6501.

31. Byrd, G. D.; Freiser, B. S. J. Am. Chem. Soc. 1982, 104, 5944.

32. The 14 electron cyclopentadienyl nickel ion, $CpNi^+$, is unreactive with both ethane and formaldehyde but does exclusively dehydrogenate larger alkanes[7]. Because $CpNi^+$ has added vibrational degrees of freedom compared to the bare metal ion, the above argument concerning the lifetimes of the intermediate 5 is not as relevant. It has been suggested that $CpNi^+$ reacts by first abstracting H^-. Thus, reaction should be observed with hydrocarbons having a greater hydride affinity than $CpNi^+$ (Corderman, R. R., Ph.D. Thesis, California Institute of Technology, 1977)[7].

33. Ethene-d_4 is observed to displace CO from $Ni(CO)^+$ (Reference 6) and $Fe(CO)^+$, Foster, M.S.; Beauchamp, J. L. J. Am. Chem. Soc. 1975, 97, 4808.

34. Also observed in the reactions of 2-butanone and 2-butanone-α,α'-d_5 is a small amount (3-6%) of $Co(COCH_2)^+$ which appears to be formed in an exothermic process. The generation of this product from the labeled butanone is difficult to explain.

35. Houriet, R.; Halle, L. F.; Beauchamp, J. L. Organomet., submitted for publication.

36. Hydridoacylmethyl iridium compounds have also been generated in solution, see for example, Milstein, D.; Calabrese, J. C. J. Am. Chem. Soc. 1982, 104, 3773.

37. The $C_7H_3O^+$ ion has the same mass as $Co(C_4H_6)^+$.

38. Beta-methyl transfers have been observed in condensed phase reactions as well; Watson, P. L.; Roe, D. C. J. Am. Chem. Soc. 1982, 104, 6471.

39. Studies of the reaction of Co^+ with ^{18}O-labeled cyclopentanone indicate that decarbonylation is the major process in which a neutral of 28 amu using the unlabeled reactant is eliminated, accounting for greater than 90% of the product. A minor product results in loss of ethene from the 3,4 sites on the ring (Kalmbach, K. A.; Ridge, D. P., unpublished results). The neutral products of reaction 13 are uncertain. Possibilities are H_2CO or H_2 + CO.

40. Jacobson and Freiser have also examined the reactions of Co^+ with cyclopentanone[10b]. The product distribution they resport is very similar to the one we observe at 1 eV relative kinetic energy.

41. Jacobson, D. B.; Freiser, B. S., submitted for publication.

42. This ion could also be partially due to loss of ethene in the reaction of Co^+ with cyclopentanone-α,α'-d_3, an impurity in our labeled compound.

43. Interestingly, in the reactions of group 8 metal ions with alkanes, deuterium scrambling processes appeared to play a significant role only for Co^+ in contrast to Fe^+ and Ni^+[2,35]. Evidence for scrambling processes was also noted above for the reaction of Co^+ with 3-pentanone-α,α'-d_4, Scheme V.

44. Grubbs, R. H.; Miyashita, A. J. Am. Chem. Soc. 1978, 100, 1300. Stockis, A.; Hoffmann, R. J. Am. Chem. Soc. 1980, 102, 2952, and references therein.

45. Hanratty, M. A.: Beauchamp, J. L., unpublished results.

46. Only ligand displacement reactions were seen in the reactions of $Co(NO)(Co)_n^+$, n = 1-3, with C_2D_4. No olefin coupling reactions were observed. Weddle, G. H.; Allison, J.; Ridge, D. P. J. Am. Chem. Soc. 1977, 99, 105.

47. Suggs, J. W. J. Am. Chem. Soc. 1978, 100, 640.

48. Schwartz, J.; Cannon, J. B. J. Am. Chem. Soc. 1974, 96, 4721.

49. An additional reaction of interest is the pyrolysis of acetyl complexes of the type $[PtXMe_2(COMe)L_2]$ (X = halogen, L = PMe_2Ph or $AsMe_2Ph$) which gives acetone and trans-$[PtXMeL_2]$ in quantitative yields. Ruddick, J. D.; Shaw, B. L. J. Chem. Soc. (A) 1969, 2969.

50. Lochow, C. F.; Miller, R. G. J. Am. Chem. Soc. 1976, 98, 1280.

51. Jones, R. W.; Staley, R. H. Int. J. Mass Spec. Ion Phys. 1981, 39, 35.

52. Halpern, J. Acc. Chem. Res. 1982, 15, 238.

53. Martinho Simões, J. A.; Beauchamp, J. L., to be published.

54. Connor, J. A.; Zafarani-Moattar, M. T.; Bickerton, J.: El Saied, N. I.; Suradi, S.; Carson, R.; Al Takhin, G.; Skinner, H. A. Organomet. 1982, 1, 1166.

55. Jones, R. W.; Staley, R. H. J. Phys. Chem. 1982, 86, 1387.

56. Corderman, R. R.; Beauchamp, J. L. J. Am. Chem. Soc. 1976, 98, 3998.

57. Aue, D. H.; Bowers, M. T., "Gas Phase Ion Chemistry," Vol. 2; Bowers, M. T., ed., Academic Press: New York, 1979.

58. Vogt, J.; Williamson, A. D.; Beauchamp, J. L. J. Am. Chem. Soc. 1978, 100, 3478.

59. Stevens, A. E.; Beauchamp, J. L. J. Am. Chem. Soc. 1978, 100, 2584.

60. Yoneda, G.; Blake, D. M. Inorg. Chem. 1981, 20, 67. See also, Yoneda, G.; Lin, S.-M.; Wang, L.-P.; Blake, D. M. J. Am. Chem. Soc. 1981, 103, 5768.

61. Brown, M. P.; Puddephatt, R. J.; Upton, C. C.; Lavington, S. W. J. Chem. Soc., Dalton Trans. 1974, 1613.

62. $D[R\text{-}Mn(CO)_5]$ for R = CH_3CO has been determined to be ~6 kcal/mol greater than for R = CH_3; reference 54.

63. Corderman, R. R. Ph.D. Thesis, California Institute of Technology, 1977.

64. Distefano, G. J. Res. Natl. Bur. Stand., Sect. A. 1970, 74, 233. The Fe^+-CO bond energy is given as 2.62 ± 0.1 eV (60.5 ± 2 kcal/mol). This latter value may be too high. The threshold for formation of $FeCO^+$ appears closer to 12.40 eV rather than 11.53 eV as suggested by Distefano. This lowers $D^o(Fe^+\text{-}CO)$ to 1.63 eV (37.6 kcal/mol).

65. Moore, S. S.; DiCosimo, R.; Sowinski, A.F.; Whitesides, G. M. J. Am. Chem. Soc. 1981, 103, 948. Steigerwald, M. L.; Goddard, W. A., III, private communication.

66. Estimates for $\Delta H_f(\cdot CH_2(CH_2)_2CH_2\cdot)$ are in the range of 61-67 kcal/mol; Doering, W. von E. Proc. Natl. Acad. Sci., USA 1981, 78, 5279. We have used a value of 62 kcal/mol in our calculations.

CHAPTER IV

FLUORINE SUBSTITUENT EFFECTS ON METAL-CARBENE BOND DISSOCIATION ENERGIES. IMPLICATIONS FOR METATHESIS REACTIONS OF FLUORINATED OLEFINS.

FLUORINE SUBSTITUENT EFFECTS ON METAL-CARBENE BOND DISSOCIATION ENERGIES. IMPLICATIONS FOR METATHESIS REACTIONS OF FLUORINATED OLEFINS

L. F. Halle, P. B. Armentrout[1], and J. L. Beauchamp

Contribution No. 6816 from the Arthur Amos Noyes Laboratory of Chemical Physics, California Institute of Technology, Pasadena, California 91125.

Abstract

The reactions of singly charged atomic nickel ions with ethylene oxide, cyclopropane, ethene, and several fluorinated hydrocarbons are examined by using an ion beam apparatus. Analysis of the thresholds for endothermic processes leading to the formation of nickel ion carbene species yields the bond dissociation energies, $D^{o}(Ni^{+}\text{-}CH_2)$ = 86 ± 6 kcal/mol and $D^{o}(Ni^{+}\text{-}CF_2)$ = 47 ± 7 kcal/mol. Although fluorine substitution results in a substantially weakened bond, the difluorocarbene is, in fact, more stable as judged by several criteria. For example, the reaction of $NiCH_2^{+}$ with C_2F_4 to yield $NiCF_2^{+}$ and CH_2CF_2 is exothermic by 20 kcal/mol. The implications of these carbene bond strengths for the metathesis of various fluorinated olefins is discussed.

Introduction

Metal carbenes are considered to be propagating intermediates in reactions such as olefin metathesis[2] and possibly olefin polymerization[3]. Little is known about the strength of the metal-carbene bond. Estimates of the relative strengths of π bonds in these species are sometimes derived from measured rotational barriers[4]. This analysis may lead to erroneous conclusions for metal systems in which more than a single d orbital is available for π-bonding[5]. Theoretical calculations for model metal carbene systems have provided some estimates of bond strengths[6,7]. Where comparison with experiment has been possible, the agreement is sufficiently poor to suggest that caution must be used in regarding the calculated bond strengths as useful estimates[7-9]. In our laboratory, we have developed experimental methods to directly measure carbene bond strengths to metal ions in the gas phase[9-11]. The present study reports the results of ion beam reactions of Ni^+ with various organic compounds which yield the metal carbene ions $NiCH_2^+$ and $NiCF_2^+$. Bond energies are derived from an examination of thresholds of endothermic reactions using theoretical techniques described previously. These bond strengths can be used to assess fluorine substituent effects on carbene stability and evaluate the energetics of gas phase metathesis reactions of fluorinated olefins with $NiCH_2^+$ and $NiCF_2^+$ as the propagating intermediates.

Experimental

The ion beam apparatus is described in detail elsewhere[10]. Ions from a surface ionization source are accelerated and focused into a 60^o sector magnet for mass separation. The mass selected beam in deceler-

ated to a chosen energy and focused into a collision chamber containing the reactant gas. Product ions scattered in the forward direction are focused into a quadrupole mass filter, and detected using a channeltron electron multiplier operated in a pulse counting mode. Ion signal intensities are corrected for the mass discrimination of the quadrupole mass filter.

The ion source, previously described, is comprised of a tubular stainless steel oven attached to the side of a U-shaped repeller plate which surrounds a rhenium ionization filament. The oven is loaded with $NiCl_2 \cdot 6H_2O$ in these experiments. The filament generates sufficient heat to dehydrate the nickel complex and vaporize $NiCl_2$. This vapor is directed at the filament where dissociation and ionization of the resulting Ni occurs. At the filament temperature used, $\sim$2500K, it is estimated that over 98% of the nickel ions produced are in the $3d^9$ ground state configuration (^2D), while less than 2% have the first excited state configuration, $4s3d^8(^4F)$, which lies 1.04 eV above the ground state[12].

The nominal collision energy of the ion beam is taken as the difference in potential between the collision chamber and the center of the filament, the latter being determined by a resistive divider. This energy is verified by use of a retarding field energy analyzer. Agreement was always within 0.3 eV. The energy distribution of the Ni^+ beam was also obtained using the retarding grid and was determined to be 0.7 eV (FWHM). In the center of mass frame, this introduces an uncertainty of less than $\pm$0.23 eV for reactions in which bond energies were determined. No specific account of the energy distribution of the ion beam is taken in the treatment below. A more severe problem concerning the actual energy

of interaction is the effect of the thermal motion of the reactant gas. This energy distribution effectively broadens any sharp features in the excitation function, including threshold. To account for this effect, the proposed excitation function is convoluted with this distribution before comparison with the data using the method outlined by Chantry[13].

Reaction cross sections for a specific product, σ_i, are calculated from

$$\sigma_i = \sigma I_i / \Sigma I_i \qquad (1)$$

where the sum is over all products and I_i refers to a particular measured product ion intensity. The total reaction cross section, σ, is evaluated using

$$I_o = (I_o + \Sigma I_i) \exp(-n\sigma\ell) \qquad (2)$$

where I_o is the transmitted reactant ion beam intensity, n is the number density of the target gas, and ℓ is the length of the interaction region. The pressure of the target gas, measured using an MKS Baratron Model 90H1 capacitance manometer, is kept sufficiently low, $1\text{-}5 \times 10^{-3}$ Torr, that attenuation of the ion beam is minimal. The length of the interaction region is 5 mm and is uncorrected for entrance and exit aperture effects [14] (1.0 and 1.5 mm in diameter, respectively).

The greatest uncertainty in measurements of reaction cross sections is the ion detection efficiency. At laboratory energies below about 10 eV, a small field of 0.5 V is placed across the specially designed collision chamber[15] to extract low energy ions. This field introduces an additional uncertainty in the energy of interaction. Relative cross sections are well reproduced, and we estimate that the absolute cross

sections reported are accurate to a factor of two.

In a previous paper[10], a functional form for the energy-dependent cross section was suggested. This formula, used in examining the endothermic reactions presented here, is:

$$\sigma = \begin{cases} 0 & E \leqslant E_o \\ \sigma_o\left(\frac{E-E_o}{E}\right)^n & E_o < E < E_o + D/a \\ \sigma_o\left(\frac{D}{aE}\right)^n & E \geqslant E_o + D/a \end{cases} \qquad (3)$$

where E is the total energy of the reactants and E_o is the endothermicity of the reaction, taken to be the difference between the bond energy of the ionic product, D, and the bond energy of the neutral reactant. The average fraction of the total internal energy of the products in the ionic fragment is given by a , and n is a variable exponent which equals one when using the line of centers model[16]. If the reaction involves a long-lived intermediate, n is large and may be a sizable fraction of the total number of vibrational degrees of freedom[10]. In fitting the data, the curves equation 3 describes are convoluted using the method of Chantry[13] to account for the thermal motion of the reactant gas as discussed above. Often, within experimental error, several sets of parameters fit the data equally well and thus give a range of possible threshold energies. This is how the uncertainty in E_o is determined.

It is important to point out that in these experiments neutral products are not detected. However, except at higher energies, the identity of these products can usually be inferred without ambiguity. In addition, these experiments provide no direct structural information about

the ionic products. However, straightforward thermochemical arguments can often distinguish possibilities for isomeric structures.

Results

Nickel Carbene. Reaction of nickel ions with ethylene oxide at low energies yields a number of products having large cross sections which decrease with increasing energy (Figure 1). This behavior implies that these processes are exothermic. Scheme I outlines a possible mechanism

Scheme I

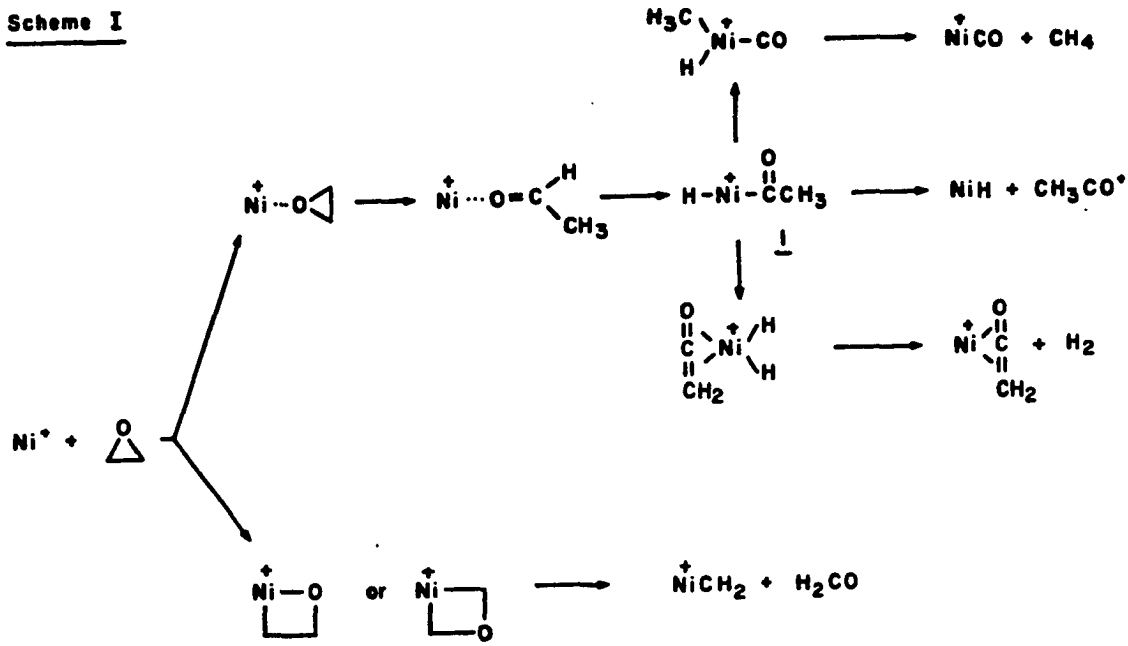

for the production of these species. Initial interaction of Ni^+ with ethylene oxide may be associated with the basic oxygen center to produce a chemically activated species which can rearrange to acetaldehyde. A hydrido acyl compound, analogous to 1, is formed in the reaction of $Rh(PPh_3)_3Cl$ with ethylene oxide[17]. Moreover, this same hydridoacyl is formed in the reaction of $Rh(PPh_3)_3Cl$ with acetaldehyde. Upon heating, methane is evolved[18]. In experiments using the technique of ion

Figure 1. Variation in experimental cross section for the interaction of Ni^+ with ethylene oxide as a function of kinetic energy in the center of mass frame (lower scale) and laboratory frame (upper scale).

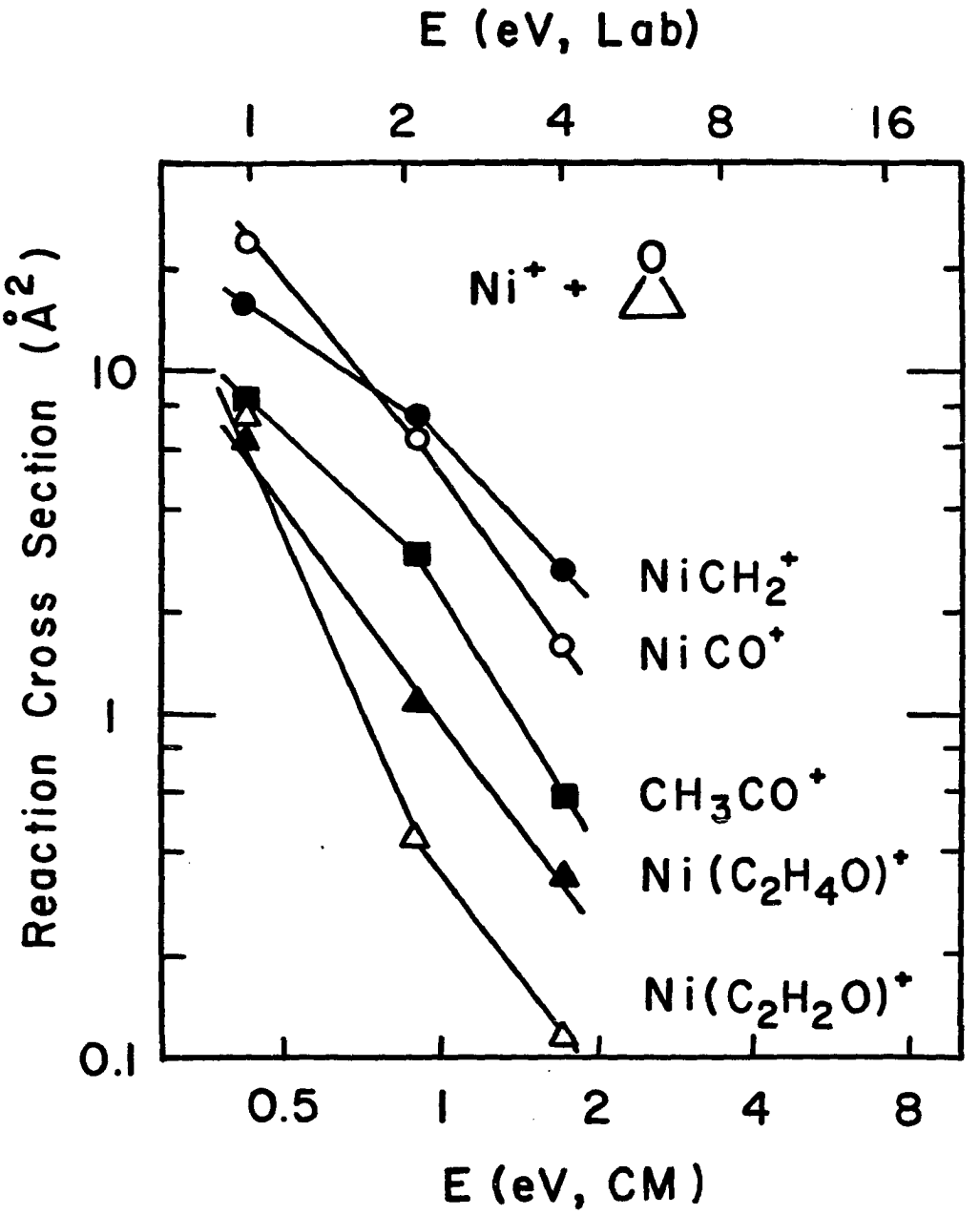
E (eV, Lab)
1
2
4
8
16
Reaction Cross Section (Å²)
10
1
0.1
Ni⁺ +
NiCH₂⁺
NiCO⁺
CH₃CO⁺
Ni(C₂H₄O)⁺
Ni(C₂H₂O)⁺
0.5
1
2
4
8
E (eV, CM)

cyclotron resonance mass spectrometry, reaction of $(\eta^5\text{-}C_5H_5)Ni^+$ with CH_3CHO yielded only the $(\eta^5\text{-}C_5H_5)NiCO^+$ product[19]. Other studies have shown that $M(CO)^+$, M = Co, Fe, is the only exothermic product formed in the interaction of M^+ with acetaldehyde[20,21]. Ni^+ may also insert into the carbon-carbon or a carbon-oxygen bond of ethylene oxide as steps prior to formation of the carbene.

The exothermic formation of $C_2H_3O^+$ indicates that the bond energy for NiH must be greater than 1.98 eV (see Table I). This is consistent with Gaydon's value of 2.6 eV[22]. In order for the process forming $NiCH_2^+$ to be exothermic, the metal ion carbene bond energy must be greater than the enthalpy change, ΔH = 3.43 eV (see Table I for thermochemical data used), for reaction 4.

$$\text{cyclo-}C_2H_4O \rightarrow CH_2O + CH_2 \qquad (4)$$

At low energies, the cross section for formation of $NiCH_2^+$ from the reaction of Ni^+ with cyclopropane, Figure 2, is small. As reaction energy is increased, the cross section reaches a maximum and then falls off. This is typical behavior for an endothermic process. Thus, the bond energy for $NiCH_2^+$ must be less than the enthalpy change, ΔH = 3.99 eV (see Table I) for reaction 5.

$$\text{cyclo-}C_3H_6 \longrightarrow C_2H_4 + CH_2 \qquad (5)$$

The lines drawn in Fig. 2 show three fits to the data using equation 3, giving rise to a range of threshold energies, E_o = 0.48 - 0.60 eV. The fit chosen as the best description of the data uses n = 5, $\sigma_o = 6.1 \text{Å}^2$, E_o = 0.55 eV, and a = 0.68. In this case, the uncertainties

Table I. Thermochemical Data Used in This Study

Species	$\Delta H^o_{f,298}$(eV)	$\Delta H^o_{f,298}$(kcal/mol)	Reference
CH_2	4.01	92.4 ± 1.0	a
CF_2	-1.91	-44.0 ± 1.0	b
C_2H_4	0.534	12.45 ± 0.3	c
CH_2CF_2	-3.47	-80.1 ± 0.8	c
C_2F_4	-8.47	-157.9 ± 0.4	c
c-C_3H_6	0.552	12.7 ± 0.1	c
H_2CO	-1.13	-25.98 ± 0.2	c
CH_2CO	-0.494	-11.4 ± 0.6	c
c-C_2H_4O	-0.545	-12.6 ± 0.15	c
H^-	1.505	34.7	d
CH_3CO^+	7.167	157.0 ± 0.4	e
Ni^+	12.07	278.3	f

a) Chase, M. W.; Curnett, J. L.; Prophet, H.; McDonald, R. A.; Syverud, A. N. J. Phys. Chem. Ref. Data, Suppl. 1975, 4, No. 1.

b) Schug, K. P.; Wagner, H. G. Ber. Bunsenges, Phys. Chem. 1978, 82, 719.

c) Pedley, J. B.; Rylance, J. "Sussex-N.P.L. Computer Analysed Thermo-Chemical Data: Organic and Organometallic Compounds" Sussex University: Sussex, 1977.

d) EA(H) = 0.754 eV from Wagman, D. D.; Evans, W. H.; Parker, V. B.; Halow, I.; Bailey, S. M.; Schumm, R. H. Natl. Bur. Stand. Tech. Note 270-3, 1968.

Table I. continued

e) Traeger, J. C.; McLoughlin, R. G.; Nicholson, A. J.C. J. Am. Chem. Soc. 1982, 104, 5318.

f) Rosenstock, H. M.; Draxl, K.; Steiner, B. W.; Herron, J. T. J. Phys. Chem. Ref. Data 1977, 6, Suppl. 1.

Figure 2. Variation in experimental cross section as a function of kinetic energy in the center of mass frame (lower scale) and the laboratory frame (upper scale) for the formation of $NiCH_2^+$ from reaction of Ni^+ with cyclopropane. Arrows mark the threshold at 0.55 eV and the energy needed to produce methylene and ethene from cyclopropane, 4.0 eV. The curves are the convoluted fits to the data as discussed in the text.

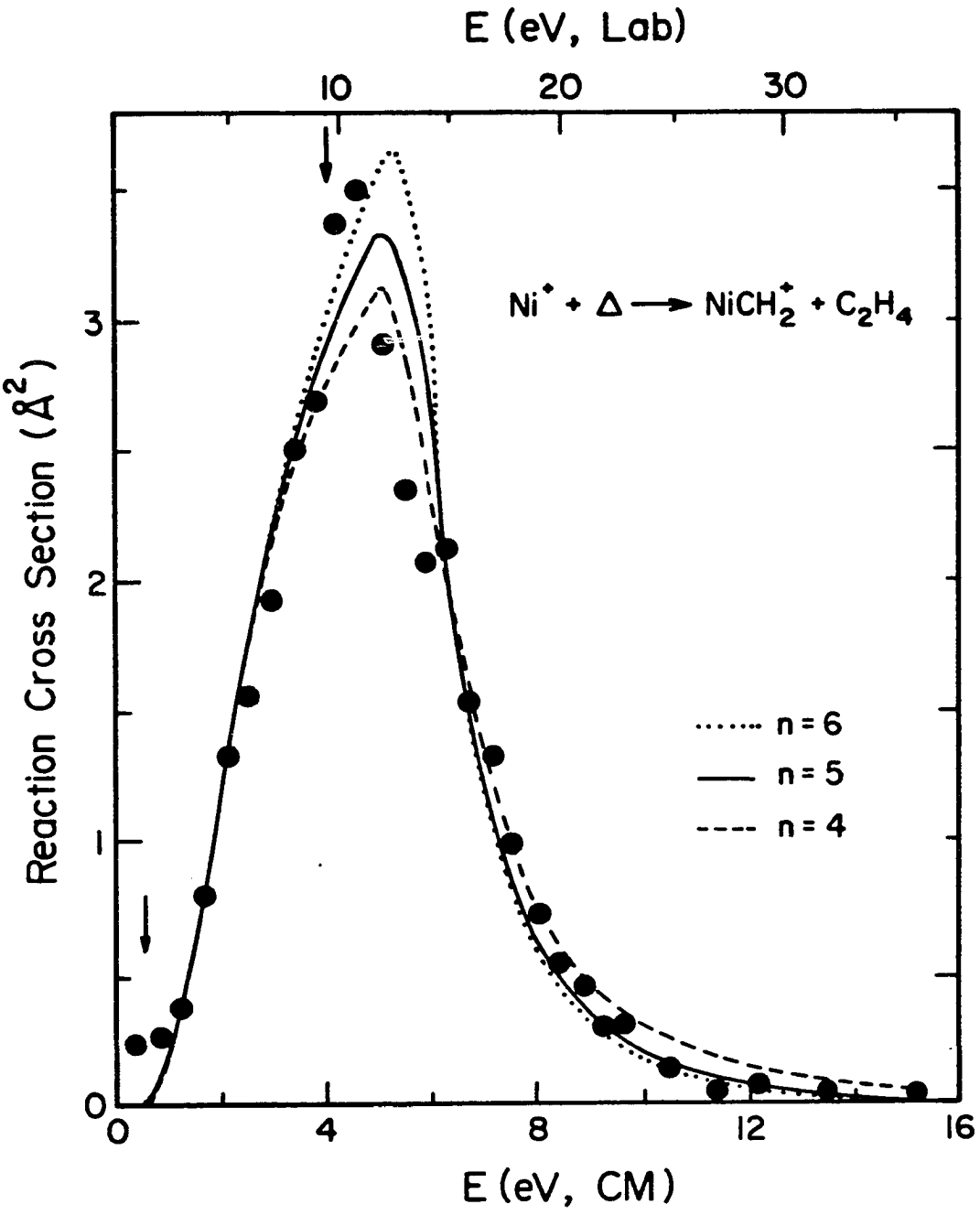
E (eV, Lab)
10
20
30
Reaction Cross Section (Å²)
3
2
1
0
Ni⁺ + Δ → NiCH₂⁺ + C₂H₄
n = 6
n = 5
n = 4
0
4
8
12
16
E (eV, CM)

set by the various good fits are small due to the low E_o, and do not accurately represent the uncertainty in the experimental data. From this last fit, a bond energy $D^o(Ni^+-CH_2) = 3.45 \pm 0.3$ eV is calculated.

Results for reaction of Ni^+ with ethene to yield $NiCH_2^+$ are shown in Figure 3. The theoretical fit uses n = 5, $\sigma_o = 8.5 Å^2$, $E_o = 3.4$ eV, and a = 0.81. From this threshold, a bond strength $D^o(Ni^+-CH_2) = 4.1 \pm 0.3$ eV is derived.

Nickel Fluorocarbenes. The products formed in the reaction of Ni^+ with C_2F_4 are given in equations 6-8. All of these products are formed

$$Ni^+ + C_2H_4 \rightarrow \begin{cases} NiF^+ + C_2F_3 & (6) \\ NiCF_2^+ + CF_2 & (7) \\ NiC_2F_3^+ + F & (8) \end{cases}$$

in endothermic processes. The thresholds for reactions 6 and 8 were not examined. Detailed cross section data for reaction 7 are shown in Figure 4. The maximum cross section occurs at ~3.8 eV relative kinetic energy. At this energy, reaction 7 accounts for 80% of the products observed. At higher energies, NiF^+ becomes the dominant product ($\sigma[NiF^+] = 1 Å^2$ at 6.3 eV relative kinetic energy). The fit to the data shown in Figure 4 is given by equation 3 with n = 4, $\sigma_o = 4.7 Å^2$, $E_o = 1.0$ eV, and a = 0.60. Given the F_2C-CF_2 bond energy in tetrafluoroethene of 69.9 kcal/mol (see Table I), a bond energy $D^o[Ni^+-CF_2]$ of 47 ± 7 kcal/mol (2.0 ± 0.3 eV) is calculated.

In unsuccessful attempts to find other sources for the fluorocarbenes, we briefly examined the reaction of Ni^+ with carbon tetrafluoride,

Figure 3. Variation in experimental cross section with kinetic energy in the center of mass frame (lower scale) and the laboratory frame (upper scale) for the formation of $NiCH_2^+$ from the reaction of Ni^+ with ethene. Arrows indicate the threshold energy for reaction, 3.4 eV, and the carbon-carbon bond energy of ethene, 7.47 eV. The curve is the fit to the data given in the text and convoluted as discussed.

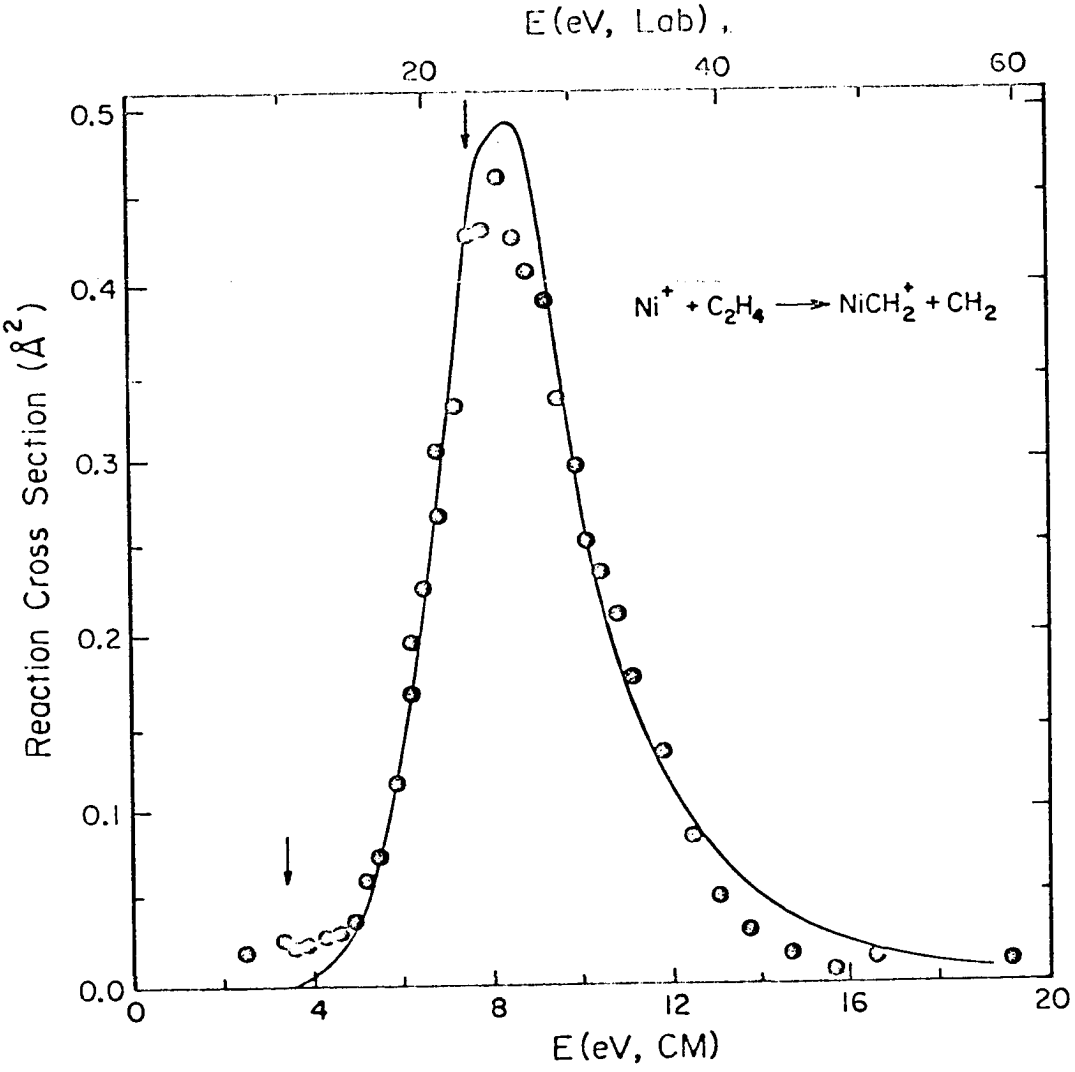
E(eV, Lab)
20
40
60
0.5
0.4
0.3
0.2
0.1
0.0
Reaction Cross Section (Å²)
Ni⁺ + C₂H₄ → NiCH₂⁺ + CH₂
0
4
8
12
16
20
E(eV, CM)

Figure 4. Variation in experimental cross section with kinetic energy in the center of mass frame (lower scale) and the laboratory frame (upper scale) for the formation of $NiCF_2^+$ from the reaction of Ni^+ with tetrafluoroethene. Arrows indicate the threshold energy for reaction, 1.0 eV, and the carbon-carbon bond energy of C_2F_4, 3.03 eV. The curve is the fit to the data given in the text and convoluted as discussed.

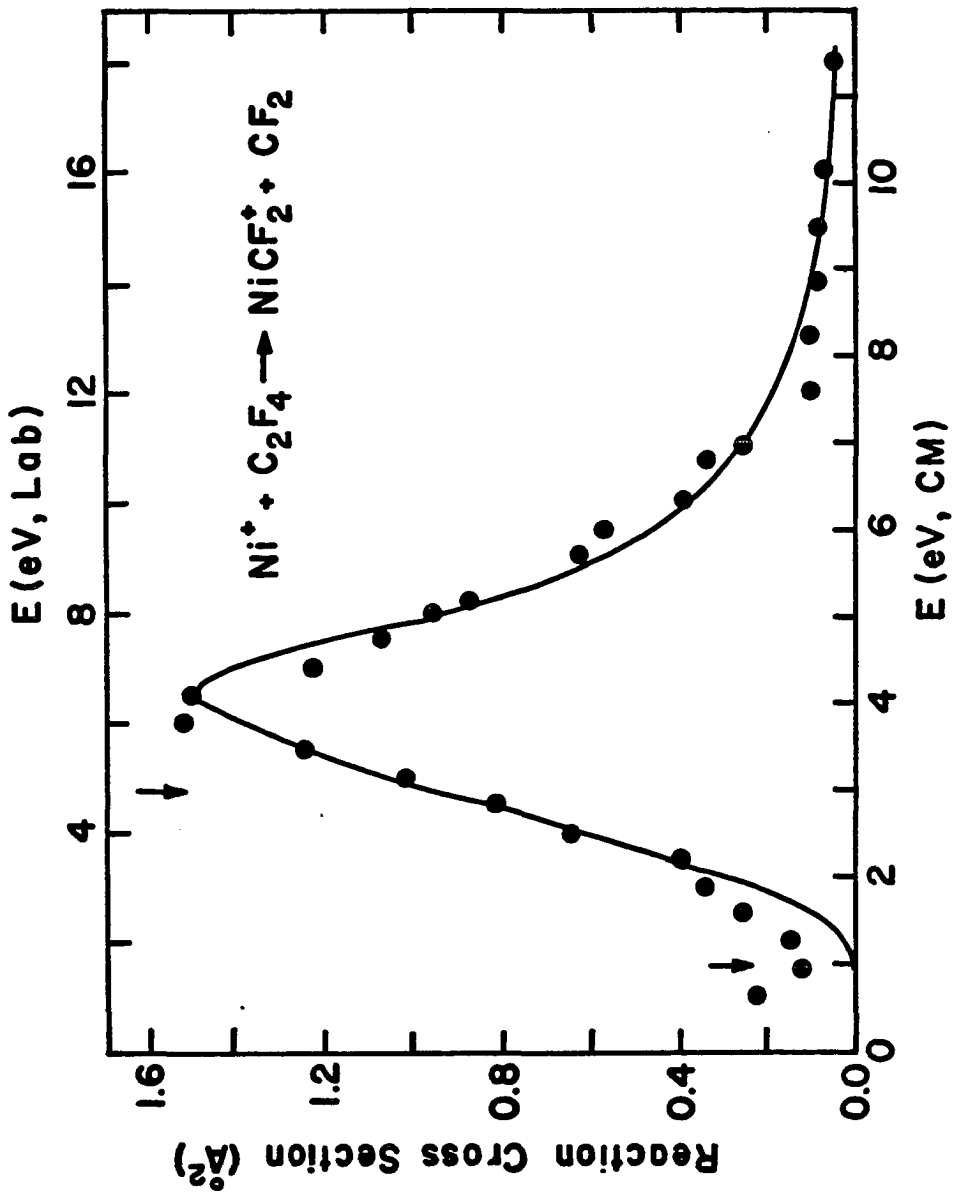
Reaction Cross Section (Å²)
0.0
0.4
0.8
1.2
1.6
E (eV, Lab)
4
8
12
16
E (eV, CM)
2
4
6
8
10
Ni⁺ + C₂F₄ → NiCF₂⁺ + CF₂

1,1-difluoroethene and cis-1,2-difluoroethene. Only endothermic processes were observed, but no thresholds were derived. The lowest energy processes in the interaction of Ni^+ with CF_4 are given in reactions 9 and 10. At higher energies (>7 eV relative kinetic energy) small

$$Ni^+ + CF_4 \longrightarrow NiF^+ + CF_3 \quad (9)$$

$$Ni^+ + CF_4 \longrightarrow CF_3^+ + NiF \quad (10)$$

amounts of CF^+ and CF_2^+ appear. A small amount (< 0.3 $Å^2$) of $NiCH_2^+$ is formed in the reaction with 1,1-difluoroethene, but no $NiCF_2^+$ is observed. The largest product (σ_{max} ~ 2 $Å^2$ at 0.7 eV relative kinetic energy) is NiF^+, and some $C_2H_2F^+$ and NiC_2H^+ are also seen. These latter three products are the only ones observed in the reaction of Ni^+ with 1,2-difluoroethene.

Discussion

$NiCH_2^+$. Table II lists the thermochemical results obtained from the reactions of Ni^+ studied leading to formation of $NiCH_2^+$. The bond strength of the nickel carbene species is estimated to be $D^o(Ni^+-CH_2)$ = 3.75 ± 0.25 eV (86 ± 6 kcal/mol), an average value determined from the threshold of cyclopropane reaction and the limit set by the endothermicity of this reaction. The bond energy derived from the results with ethene, $D^o(Ni^+-CH_2)$ > 4 eV, reflects the experimental errors as well as possible inaccuracies in the theoretical analysis.

It is useful to compare the results and analysis of reactions of Ni^+ with previous experiments in which the reactant ion was Co^+ [10]. In particular, the comparison for Co^+ reacting with ethene to yield $CoCH_2^+$

Table II. Experimental Results for $D^0(Ni^+-CH_2)$

Reaction	$D^0(Ni^+-CH_2)$, eV	kcal/mol
$Ni^+ + C_2H_4O \rightarrow NiCH_2^+ + CH_2O$	>3.43	79.0
$Ni^+ + C_3H_6 \rightarrow NiCH_2^+ + C_2H_4$	<3.99	92.1
	3.45 ± 0.3[a]	79.6 ± 7
$Ni^+ + C_2H_4 \rightarrow NiCH_2^+ + CH_2$	4.1 ± 0.3[a]	95 ± 7

a) Calculated from threshold for reaction using theory as described in text.

is shown in Figure 5 [23]. Also shown are the data for $NiCH_2^+$ from this system normalized to the corresponding $CoCH_2^+$ data, as well as the excitation function for $NiCH_2^+$ multiplied by this same normalization factor. The theoretical fits to the data for formation of $NiCH_2^+$ and $CoCH_2^+$ from reaction with ethene have very similar shapes, and both use the same value of n = 5. The excitation function for the $CoCH_2^+$ product is diplaced approximately 0.3 eV higher than that for $NiCH_2^+$. The threshold for formation of $CoCH_2^+$ from ethene is 3.8 eV [10], which suggests that the $NiCH_2^+$ product should have a threshold of about 3.5 eV, or a bond energy of about 4 eV. This value is in reasonable agreement with the threshold energy taken directly from Figure 3, D_o = 3.4 ± 0.3 eV, and is in slightly better agreement with the other determinations of this bond energy than the latter value. It is not clear why the maximum cross section for the metal carbene ion from reaction with ethene is three times larger for the Co^+ system compared to the Ni^+ system. The analogous reaction of Fe^+ has a maximum cross section of 1.8 $Å^2$ [24]. A comparison of metal ion carbene bond strengths is discussed elsewhere[9,11]. Briefly, we note that the group 8 metal ion bond energies are similar, with the iron system having a slightly higher bond strength; $D^o(Co^+-CH_2)$ = 85 ± 6 kcal/mol, and $D^o(Fe^+-CH_2)$ = 96 ± 5 kcal/mol.

The results of these studies indicate that the Ni^+-CH_2 bond (86 kcal/mol) is almost twice as strong as the Ni^+-CF_2 bond (47 kcal/mol). A similar weakening of the metal carbene bond energies by successive fluorine substitution has been noted previously for the bond energies of $(CO)_5Mn^+-CXY$ where X,Y = H or F [11]. The bond strengths for these systems were determined by photoionization mass spectrometry and are

Figure 5. Variation in experimental cross section with kinetic energy in the center of mass frame (lower scale) and the laboratory frame (upper scale) for the formation of MCH_2^+ from the reaction of M^+ with ethene. Dotted line is the fit to the data for $M^+ = Ni^+$, dashed line is the same multiplied by 3.24. Solid curve is the fit to the data for $M^+ = Co^+$. Arrows indicate the threshold for the Ni^+ reaction at 3.4 eV, the threshold for the Co^+ reaction at 3.8 eV, and the carbon–carbon bond energy of ethene, 7.47 eV.

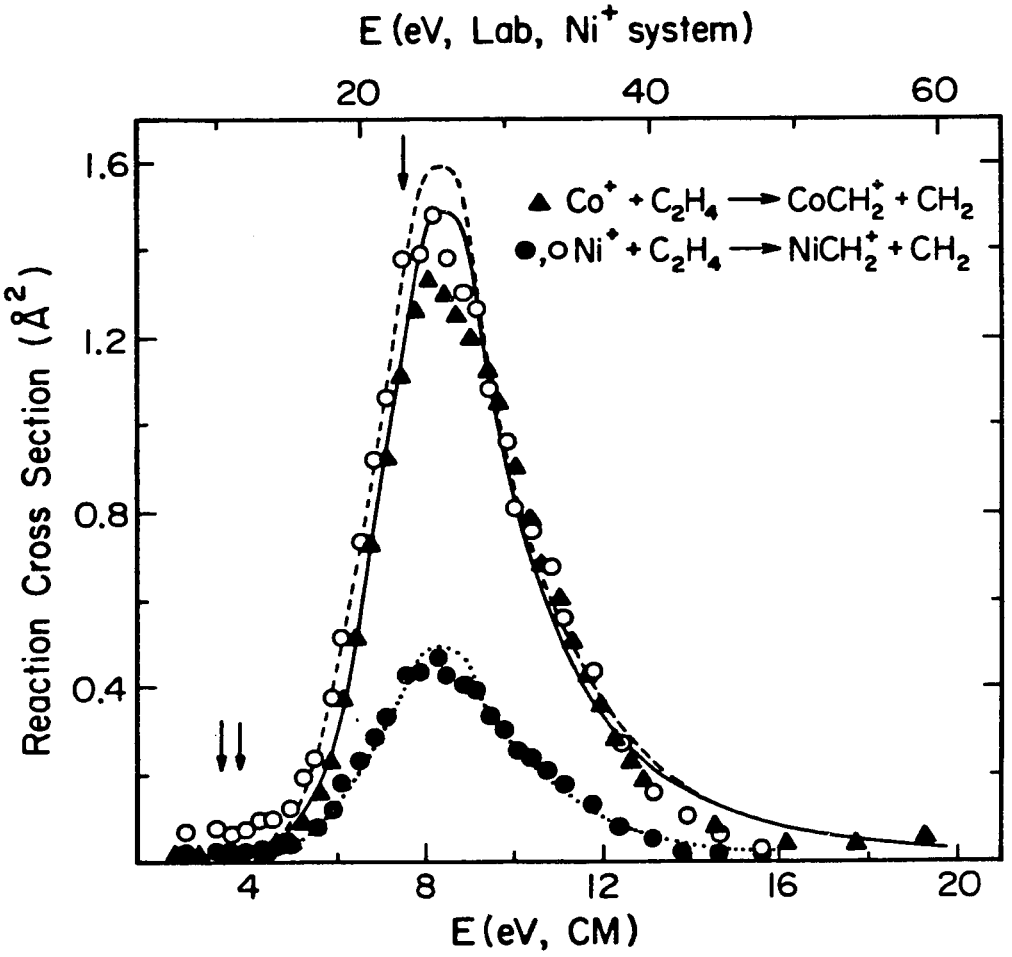
E (eV, Lab, Ni+ system)
20
40
60
1.6
1.2
0.8
0.4
Reaction Cross Section (Å2)
▲ Co+ + C2H4 → CoCH2+ + CH2
●,○ Ni+ + C2H4 → NiCH2+ + CH2
4
8
12
16
20
E (eV, CM)

listed along with the present results in Table III. A difference of 14 kcal/mol between the bond strength of $(CO)_5Mn^+-CH_2$ and $(CO)_5Mn^+-CF_2$ is measured. This difference is smaller than that of the bare nickel ion, but still substantial[25]. It is interesting to note that the carbon-carbon bond energy in tetrafluoroethene is over 100 kcal/mol less than that of ethene.

The thermochemical data of the present study can be used to assess the enthalpy changes of the metathesis reactions 11 and 12. The enthalpy

$$NiCH_2^+ + CF_2CF_2 \rightarrow NiCF_2^+ + CH_2CF_2 \qquad (11)$$

$$NiCH_2^+ + CH_2CF_2 \rightarrow NiCF_2^+ + CH_2CH_2 \qquad (12)$$

change for reaction 12 is calculated to be $\Delta H = -20$ kcal/mol, and that for reaction 11 is $\Delta H = -5$ kcal/mol (see Tables I and III). The exothermicity of these processes leading to $NiCF_2^+$ suggests that the weak Ni^+-CF_2 bond should not be interpreted to imply a lack of stability of this species.

The thermochemistry determined above is also useful in judging whether these carbenes can act as catalytic intermediates in the olefin metathesis reaction 13. The catalytic cycle is

$$CH_2CH_2 + CF_2CF_2 \rightarrow 2CH_2CF_2 \qquad (13)$$

given by reaction 11 followed by the reverse of reaction 12. For both these steps to be exothermic in the general case, the inequalities shown in equation 14 must hold. The limits depend only on the heats of

Table III. Carbene Bond Energies[a]

Ion	$D[Ni^+-CX_2]$	$D[(CO)_5Mn^+-CXY]$[b]
$NiCH_2^+$	86 ± 6	
$NiCF_2^+$	47 ± 7	
$(CO)_5MnCH_2^+$		93 ± 8
$CO)_5MnCHF^+$		91 ± 9
$(CO)_5MnCF_2^+$		79 ± 3

a) All values in kcal/mol at 298 K.

b) Data from Reference 11.

$$43.9 \text{ kcal/mol} < D^{o}(M\text{-}CH_2) - D^{o}(M\text{-}CF_2) < 58.6 \text{ kcal/mol} \quad (14)$$

formation of the olefins, given in Table I. The difference in carbene bond energies for the nickel ion system considered in the present study is 39 ± 9 kcal/mol (Table III). Thus, the nickel ion carbene and difluorocarbene may be only marginally able to catalyze reaction 13. Other systems may prove to be better candidates for this process.

Acknowledgments

This research was supported in part by the U.S. Department of Energy. Graduate fellowship support from Bell Laboratories, SOHIO, and the Shell Companies Foundation (L.F.H.) is gratefully acknowledged.

References

1. Present address: Department of Chemistry, University of California, Berkeley, California 94720.
2. Calderon, N.; Lawrence, J. P.; Ofstead, E. A. Adv. Organomet. Chem. 1979, 17, 449.
3. Ivin, K. J.: Rooney, J. J.; Stewart, C. D.; Green, M. L. H.; Mahtab, R. J. Chem. Soc., Chem. Commun. 1978, 604.
4. Kiel, W. A.; Lin, G. Y.; Constable, A. G.; McCormick, F. B.: Strouse, C. E.; Eisenstein, O.; Gladysz, J. A. J. Am. Chem. Soc. 1982, 104, 4865. See also Kegley, S. E.; Brookhart, M. Organomet. 1982, 1, 760.
5. Francl, M. M.; Pietro, W. J.: Hout, R. F., Jr.; Hehre, W. J. Organomet., submitted for publication.
6. Rappé, A. K.; Goddard, W. A., III J. Am. Chem. Soc. 1977, 99, 3966.
7. a) Brooks, B. R.; Schaefer, H. F., III Molec. Phys. 1977, 34, 193. b) Vincent, M. A.; Yoshioka, Y.; Schaefer, H. F., III J. Phys. Chem. 1982, 86, 3905.
8. Stevens, A. E.; Beauchamp, J. L. J. Am. Chem. Soc. 1979, 101, 6449.
9. Armentrout, P. B.; Halle, L. F.; Beauchamp, J. L. J. Am. Chem. Soc. 1981, 103, 6501.
10. Armentrout, P. B.; Beauchamp, J. L. J. Chem. Phys. 1981, 75, 2819.
11. Stevens, A. E.; Berman, D. W.; Beauchamp, J. L. J. Am. Chem. Soc., submitted for publication.
12. Moore, C. E. "Atomic Energy Levels," Natl. Bur. Stand., Washington, D.C., 1949.
13. Chantry, P. J. J. Chem. Phys. 1971, 55, 2746.

14. Nenner, T.; Tien, H.; Fenn, J. B. J. Chem. Phys. 1975, 63, 5439.

15. Armentrout, P. B.; Hodges, R. V.; Beauchamp, J. L. J. Chem. Phys. 1977, 66, 4683.

16. Levine, R. D.; Bernstein, R. B. "Molecular Reaction Dynamics," Oxford: New York, 1972.

17. Milstein, D. J. Am. Chem. Soc. 1982, 104, 5228. See also Milstein, D.; Calabrese, J. C. J. Am. Chem. Soc. 1982, 104, 3773.

18. Milstein, D. Organomet. 1982, 1, 1549.

19. Corderman, R. R.; Beauchamp, J. L. J. Am. Chem. Soc. 1976, 98, 5700.

20. Burnier, R. C.; Byrd, G. D.; Freiser, B. S. J. Am. Chem. Soc. 1981, 103, 4360.

21. Halle, L. F.; Crowe, W. E.; Armentrout, P. B., Beauchamp, J. L., to be submitted for publication.

22. Gaydon, A. G. "Dissociation Energies and Spectra of Diatomic Molecules," Chapman and Hall: London, 1968.

23. Data for the reaction of Co^+ with ethylene oxide are similar to that to Ni^+, indicating exothermic production of $CoCH_2^+$. The excitation function for the carbene product formed in the reaction of Co^+ with cyclopropane shows complications which are not observed in the Ni^+ reaction. See Reference 10.

24. It is interesting to note that the maximum cross section for formation of MCH_3^+ from the reaction of M^+ with ethane is 2.1 $\AA^2$ for Co^+ and Ni^+, but lower for Fe^+(0.7 $\AA^2$).

25. Theoretical calculations (STO-3G level) for substituted titanium carbenes predict systems for which the monofluoro-carbene bond to the metal should be stronger than the M-CH_2 bond. The difluoro-carbene

was not examined. Francl, M. M.; Pietro, W. J.; Hout, R. F., Jr.; Hebre, W. J. Organomet. 1983, 2, 281.

CHAPTER V

PROPERTIES AND REACTIONS OF ORGANOMETALLIC FRAGMENTS IN THE GAS PHASE. ION BEAM STUDIES OF FeH^+.

PROPERTIES AND REACTIONS OF ORGANOMETALLIC FRAGMENTS IN THE GAS PHASE. ION BEAM STUDIES OF FeH^+

L. F. Halle, F. S. Klein[1], and J. L. Beauchamp

Contribution No. 6813 from the Arthur Amos Noyes Laboratory of Chemical Physics, California Institute of Technology, Pasadena, California 91125.

Abstract

Analysis of the thresholds for the reactions of Fe^+ with H_2 and D_2 studied with an ion beam apparatus yield the bond dissociation energy $D^o(Fe^+-H) = 59 \pm 5$ kcal/mol. From this bond strength the proton affinity of an iron atom, $PA(Fe) = 190 \pm 5$ kcal/mol is calculated. Ion beam studies of the deprotonation of FeH^+ by bases of various proton affinities are consistent with this value. Hydride transfer reactions of these bases with FeH^+ yield a lower limit for the hydride affinity of FeH^+, $D^o(HFe^+-H^-) > 232$ kcal/mol. These energetics indicate that oxidative addition of H_2 to an iron atom is exothermic by at least 22 kcal/mol. The nearly thermoneutral formation of FeD^+ in the reaction of FeH^+ with D_2 occurs only with a small cross section at higher energies and exhibits a threshold of 20 ± 7 kcal/mol. If oxidative addition of D_2 to iron precedes reductive elimination of HD, then this activation energy implies a significant barrier for formation of an Fe(IV) intermediate. Alternatively, if the exchange process involves a 4-center transition state, the observation of a significant activation energy is consistent with recent theoretical predictions that such processes are unfavorable if the metal-hydrogen bond has predominantly metal-s or p character. Correlations of experimental bond energies with promotion energies provide evidence that the Fe^+-H bond is primarily metal-s in character. Formation of FeD^+ is observed with a moderate cross section at low energies in the reaction of FeH^+ with ethene-d_4. This results from reversible olefin insertion into the metal hydrogen bond, a process which does not involve higher oxidation states of iron. Reactions of FeH^+ with several alcohols, aldehydes, ethers, and alkanes are also

presented. Facile oxidative addition reactions to C-C and C-H bonds of alkanes do not occur at low energies, presumably due to the requisite formation of an Fe(IV) intermediate. The reactions of FeH^+ with the oxygenated compounds are generally of the type expected for strong Lewis acids.

Introduction

Activation of molecular hydrogen by a metal center is an important step in catalytic processes both in solution and on surfaces[2]. Because of this, the properties and reactivity of the intermediate metal hydrides are of great interest. Additional interest stems from the observation of diatomic metal hydrides, such as FeH, in spectra of stellar atmospheres[3,4]. These species have been observed in matrix isolation experiments[5], and several theoretical papers have explored their electronic structures[6]. Metal hydrides have also been studied by using ion cyclotron resonance spectroscopy[7a] and electron photodetachment techniques[8]. Using an ion beam apparatus, we have prepared metal ion hydrides in the gas phase by the endothermic reactions of the atomic metal ions with hydrogen[9-11]. Interpretation of the threshold for this process yields the bond energy for the metal hydride ion. From this bond energy the base strength, or proton affinity (PA), of the metal can be calculated. The present work reports the results of this analysis for Fe^+.

Further reactions of the ionic products formed in the collision chamber cannot be studied with our present apparatus. However, a beam consisting of FeH^+ can be generated in the source region from electron impact fragmentation of 1,1'-dimethylferrocene. Using this approach, the reactions of FeH^+ have been examined. Ion cyclotron resonance (ICR) studies of the deprotonation of diatomic transition metal hydride ions have been used to quantify the proton affinities of metal atoms and complexes[7,12]. Similar experiments using the ion beam apparatus are reported here for the deprotonation of FeH^+ by various bases. The limits given for PA(Fe)

agree well with the value calculated from the metal ion-hydrogen homolytic bond dissociation energy determined from the analysis of the reaction of Fe^+ with H_2 and D_2.

Exothermic hydride transfer reactions have also been examined; these experiments provide limits for the hydride affinity of FeH^+, $D^0(HFe^+-H^-)$, which are discussed in terms of the stability of FeH_2. The reactions of FeH^+ with several alcohols, aldehydes, ethers, and alkanes are reported. In contrast to the reactions of bare group 8 transition metal ions[10,12], facile exothermic bond insertion processes are not observed; instead reactions characteristic of a strong Lewis acid are observed.

Experimental

The ion beam apparatus, described in detail elsewhere[13] is shown schematically in Figure 1. The reactant ions are mass analyzed using a 60^0 sector magnet which provides unit mass resolution to greater than 100 m/z. This mass-selected beam is decelerated to the desired energy and focused into a collision chamber containing the reactant gas. Product ions exit the chamber and are focused into a quadrupole mass filter and detected using a Channeltron electron multiplier operated in a pulse counting mode. Ion signal intensities are corrected for the mass discrimination of the quadrupole mass filter.

The surface ionization source used to generate atomic iron ions[13] is sketched in Figure 2a. The oven, a stainless steel tube 1 cm long with 1/8" i.d., is attached to a U-shaped repeller. The sides of the repeller have dimensions 10 mm x 7 mm and are spaced 5 mm apart. A

Figure 1. Schematic drawing of the ion beam apparatus.

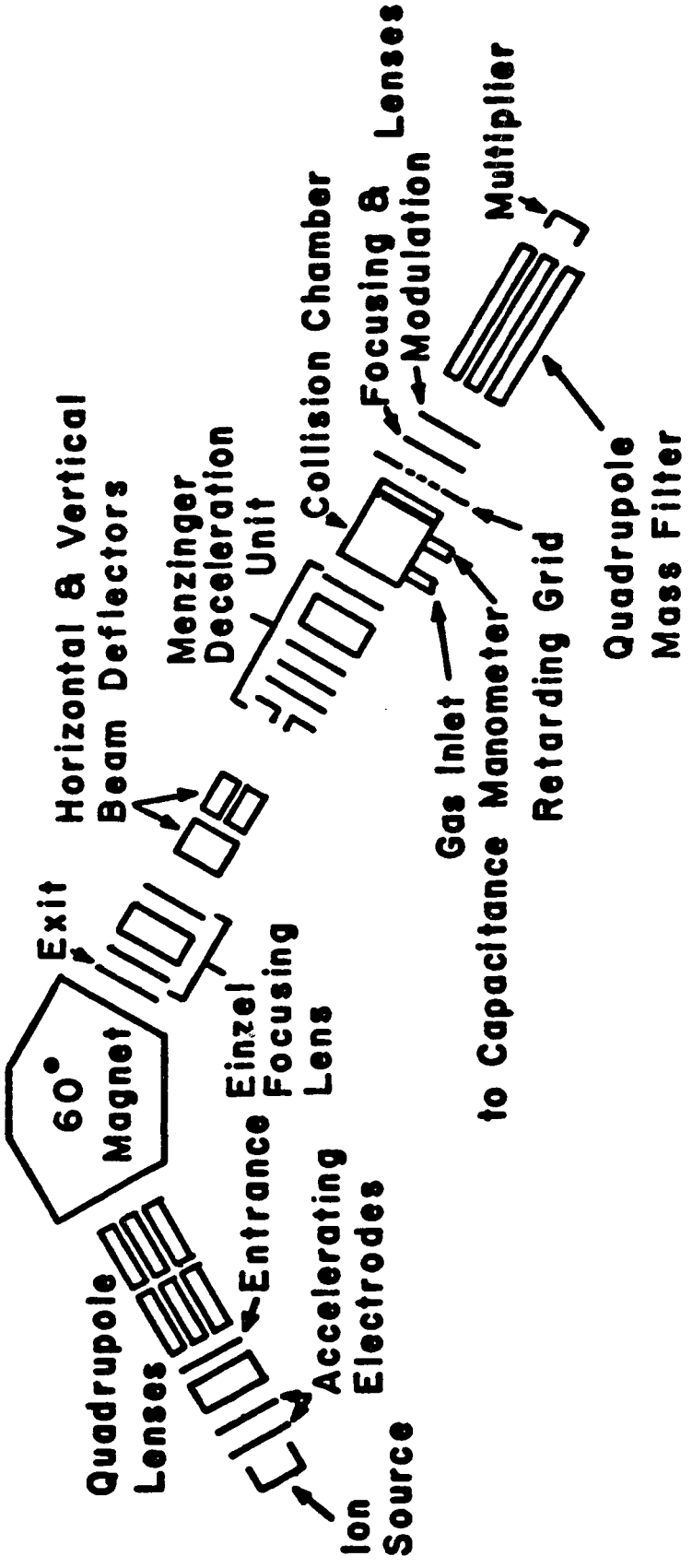
Ion Source
Quadrupole Lenses
Accelerating Electrodes
Entrance
Einzel Focusing Lens
60° Magnet
Exit
Horizontal & Vertical Beam Deflectors
Menzinger Deceleration Unit
Collision Chamber
Gas Inlet
to Capacitance Manometer
Retarding Grid
Focusing & Modulation Lenses
Quadrupole Mass Filter
Multiplier

Figure 2. Schematic drawing of a) the surface ionization source,
b) the electron impact source.

(a) SURFACE IONIZATION SOURCE

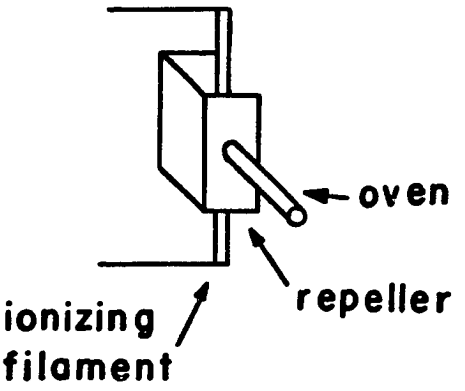

(b) ELECTRON IMPACT SOURCE

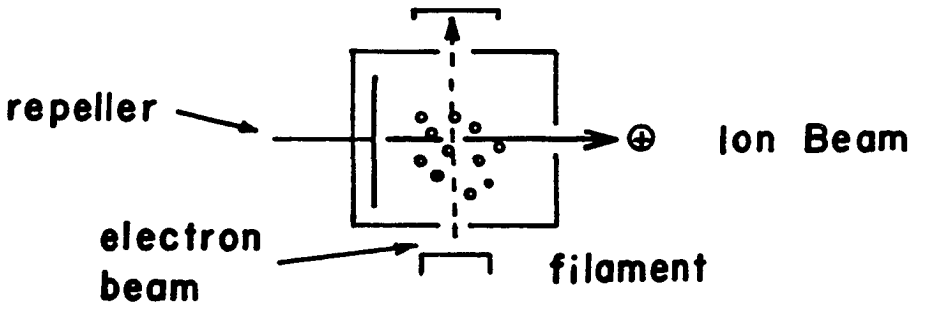

rhenium ribbon (0.03" wide x 0.0012" thick) is used for the filament (~12 mm long). In these experiments, the oven is loaded with $FeCl_3$. The filament generates enough heat to vaporize the complex. The metal chloride vapor is directed at the filament where dissociation and ionization of the resulting Fe occurs. This method of ionization minimizes the production of excited metal ion states. It is estimated that at the filament temperature used, ~2500 K, 77% of the Fe^+ ions produced are in the ^6D ground state manifold and 22% are in the ^4F excited state manifold at 0.232 eV[14].

The FeH^+ ion is formed from 1,1-dimethylferrocene by electron impact. All experiments were done at an electron energy of 70 eV unless otherwise noted. This source, sketched in Figure 2b, is of standard design in which an ion beam is extracted at a right angle from an electron beam with the aid of a small repeller field. The source is easily dissembled and cleaned. The inner dimensions of the surrounding chamber are approximately 5 mm x 6 mm x 5 mm. The same type of rhenium ribbon is used for this filament, ~4 mm long, as in the surface ionization source.

Electron impact ionization of organometallic compounds has been known to create electronically excited metal ions[15]. In addition, the FeH^+ ion formed by electron impact may possess some excess vibrational energy. When proton transfer and deuterium exchange reactions were monitored as a function of electron impact energy (~30 - 70 eV), no change in cross section was noted. This suggests excited state reactions of FeH^+ are not observed. In addition, the ratio of $^{56}FeH^+$ to $^{56}Fe^+$ varied by less than 4% over the range of 30 to 100 eV of electron impact energy.

The FeH^+ ion was first reported to appear in the mass spectrum of

$(CH_3C_5H_4)_2Fe$ by Mysov et al.[16]. The hydride of the major isotope of hydrogen, $^{56}FeH^+$, coincides with a minor isotope of iron, $^{57}Fe^+$(2.19%). Because of possible competing reactions from $^{57}Fe^+$, we found it more convenient at times to use $^{54}FeH^+$ as our reactant ion beam. This ion beam (mass 55) was not pure $^{54}FeH^+$, as indicated by fragmentation products at mass-to-charge ratios of 27, 29, and 39 which were observed when this ion beam was directed into the collision cell containing a nonreactive gas such as Ar. The impurity is most likely $C_4H_7^+$, an ion produced by the electron impact fragmentation of the methylcyclopentadienyl rings of $(CH_3C_5H_4)_2Fe$. A beam of $C_4H_7^+$ can be formed from electron impact of trans-2-butene. From a comparison of the fragmentation pattern of this $C_4H_7^+$ species upon collision with Ar to that of the 55 amu ion formed from $(CH_3C_5H_4)_2Fe$ (the patterns were similar but not identical), we estimate that 10% of the beam at 55 amu formed from the iron compound is due to $C_4H_7^+$. The interactions of the $C_4H_7^+$ ion formed from trans-2-butene with the reactant gases used in the $^{54}FeH^+$ studies were examined. In virtually all cases only collision-induced dissociation and proton transfer reaction occurred. The proton transfer cross sections were similar, and therefore do not affect our results (since the ratio of product to reactant beam, both due to $^{54}FeH^+$, remains the same).

The beam of ions of mass 57 amu from $(CH_3C_5H_4)_2Fe$ shows a very small amount of collision-induced fragmentation products at m/e = 29 ($\sigma \sim 0.02$ Å^2) and m/e = 31 ($\sigma \sim 0.006$ Å^2). These could be due to $C_4H_9^+$ formed in a complex rearrangement of the methylcyclopentadienyl rings upon electron impact or perhaps is due to ionization of the background gas.

The nominal collision energy of the ion beam is taken as the difference in potential between the collision chamber and either the center of the filament (determined by a resistive divider) of the surface ionization source, or the gas chamber of the electron impact source. This collision energy is checked by use of a retarding field energy analyzer. Agreement was always between 0.3 eV for the surface ionized beam. The beam produced by the electron impact source has a more uncertain energy, which can be up to 1.8 eV off the nominal value. This will not affect the trends observed for the exothermic reactions reported. In the one endothermic reaction studied, FeH^+ with D_2, the uncertainty caused by this energy is only 0.13 eV in the center of mass frame. By use of the retarding field analyzer, the energy distribution of the Fe^+ beam produced by surface ionization is 0.7 eV (FWHM), and that of the FeH^+ beam produced by electron impact of $(CH_3C_5H_4)_2Fe$ is not greater than 1.1 eV (FWHM). This latter effect is small in the present experiments.

The effect of the thermal motion of the reactant gas in ion beam collision chamber experiments has been discussed in detail elsewhere[17]. The energy broadening due to this motion washes out any sharp features in reaction cross sections. For exothermic reactions this has little effect on the observed cross sections and branching ratios. Consequently, we report such data without taking this energy distribution into account. For endothermic reactions, the thermal motion obscures the threshold energy for reactions. By convoluting a functional form for the reaction cross section, $\sigma(E)$, with the thermal energy distribution, using the method of Chantry[17], and fitting this new curve to the data, we take

specific account of this factor.

Our choice for the functional form of the reaction cross-section is discussed in detail elsewhere[13]. The form used, equation 1, has

$$\sigma(E) = \sigma_0[(E - E_0)/E]^n \qquad (1)$$

three variable parameters: σ_0, an effective cross section; E_0, the energy threshold for reaction [taken equal to the difference in bond energies of the netural reactant (bond broken) and ionic product (bond formed)]; and n. Equation 1 is expected to apply for energies below the threshold for dissociation of the product ion. This threshold corresponds to the energy of the bond broken in the neutral reactant. Detailed treatments of the effect of dissociation on the observed reaction cross section also have been discussed previously[9,13,18].

Reaction cross sections for specific products, σ_i, are obtained using equations 2 and 3 which relate the total reation cross section,

$$I_0 = (I_0 + \Sigma I_i) \exp(-n_0\sigma\ell) \qquad (2)$$

$$\sigma_i = \sigma I_i/\Sigma I_i \qquad (3)$$

σ, the number density of the target gas, n_0, and the length of the collision chamber, ℓ(5 mm), to the transmitted reactant ion beam intensity, I_0, and the sum of the product ion intensities, ΣI_i. The pressure of the target gas, measured using an MKS Baratron Model 90H1 capacitance manometer, is usually kept low, $<2.5 \times 10^{-3}$ Torr, to minimize attenuation of the beam and ensure that reactions are the result of only a single bimolecular collision.

It is important to point out that neutral products are not detected in these experiments. However, except where noted below, the identity of these products can usually be inferred without ambiguity. In addition, these experiments provide no direct structural information about the ionic products. Thermochemical arguments can often distinguish possibilities for isomeric structures.

Results and Discussion

Reaction of Fe^+ with H_2, D_2 and HD. Iron ions react with H_2 to form FeH^+ as indicated in equation 4. The variation of the cross section

$$Fe^+ + H_2 \rightarrow FeH^+ + H \qquad (4)$$

with energy for this reaction is shown in Figure 3 and is characteristic of an endothermic reaction. In analogy to previous studies of such metal-ion hydrogen systems, the data have been interpreted by using equation 1 with n = 1[9,18]. The fit shown in Figure 3 gives σ_o = 1.76 $Å^2$ and E_o = 2.0 ± 0.15 eV, and is convoluted as discussed above. Combined with the bond energy of H_2, $D^o(H_2)$ = 4.52 eV, this threshold yields a value for $D^o(Fe^+\text{-}H)$ of 2.52 ± 0.15 eV. At high energies the cross section for reaction 4 decreases due to dissociation of FeH^+. This process has a thermodynamic threshold equal to the bond energy of H_2. The fit to the data above this energy uses an analysis discussed in detail elsewhere[9,18].

The reaction of Fe^+ with D_2 was also studied, process 5. The data

$$Fe^+ + D_2 \rightarrow FeD^+ + D \qquad (5)$$

Figure 3. Variation in experimental cross section for reaction 4 as a function of kinetic energy in the center-of-mass frame (lower scale) and the laboratory frame (upper scale). The solid line is the fit to the data described in the text. Arrows mark the threshold energy at 2.0 eV, and the bond energy of H_2 at 4.52 eV.

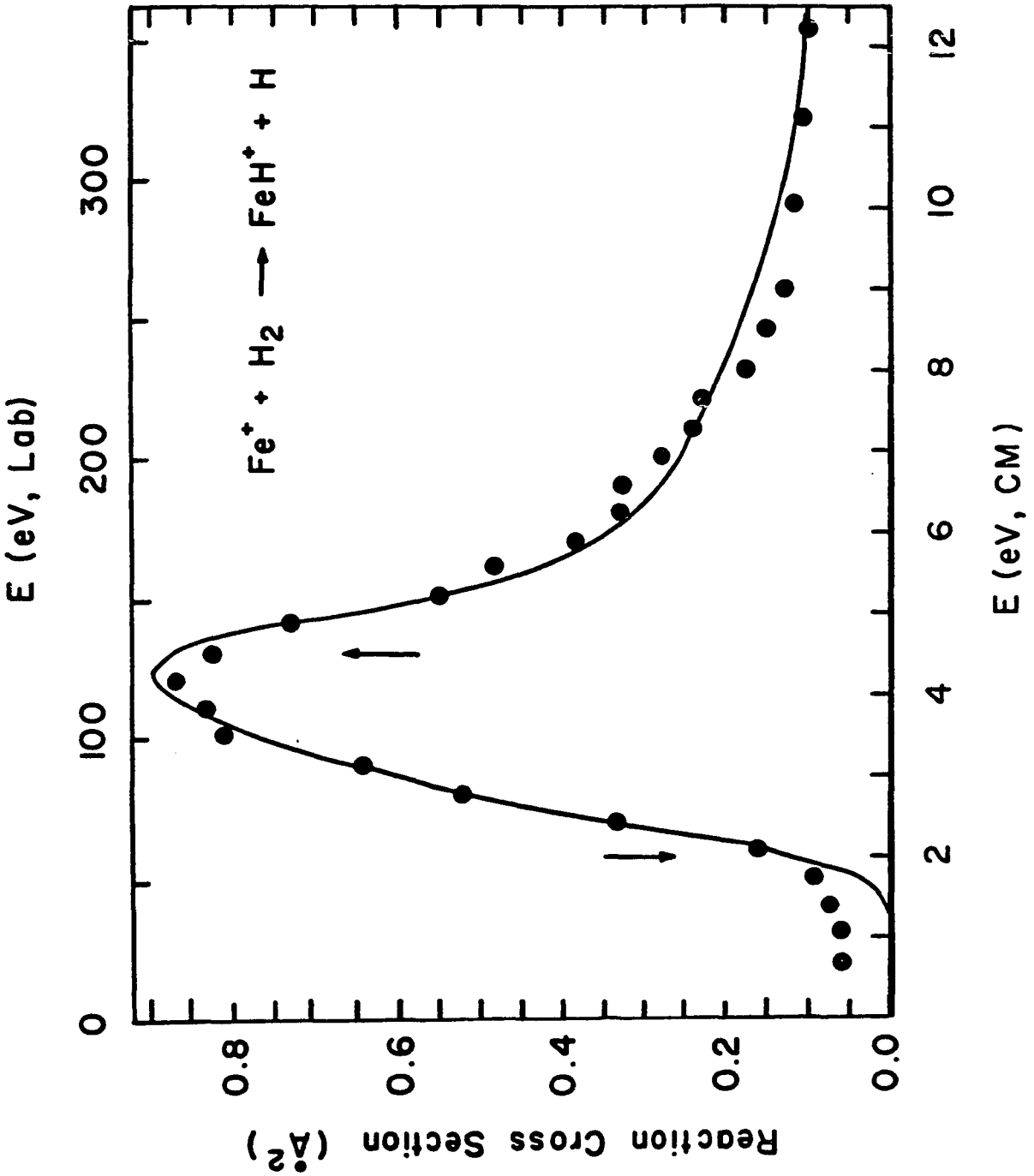
Fe⁺ + H₂ → FeH⁺ + H
E (eV, Lab)
E (eV, CM)
Reaction Cross Section (Å²)
0
100
200
300
2
4
6
8
10
12
0.0
0.2
0.4
0.6
0.8

for this reaction are not shown, but look very similar to those plotted in Figure 3. The cross section rises to a maximum of ~5 Å at 4 eV relative kinetic energy. The best fit using equation 1 with n = 1 gives σ_o = 0.84 Å^2 and E_o = 2.0 ± 0.15 eV. From this threshold and $D^o(D_2)$ = 4.60 eV, a value of $D^o(Fe^+\text{-}D)$ = 2.60 ± 0.2 is determined. Making a zero-point energy correction of 0.03 eV[19], yields $D^o(Fe^+\text{-}H)$ = 2.57 ± 0.15. Taking an average of the two determinations of the iron ion-hydrogen bond energy, a value of $D^o(Fe^+\text{-}H)$ = 2.55 ± 0.2 eV (59 ± 5 kcal/mol) is obtained. This value agrees well with the limit, $D^o(Fe^+\text{-}H)$ < 71 kcal/mol obtained by Allison and Ridge[20]. The proton affinity of the iron atom, PA(Fe) can now be calculated from equation 6. The

$$PA(Fe) = D^o(Fe^+\text{-}H) + IP(H) - IP(Fe) \qquad (6)$$

term IP(X) denotes the ionization potential of species X. The proton affinity obtained, PA(Fe) = 190 ± 5 kcal/mol, is only slightly larger than those of the other first row group 8 metals [PA(Co) = 184 ± 4 kcal/mol[10] and PA(Ni) = 180 ± 3 kcal/mol[9]].

The reaction of Fe^+ with HD was also briefly examined. The results are similar to the reaction of Ni^+ with HD in that formation of FeH^+ is favored over FeD^+ at all energies[9]. From threshold to the maximum of the FeH^+ peak, σ ~ 0.34 Å^2 at 4 eV relative kinetic energy, the cross section for FeH^+ is three to four times as large as that for FeD^+. At higher energies, the ratio of FeH^+ to FeD^+ is approximately equal to two.

Reaction of FeH^+ with D_2. The reaction of FeH^+ with D_2 was examined in an attempt to further characterize the intermediate formed

in reaction 4, presumably $Fe(H)_2^+$. In addition, we wished to probe the thermoneutral exchange reaction 7. No $Fe(HD)^+$ was observed in the

$$FeH^+ + D_2 \rightarrow FeD^+ + HD \qquad (7)$$

interaction of FeH^+ with D_2. If D_2 does add to FeH^+ to form 1, an Fe(IV)

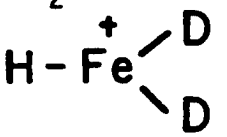

1

species, then the energetics for reductive elimination of molecular hydrogen (HD or D_2) are probably more favorable than for cleavage of an Fe^+-H or Fe^+-D bond. It is interesting to note that while dihydrides of nickel ions are present in slow field tip evaporation studies, no FeH^+ or FeH_2^+ is observed[21]. If the latter ion is formed, rapid reductive elimination of H_2 may prevent its observation.

Data for the exchange reaction 7 are presented in Figure 4. The maximum cross section is quite low for a thermoneutral reaction, $\sigma_{max} < 0.54$ Å^2. In addition, the variation of the cross section with energy indicates a substantial activation energy for this reaction. The fit to the data shown in Figure 4 uses equation 1 with $n = 3$, $\sigma_o = 0.73$ Å^2, and $E_o = 0.9$ eV. This threshold, $E_o = 20 \pm 7$ kcal/mol, is equal to the activation energy for this process[22].

Two possibilities exist for the intermediate of reaction 7. The first is formed by oxidative addition of D_2 to the metal center to form the Fe(IV) species, 1. This is not a preferred oxidation state of the metal. Another possible structure is a four-centered intermediate, 2.

Figure 4. Variation in experimental cross section for reaction 7 as a function of kinetic energy in the center-of-mass frame (lower scale) and the laboratory frame (upper scale). The solid line is the fit to the data described in the text. Arrows mark the threshold energy at 0.9 eV and the bond energy of D_2 at 4.6 eV.

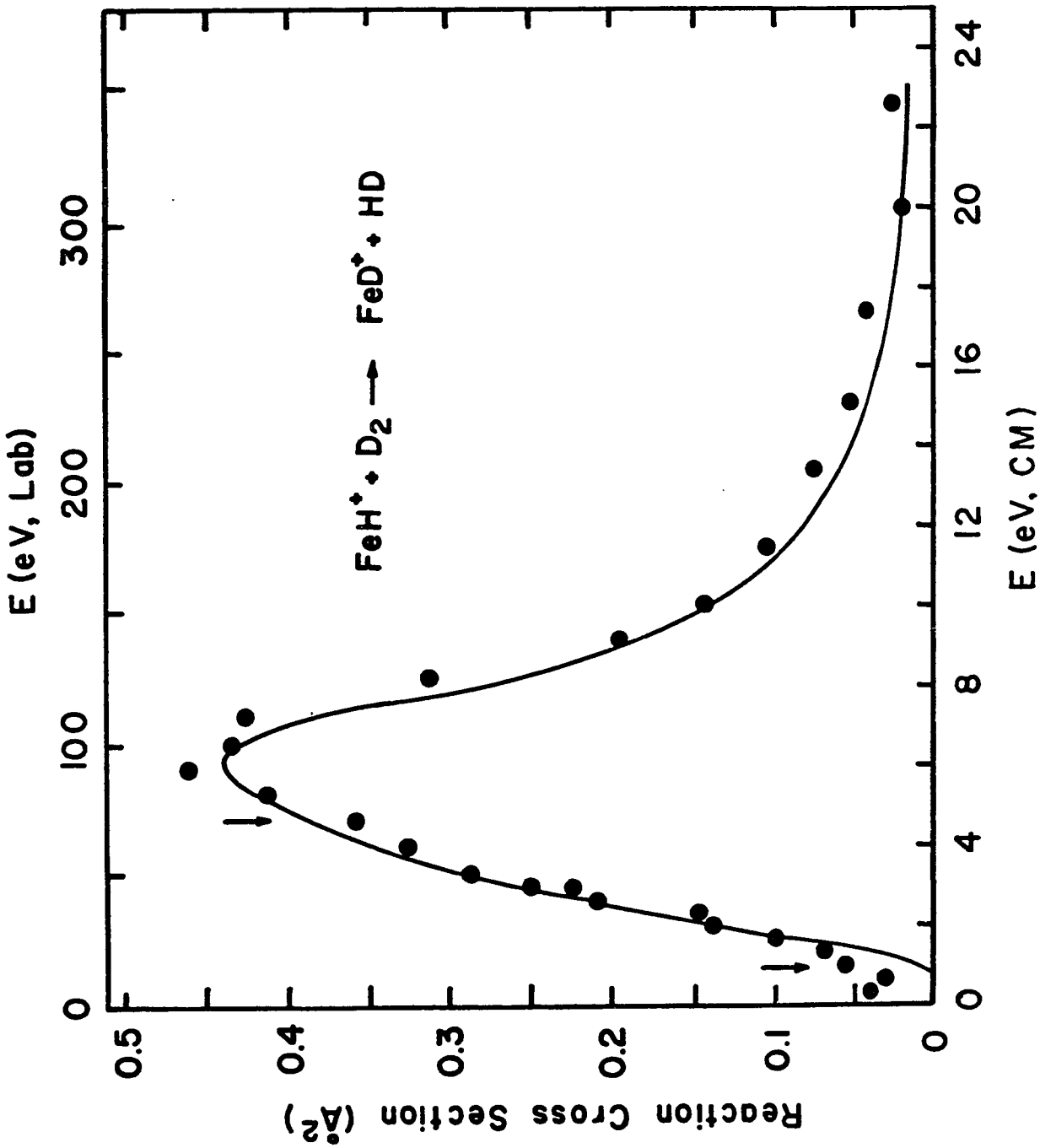
FeH⁺ + D₂ ⟶ FeD⁺ + HD
E (eV, Lab)
E (eV, CM)
Reaction Cross Section (Å²)
0
100
200
300
0
4
8
12
16
20
24
0.5
0.4
0.3
0.2
0.1
0

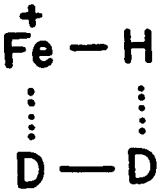

2

The exchange reactions with D_2 of Cl_2M-H, M = Sc, Ti, Ti^+, proceeding through a structure analogous to 2 have been studied by Steigerwald and Goddard using generalized valence bond methods[23]. These calculations indicate that the activation barrier for this process will be large for systems with a large amount of metal-s or p character in the M-H bond. Correlation of experimental metal ion-hydrogen bond strengths with electronic promotion energies of the metal ion indicate that the metal orbital in the Fe^+-H bond is primarily s in character[11]. This is supported by preliminary calculations on the FeH^+ molecule[24]. Thus, these calculations would predict that a four-centered intermediate for reaction 7 will result in a large activation barrier. Given these considerations, both structures 1 and 2 are expected to be high-energy intermediates, consistent with the experimental observation of a large activation barrier for reaction 7. The experiments do not distinguish the two possibilities.

Proton Transfer Reactions of FeH^+. In the studies reported above, the proton affinity of Fe was determined by measuring the energy required to form FeH^+ from the reaction of Fe^+ with hydrogen. A complementary method of determining this value is to measure the energy required to remove a proton from FeH^+. This can be accomplished by using

the ion beam apparatus to measure the cross section for proton transfer from FeH^+ to bases of varying proton affinity (process 8). The enthalpy

$$FeH^+ + B \rightarrow Fe + BH^+ \quad (8)$$

$$\Delta H_{rxn} = PA(Fe) - PA(B) \quad (9)$$

for this process is given in equation 9.

Proton transfer processes are commonly observed in gas phase studies of the reactions of organic ions with n-donor bases[25]. The observation of large cross sections for reaction 8 would be consistent with an exothermic process. Endothermic proton transfer reactions can be made to occur by supplying excess translational energy to the system. The variation of cross section for reaction 8 with relative kinetic energy was examined for bases of varying proton affinities[25]. Formaldehyde has the lowest proton affinity of the bases used, $\delta PA = -27.8$ kcal/mol, where the proton affinity is given relative to ammonia, equation 10.

$$\delta PA(B) = PA(B) - PA(NH_3) \quad (10)$$

The best estimate for $PA(NH_3)$ is discussed below. No ion corresponding to CH_2OH^+ was observed at low energies in the reaction of FeH^+ with formaldehyde, and only a very small amount (~0.04 $Å^2$) of this product appeared at a higher energy (~2 eV relative kinetic energy). The proton transfer cross section for reaction of FeH^+ with methanol, $\delta PA = -20.1$ kcal/mol is ~0.3 $Å^2$ at the lowest energy measured (~0.09 eV in the center-of-mass frame (CM)), increases slowly to a maximum of ~0.7 $Å^2$ at ~1.8 eV (CM), and then decreases. This suggests the reaction

is slightly endothermic. The behavior of the cross section for reaction 8 with bases having $\delta PA \geq \delta PA(CH_3CHO) = 16.1$ kcal/mol is characteristic of exothermic processes, suggesting a value for $\delta PA(Fe)$ between -20.1 and -16.1 kcal/mol.

A comparison of the proton transfer cross sections for the various bases measured at the same interaction energy, ~0.5 eV (CM), is shown in Figure 5. The cross section for reaction 8 is plotted for each base according to its proton affinity relative to ammonia. Overall, the trend is as expected, with higher cross sections for the bases with higher proton affinities. The line shown is a least-squares fit to the data in the range of δPA = -16.1 kcal/mol to δPA = -4 kcal/mol. These data appear to extrapolate to a value of δPA = -16.0 kcal/mol, which can be considered as an estimate of the threshold for the proton transfer reaction to occur. However, there are numerous competing reactions discussed below which complicate any quantitative analysis. It is not clear why the proton transfer cross section for the group V bases are low. While the reaction with PH_3 may be only thermoneutral, proton transfer to ammonia should be highly exothermic. Formation of $Fe(NH_2)^+$ and the adduct $HFe(NH_3)^+$ do occur in the reaction with ammonia. It is possible that coordination to the metal cation ties up the site to which the proton can be transferred, in which case the presence of an additional lone pair in the base may be required to observe proton transfer near the thermodynamic threshold[26]. If such an adduct is formed, the reductive elimination of NH_4^+ may have a sizable activation barrier relative to loss of NH_3 to regenerate the reactants.

An absolute value for the proton affinity of Fe is determined from

Figure 5. Experimental cross sections for reaction 8 plotted as a function of the proton affinity of base. All measurements shown were taken at ~0.5 eV relative kinetic energy. The arrow marks δPA(Fe) calculated from the thresholds of reactions 4 and 5, and assuming $PA(NH_3)$ = 204 kcal/mol.

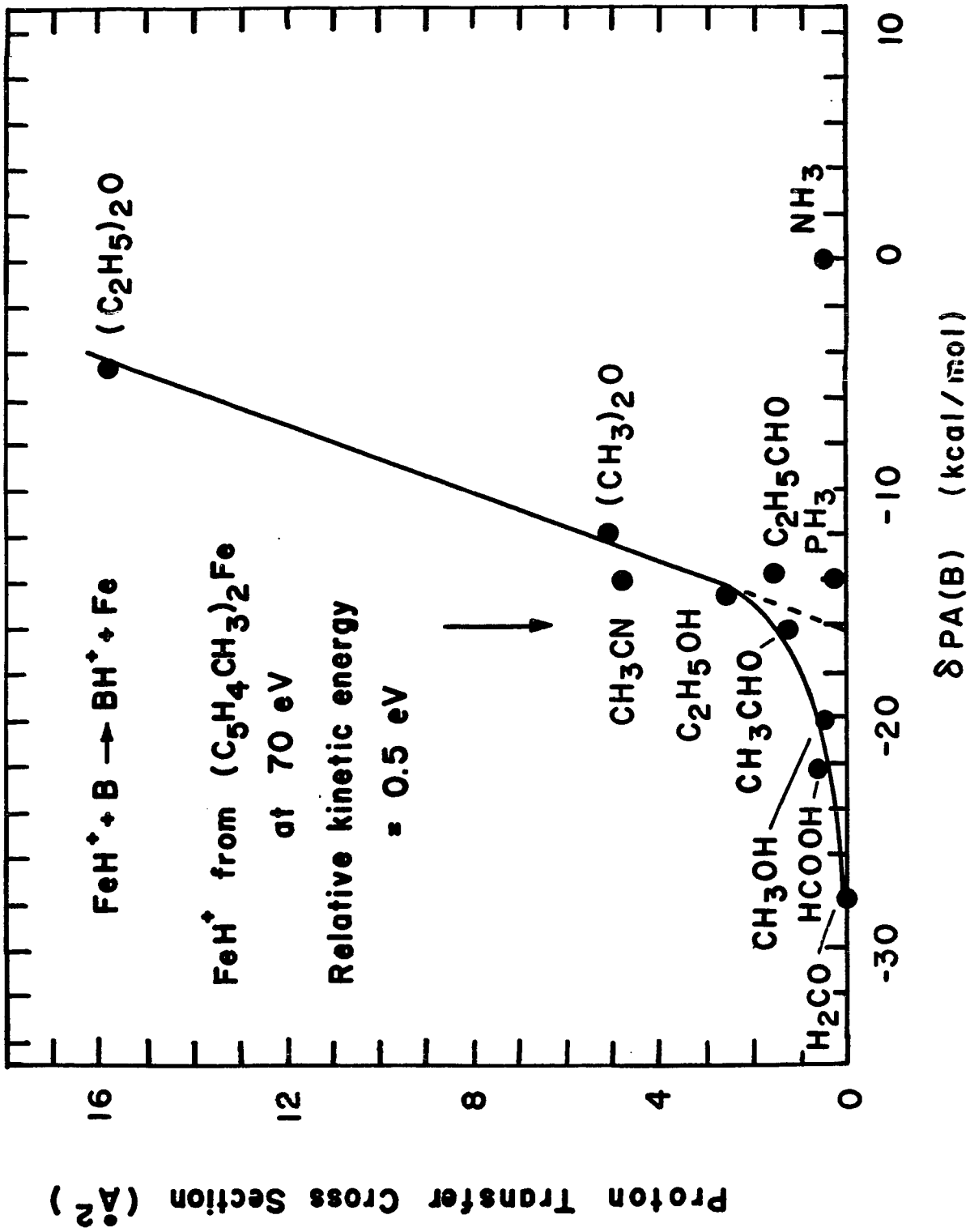
Proton Transfer Cross Section (Å²)
16
12
8
4
0
10
0
-10
-20
-30
δ PA(B) (kcal/mol)
FeH⁺ + B → BH⁺ + Fe
FeH⁺ from (C5H4CH3)2Fe
at 70 eV
Relative kinetic energy
= 0.5 eV
(C2H5)2O
(CH3)2O
CH3CN
C2H5OH
CH3CHO
C2H5CHO
PH3
NH3
CH3OH
HCOOH
H2CO

the proton affinity of ammonia. Photoionization appearance potential measurements of NH_4^+ from NH_3 dimers made by Ceyer et al. yield a value of $PA(NH_3)$ = 203.6 kcal/mol[27] (298 K) though other estimates are higher[28]. Combining $PA(NH_3)$ = 204 ± 2 kcal/mol with $\delta PA(Fe)$ = 16 kcal/mol yields a value for the proton affinity of Fe, PA(Fe) = 188 kcal/mol. This number agrees very well with the above determination, PA(Fe) = 190 ± 5, derived from the Fe^+-H bond energy.

As noted in the experimental section, FeH^+ formed by electron impact of the 1,1'-dimethylferrocene may possess excess vibrational energy. The agreement between the values for the proton affinity of Fe derived from threshold measurements of the reactions of Fe^+ with H_2 and D_2 and from proton transfer reactions of FeH^+ suggests that the latter ion has little vibrational excitation. If it were vibrationally excited, the proton transfer studies would lead to a lower proton affinity for Fe.

Hydride Transfer Reactions of FeH^+. In addition to proton transfer from FeH^+ to the above bases, the interaction with these compounds can also result in a hydride ion being transferred from the neutral reactant to FeH^+, to form FeH_2 (reaction 11). Reaction 11 will occur when the hydride affinity of FeH^+, $D[HFe^+\text{-}H^-]$, is greater than that of the base (represented by AH in equation 11). The enthalpy change for reaction 11

$$FeH^+ + AH \xrightarrow{\Delta H} FeH_2 + A^+ \qquad (11)$$

$$\Delta H = D[A^+\text{-}H^-] - D[HFe^+\text{-}H^-] \qquad (12)$$

is given in equation 12.

Table I lists $D[A^+\text{-}H^-]$ for all species AH used in the present studies.

Table I. Calculated Bond Strengths for Hydride Transfer Reagents

AH[a]	$D(A^+-H^-)$[b-d] (kcal/mol)
$(CH_3CH_2)_2O$	214[e]
CH_3NH_2	218
CH_3CH_2CHO	224
CH_3CHO	231.4[f]
CH_3CH_2OH	231.9[g]
$(CH_3)_2O$	236[h]
CH_3OH	255
HCOOH	267
PH_3[i]	295
CH_3CN	306
NH_3[i]	348

a) Heats of formation for organic compounds taken from Reference 31 unless noted.

b) The lowest value for $D(A^+-H^-)$ is listed for compounds with different types of hydrogen bonds.

c) These values are calculated using a value for the electron affinity of H, EA(H) = 0.754 eV from Wagman, D. D.; Evans, W. H.: Parker, V. B.; Harlow, I.; Bailey, S. M.; Schumm, R. H. Natl. Bur. Stand. Tech. Note 270-3, 1968.

d) Heats of formation or selected appearance potentials for ions are taken from Rosenstock, H. M.; Draxl, K.: Steiner, B. W.: Herron, J. T. J. Phys. Chem. Ref. Data, Suppl. 1977, 6, No. 1, unless otherwise noted.

e) Calculated using appearance potential measurement of $C_4H_9O^+$ from iso-$C_3H_7OC_2H_5$ from reference listed in footnote h of this table. ΔH_f(iso-$C_3H_7OC_2H_5$) taken to be the average of $\Delta H_f[(C_2H_5)_2O]$ and

Table I. cont.

ΔH_f (iso-$C_3H_7)_2O$ from Reference 31.

f) $\Delta H_f(CH_3CO^+)$ = 157.0 ± 0.4 kcal/mol from Traeger, J. C.: McLoughlin, R. G.; Nicholson, A. J. C. J. Am. Chem. Soc. 1982, 104, 5318.

g) $\Delta H_f(C_2H_4OH^+)$ = 141 kcal/mol from Rafaey, K. M. A.; Chupka, W. A. J. Chem. Phys. 1968, 48, 5205.

h) $\Delta H_f(CH_3OCH_2^+)$ = 157 kcal/mol from Lossing, F. P. J. Am. Chem. Soc. 1977, 99, 7526.

i) Heat of formation taken from reference listed in footnote d of this table.

Appreciable yields of A^+, reaction 11, are observed for the first four compounds listed. The cross section for formation of A^+ at low energies in the reaction of FeH^+ with AH = CH_3CH_2OH and $(CH_3)_2O$ is less than 0.4 $Å^2$, indicating a lower limit for $D[HFe^+-H^-]$ of 232 kcal/mol. Hydride transfer reactions are often fast (at 300 K) and reversible, and do not require activation energies in excess of their endothermicities[32]. This suggests that the lower limit is a measure of the true value. This result gives $\Delta H_f(FeH_2) < 77.5$ kcal/mol, from which an enthalpy change greater than 22 kcal/mol is calculated for process 13. Thus, the sum of the

$$FeH_2 \rightarrow Fe + H_2 \qquad (13)$$

first two hydrogen bonds to an iron atom is greater than 126 kcal/mol. Unfortunately, both experimental and theoretical estimates for the Fe-H bond dissociation energy range from 1.0 to 2.4 eV[5a,6,33]. From electron photodetachment studies of FeD^-, Stevens et al. propose that FeH has a $^4\Delta$ ground state[8].

Sweany has observed oxidative addition of H_2 to $Fe(CO)_4$ in matrix isolation studies, which suggests there is little or no activation energy for this process[34]. The activation energy for the reverse reaction, reductive elimination of H_2 from $H_2Fe(CO)_4$, has been calculated from kinetic studies by Pearson and Mauermann to be 26 kcal/mol[35]. The above two studies indicate that the enthalpy change for addition of H_2 to $Fe(CO)_4$ is ~26 kcal/mol. It is interesting to note that even though the molecular and electronic structure of this system is very different from the FeH_2 species (which is probably linear), the energetics of reductive elimination are comparable.

Reactions of FeH^+ with Alkanes. The reactions of FeH^+ with methane, ethane, and butane were studied at low energies. The purpose of these experiments was to examine the occurrence of reaction 14. Labeled

$$FeH^+ + RH \rightarrow FeR^+ + H_2 \qquad (14)$$

substrates would then allow the site of reaction to be identified. Methane-d_4 was used to check for the deuterium exchange reaction leading to FeD^+. No products were observed at low energies with methane or ethane, despite the fact that reaction 15 is nearly thermoneutral and reactions

$$FeH^+ + CD_4 \rightarrow FeD^+ + CHD_3 \qquad (15)$$

$$FeH^+ + CD_4 \rightarrow FeCD_3^+ + HD \qquad (16)$$

16 and 17 are exothermic by 10 and 24 kcal/mol, respectively[36]. Failure to

$$FeH^+ + C_2H_6 \rightarrow FeCH_3^+ + CH_4 \qquad (17)$$

observe these reactions is perhaps not surprising since the thermoneutral exchange reaction with D_2 occurs with a significant activation energy. Accordingly, reaction 17 was observed at higher energies (the threshold was not examined). In analogy to the D_2 exchange reaction discussed earlier, the high-energy intermediate involved in these reactions may either be an Fe(IV) species or a four-centered intermediate.

At low energies FeH^+ reacts with butane to yield $Fe(C_4H_9)^+$ and $Fe(C_4H_7)^+$, processes 18 and 19. The total reaction cross-section at

$$FeH^+ + n\text{-}C_4H_{10} \xrightarrow{73\%} Fe(C_4H_9)^+ + H_2 \qquad (18)$$

$$FeH^+ + n\text{-}C_4H_{10} \xrightarrow{27\%} Fe(C_4H_7)^+ + 2H_2 \qquad (19)$$

0.5 eV is less than 3 $Å^2$. No products formed via carbon-carbon bond cleavage are observed. While the $D[s\text{-}C_4H_7^+\text{—}H^-]$ is equal to 246 kcal/mol[30,31,37], the enthalpy change for process 20 is only 229 kcal/mol[29-31],

$$n\text{-}C_4H_{10} \rightarrow t\text{-}C_4H_9^+ + H^- \qquad (20)$$

which is less than the lower bound determined above for $D[HFe^+\text{—}H^-]$. Thus, it is not unreasonable that the first step in the dehydrogenation reaction is hydride transfer to FeH^+ accompanied by rearrangement of the resulting carbocation. This mechanism would not occur for methane or ethane since $D^o[H_3C^+\text{—}H^-]$ = 315 kcal/mol and $D^o[s\text{-}C_3H_7^+\text{—}H^-]$ = 248 kcal/mol[29].

In contrast to the above reactions of FeH^+, bare iron ions oxidatively add to carbon-carbon and carbon-hydrogen bonds of alkanes larger than ethane in facile exothermic processes[12]. The resulting metal-dialkyl or metal-hydridoalkyl can undergo a ß-hydrogen transfer to the metal leading to reductive elimination of H_2 or an alkane. At the same energy at which the FeH^+ reaction with butane was performed, the cross section for dehydrogenation of butane by Fe^+ is ~10 $Å^2$, while that for the loss of alkanes is ~30 $Å^2$ [12].

Reaction of FeH^+ with C_2D_4. The insertion of olefins into metal-hydrogen bonds is a reaction of great interest to organometallic chemists[38]. In order to determine whether this reaction would occur in our gas phase system, the reaction of FeH^+ with C_2D_4 was examined. The only product observed was due to the exchange reaction 21. The cross

$$FeH^+ + C_2H_4 \rightarrow FeD^+ + C_2HD_3 \qquad (21)$$

section for this reaction, shown in Figure 6, is moderately high at

Figure. 6. Variation in experimental cross section for reaction 21 as a function of kinetic energy in the center-of-mass frame (lower scale) and laboratory frame (upper scale).

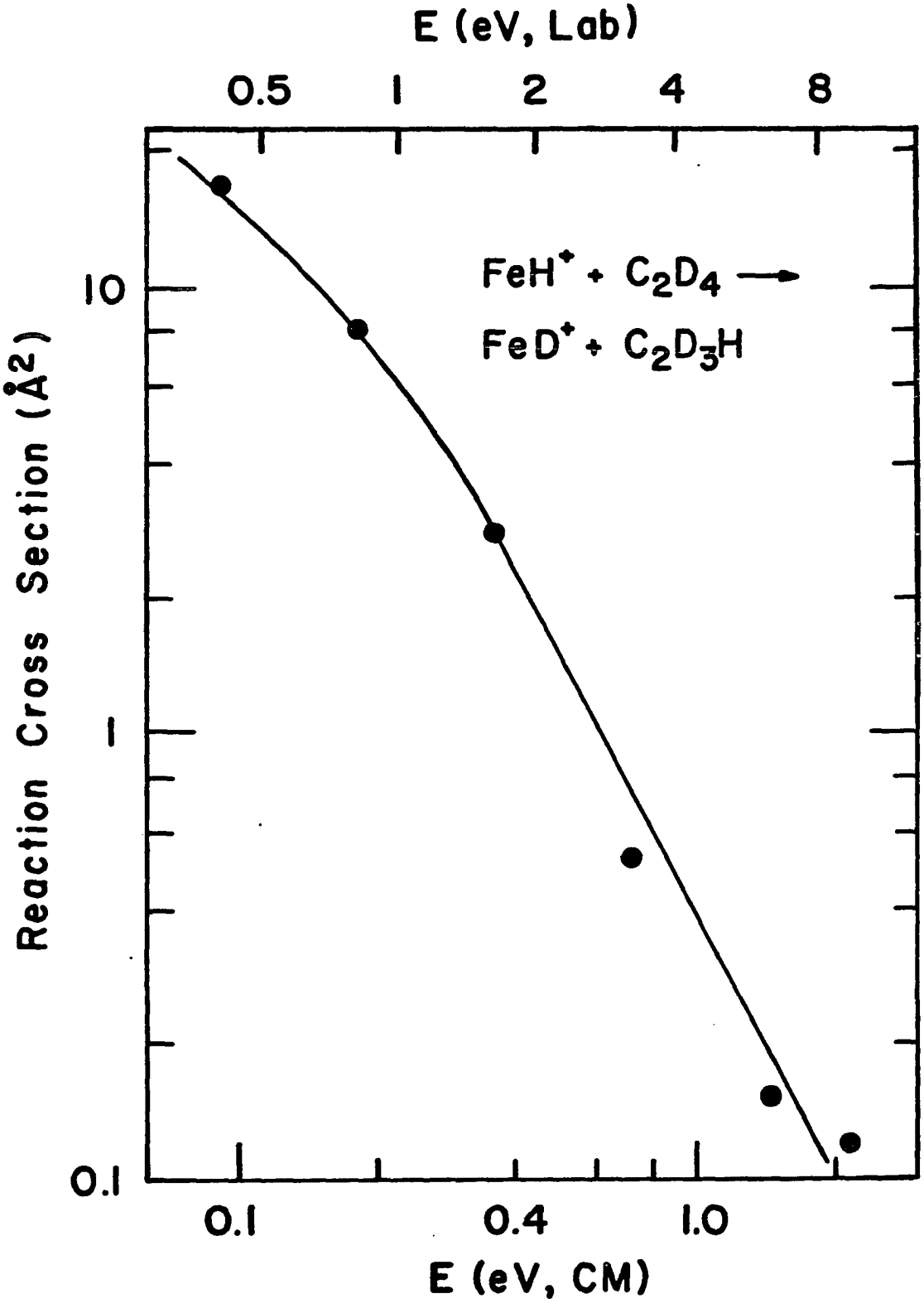
E (eV, Lab)
0.5
1
2
4
8
10
1
0.1
Reaction Cross Section (Å²)
FeH⁺ + C₂D₄ →
FeD⁺ + C₂D₃H
0.1
0.4
1.0
E (eV, CM)

low energies and decreases rapidly with increasing energy. The reaction exhibits no barrier, indicating that no high energy intermediates are involved. The likely mechanism by which this reaction occurs is presented in Scheme I. The ethene molecule initially interacts with

Scheme I

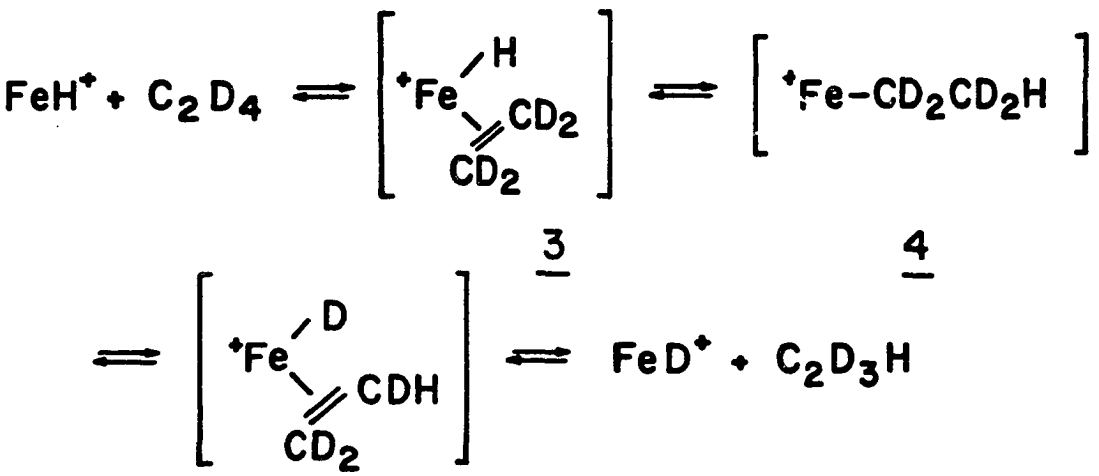

FeH^+ to form the π-bound complex, 3, after which the familiar olefin insertion can occur to form the metal alkyl species 4. The reaction continues by a β-deuterium transfer followed by elimination of ethene-d_3. No Fe(IV) species is invoked in any step of this mechanism.

Complex Reactions of FeH^+ with Oxygen Bases. In the course of examining the proton and hydride transfer processes discussed above,

additional products resulting from interaction of FeH^+ with alcohols, aldehydes, and ethers were observed at low energies. These reactions are listed in Table II. In addition, adduct formation is observed in all of these reactions, as might be expected from previous studies of cationic metal systems with oxygenated compounds[39].

The reactions listed in Table II are generally complex, involving considerable rearrangement of bonds in the reaction intermediates. In the absence of labeling data, the mechanisms by which these reactions occur cannot be determined. Possibilities include oxidative addition processes or reactions typical of a Lewis acid. Though oxidative addition processes would involve formation of Fe(IV) intermediates, these species may not be as unfavorable with the oxygenated compounds as with the hydrocarbon systems described above[40,41]. As a Lewis acid, FeH^+ may first abstract a hydride ion[20] or it may bind to n-donor bases followed by four-center rearrangements such as shown in Scheme II for an alcohol or ether. Scheme IIb is analogous

Scheme II

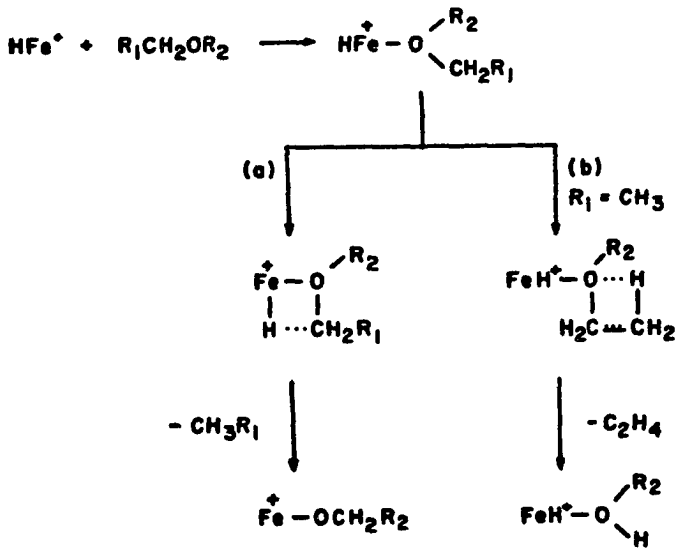

Table II. Exothermic Reactions of FeH^+ with Alcohols, Alkehydes, and Ethers[a]

	% of Total Reaction[b]	σ_{total} ($Å^2$)
Alcohols		
$FeH^+ + CH_3OH \rightarrow Fe + CH_3OH_2^+$	19	3
$\rightarrow FeOCH_3^+ + H_2$	81	
$FeH^+ + CH_3CH_2OH \rightarrow Fe + CH_3CH_2OH_2^+$	7	40
$\rightarrow FeOH^+ + C_2H_6$ [c]	42	
$\rightarrow HFe(OH_2)^+ + C_2H_4$	51	
Aldehydes		
$FeH^+ + CH_3CHO \rightarrow Fe + CH_3CHOH^+$	30	10
$\rightarrow FeH_2 + CH_3CO^+$	5	
$\rightarrow FeCH_3^+ + (H_2 + CO)$[d,e]	44	
$\rightarrow Fe(COCH_3)^+ + H_2$	21	
$FeH^+ + CH_3CH_2CHO \rightarrow Fe + CH_3CH_2CHOH^+$	6	130
$\rightarrow Fe(C_2H_5)^+ + (H_2 + CO)$[d]	11	
$\rightarrow Fe(CHO)^+ + C_2H_6$		
$\rightarrow HFe(CH_2O)^+ + C_2H_4$	12	
$\rightarrow HFe(C_2H_6)^+ + CO$		
$\rightarrow Fe(COC_2H_5)^+ + H_2$	71	
Ethers		
$FeH^+ + (CH_3)_2O \rightarrow Fe + (CH_3)_2OH^+$	31	20
$\rightarrow FeH_2 + CH_3OCH_2^+$	< 1	
$\rightarrow FeOCH_3^+ + CH_4$	69	

Table II. Continued.

	% of Total Reaction[b]	σ_{total} ($Å^2$)
Ethers (cont.)		
$FeH^+ + (CH_3CH_2)_2O \rightarrow Fe + (CH_3CH_2)_2OH^+$	16	200
$\rightarrow FeH_2 + CH_3CH_2OCHCH_3^+$	39	
$\rightarrow FeOC_2H_5^+ + C_2H_6$	28	
$\rightarrow HFe(C_2H_5OH)^+ + C_2H_4$	17	

a) Measured at ~0.2 - 0.3 eV relative kinetic energy.

b) Adduct formation is not included in calculating these product distributions.

c) Using $D^o(Fe^+\text{-}OH) = 76 \pm 5$ kcal/mol from Murad, E. J. Chem. Phys. 1980, 73, 1381, an enthalpy change of $\Delta H_{rxn} = -24$ kcal/mol is calculated for this reaction (see References 30 and 31).

d) The neutral products of this reaction may be either H_2CO or H_2 and CO.

e) Assuming the neutral products are H_2 and CO the enthalpy change for this reaction is calculated to be $\Delta H_{rxn} = -13$ kcal/mol (see References 30, 31, and 36).

to mechanisms proposed for the decomposition of proton-bound dimers of alcohols[42] and ethers[43]. In these reactions of FeH^+, the initially formed adduct may consist of a proton-bound alcohol or ether to an iron atom. The role of strong hydrogen bond formation in providing chemical activation of intermediates and lending stability to products has been previously noted in gas phase studies of the reactions of organic ions[44].

Conclusion

The present studies represent the first effort to extend our ion beam investigations of reactive intermediates in organometallic chemistry from atomic metal ions to organometallic fragments, the simplest of which is a metal hydride. The main results include (1) determination of the bond dissociation energy $D[Fe^+-H]$ by analyzing endothermic thresholds for reaction of Fe^+ with H_2 and D_2, (2) confirmation of this result by deprotonation of FeH^+ with a range of n-donor bases of varying strength, (3) demonstration that FeH_2 is stable with respect to the reductive elimination of H_2 by examining hydride abstraction reactions of FeH^+, (4) demonstration that oxidative addition of FeH^+ to H_2 or hydrocarbons to give Fe(IV) intermediates (or reaction via four-centered intermediates) is not a favorable process, and (5) reversible insertion of olefins into the FeH^+ bond is a facile process. Reactions of FeH^+ with oxygenated species suggest some complex and interesting reactions which warrant further study. Electron impact of 1,1'-dimethylferrocene provides a less than ideal source of FeH^+. We are currently developing several new sources which should permit routine preparation of a wide range of organometallic fragments, including metal hydrides and alkyls. The present results indicate that ion beam

studies of these species will reveal a rich and interesting chemistry and serve to better characterize the thermochemistry of reactive intermediates in catalytic processes.

Acknowledgments

The authors would like to thank Professor D. P. Ridge for suggesting the use of 1,1'-dimethylferrocene to generate the FeH^+ beam. This research was supported in part by the U.S. Department of Energy. Graduate fellowship support from Bell Laboratories, SOHIO, and the Shell Companies Foundation (L.F.H.) is gratefully acknowledged.

References

1. On leave from the Weizmann Institute, Rehovot, Israel.

2. Vaska, L.; Werneke, M. F. Trans. N.Y. Acad. Sci., Series 2 1971, 33, 70, and references therein.

3. Smith, R. E. Proc. Roy. Soc. London, A 1973, 332, 113.

4. Wing, R. F.; Ford, W. K. Pub. Astr. Soc. Pacific 1969, 81, 527.

5. (a) Dendramis, A.; Van Zee, R. J.; Weltner, W., Jr. Astroph. J. 1979, 231, 632.

(b) Van Zee, R. J.; Devore, T. C.; Wilkerson, J. L.: Weltner, W., Jr. J. Chem. Phys. 1978, 69, 1869.

(c) Van Zee, R. J.; Devore, T. C.; Weltner, W., Jr. ibid. 1979, 71, 2051.

6. Papers which have reported calculations on FeH include:

(a) Das, G. J. Chem. Phys. 1981, 74, 5766.

(b) Scott, P. R.; Richards, W. G. ibid. 1975, 63, 1690.

(c) Walker, J. H.; Walker, T. E. H.; Kelly, H. P. ibid. 1972, 57, 2094.

7. (a) Stevens, A. E.; Beauchamp, J. L. Chem. Phys. Lett. 1981, 78, 291.

(b) Stevens, A. E.; Beauchamp, J. L. J. Am. Chem. Soc. 1981, 103, 190.

8. Stevens, A. E.; Feigerle, C. S.; Lineberger, W. C. J. Chem. Phys. 1983, to be submitted.

9. Armentrout, P. B.; Beauchamp, J. L. Chem. Phys. 1980, 50, 37.

10. Armentrout, P. B.; Beauchamp, J. L. J. Am. Chem. Soc. 1981, 103, 784.

11. Armentrout, P. B.; Halle, L. F.; Beauchamp, J. L. J. Am. Chem. Soc. 1981, 103, 6501.

12. (a) Halle, L. F.; Armentrout, P. B.; Beauchamp, J. L. Organomet. 1982, 1, 963.

(b) Byrd, G. D.; Burnier, R. C.; Freiser, B. S. J. Am. Chem. Soc. 1982, 104, 3565.

13. Armentrout, P. B.; Beauchamp, J. L. J. Chem. Phys. 1981, 74, 2819.

14. Moore, C. E. "Atomic Energy Levels," National Bureau of Standards: Washington, D. C., 1949.

15. Halle, L. F.; Armentrout, P. B.; Beauchamp, J. L. J. Am. Chem. Soc. 1981, 103, 962.

16. Mysov, E. I.; Lyatifov, I. R.; Materikova, R. B.; Nochetkova, N.S. J. Organomet. Chem. 1979, 169, 301. We obtain a somewhat higher ratio of FeH^+:Fe^+ (~0.27) than is reported here.

17. Chantry, P.J. J. Chem. Phys. 1971, 55, 2746.

18. Armentrout, P. B.; Beauchamp, J. L. Chem. Phys. 1980, 48, 315.

19. A vibrational frequency of FeH^+ of 1629 cm^{-1} was used. Schilling, J. B.; Goddard, W. A., III, unpublished results.

20. Allison, J; Ridge, D. P. J. Am. Chem. Soc. 1979, 101, 4998.

21. Kapur, S.; Müller, E. W. Surf. Sci. 1977, 66, 45.

22. It is interesting to note that an activation energy of 17.8 ± 1.2 kcal/mol was measured for the exchange reaction of HBF_2 with D_2. Curtis, P. M.; Porter, R. F. Chem. Phys. Lett. 1976, 37, 153.

23. Steigerwald, M. L.; Goddard, W. A., III, to be submitted.

24. Preliminary calculations indicate that the hybridization of the metal orbital involved in the Fe^+-H bond is 75% s, 11% p, and only 14% d. Schilling, J. B.; Goddard, W. A., III, unpublished results.

25. Aue, D. H.; Bowers, M. T. in "Gas Phase Ion Chemistry," Vol. 2; Bowers, M. T., ed. Academic Press: New York, 1979. Values for δPA were taken from this reference.

26. Failure to observe formation of ammonia in the reaction of protonated methylamine with methylamine may be due to this same phenomenon if the reaction proceeds through a four-centered front-sided displacement mechanism. Beauchamp, J. L. in "Interactions between Ions and Molecules," vol. 6,

Ausloos, P., ed. Plenum: New York, 1975.

27. Ceyer, S. T.; Tiedemann, P. W.; Mahan, B. H.; Lee, Y. T. J. Chem. Phys. 1979, 70, 14.

28. Lias, et al. have determined $\delta PA(i\text{-}C_4H_8)$ = 8.2 kcal/mol (Lias, S. G.; Shold, D. M.; Ausloss, P. J. Am. Chem. Soc. 1980, 102, 2540). Using the value of $IP(t\text{-}C_4H_9\cdot)$ = 6.70 eV[29] and $\Delta H_f(t\text{-}C_4H_9\cdot)$ = 8.7 kcal/mol[30] gives $PA(NH_3)$ = 206.7 kcal/mol. If a higher heat of formation of the radical is used, $\Delta H_f(t\text{-}C_4H_9\cdot)$ = 12.2 kcal/mol (Tsang, W. Int. J. Chem. Kinet. 1978, 10, 821), then the value $PA(NH_3)$ = 203.1 kcal/mol is obtained. This lower value gives better agreement between values of $\delta PA(H_2O)$ derived from a recent determination of $PA(H_2O)$, and earlier studies (Collyer, S. M.; McMahon, T. B. J. Phys. Chem., submitted).

29. Houle, F. A., Beauchamp, J. L. J. Am. Chem. Soc. 1979, 101, 4067.

30. McMillen, D. F.; Golden, D. M. Ann Rev. Phys. Chem. 1982, 33, 493.

31. Heats of formation for hydrocarbons taken from Cox, J.D.; Pilcher, G. "Thermochemistry of Organic and Organometallic Compounds," Academic Press: New York, 1970.

32. Moet-Ner, M.; Field, F. H. J. Chem. Phys. 1976, 64, 277.

33. Carroll, P. K.; McCormack, P.; O'Connor, S. Astroph. J. 1976, 208, 903.

34. Sweany, R. L. J. Am. Chem. Soc. 1981, 103, 2410.

35. Pearson, R. G.; Mauermann, H. J. Am. Chem. Soc. 1982, 104, 500.

36. $D^o[Fe^+\text{-}CH_3]$ = 69 ± 5 kcal/mol from Reference 12a.

37. $IP[s\text{-}C_4H_9\cdot]$ = 7.25 ± 0.03 eV. Schultz, J. C.; Houle, F. A.; Beauchamp, J. L., to be submitted for publication.

38. Collman, J. P.; Hegedus, L. S. "Principles and Applications of Organotransition Metal Chemistry," University Science Books: Mill Valley, CA, 1980, front cover.

39. Halle, L. F.; Crowe, W. E.; Armentrout, P. B.; Beauchamp, J. L., to be submitted for publication.

40. For example, model porphyrin complexes have been prepared which contain an Fe(IV) unit; La Mar, G. N.; de Ropp, J. S.; Lechoslaw, L.-G.; Balch, A. L.; Johnson, R. B.; Smith, K. M.: Parish, D. W.; Cheng, R. J. J. Am. Chem. Soc. 1983, 105, 782.

41. Atomic iron ions are observed to add to C-OH bonds of alcohols, see Reference 20.

42. Bomse, D. S.; Beauchamp, J. L. J. Am. Chem. Soc. 1981, 103, 3292.

43. Bomse, D. S.; Woodin, R. L.; Beauchamp, J. L. J. Am. Chem. Soc. 1979, 101, 5503.

44. Ridge, D. P.; Beauchamp, J. L. J. Am. Chem. Soc. 1971, 93, 5925.